RECOVERY OF ZINC FROM ZINC FERRITE AND ELECTRIC ARC FURNACE DUST

A thesis submitted to the Department of Materials and Metallurgical Engineering in partial fulfilment of the requirements for the degree of Doctor of Philosophy

By

Dan Kui Xia

Queen's University

Kingston, Ontario, Canada

September 1997

ABSTRACT

This thesis research project addresses a very practical and troublesome problem which has been vexing Electric Arc Furnace (EAF) steelmakers and environmentalists for many years. EAF dust is generated during the EAF steelmaking process and it is designated as a hazardous waste in most industrialized countries. A suitable treatment process which is both economic and environmentally safe has not yet been found.

The major EAF dust treatment processes are pyrometallurgical at this time. However, there is an increased interest in hydrometallurgical treatment processes, because small scale on-site hydrometallurgical processes could be economic and these processes have potential environmental benefits. The major problem with the hydrometallurgical treatment processes is the low zinc recovery, since the zinc ferrite ($ZnFe_2O_4$) in EAF dust is insoluble and thus the zinc which is present in the zinc ferrite can not be recovered in the leaching process. In the present work, research on the kinetics of zinc ferrite formation, the leaching of zinc ferrite and EAF dust in caustic media were performed and evaluated. The experimental results indicated that decomposition of zinc ferrite was mainly dependent on temperature.

The major constituents of EAF dust, zincite (ZnO) and zinc ferrite ($ZnFe_2O_4$) are good microwave absorbers. Microwaves as an energy source have many advantages over the conventional heating processes and thus the microwave leaching of the dust was studied. The results showed that the microwave leaching of the electric arc furnace dust resulted in improved decomposition of the zinc

ferrite as compared to that observed in the conventional leaching process. However, the majority of the zinc ferrite in the EAF dust was still insoluble. Thus, in order to further decompose the zinc ferrite, other options were considered.

Research on the low temperature roasting of both synthetic zinc ferrite and EAF dust was performed. By adding caustic soda with EAF dust, the zinc ferrite was decomposed and formed a soluble compound during roasting at low temperatures. About 95% of the zinc was recovered in the subsequent dilute caustic leaching process. Based on the experimental findings, a hybrid low temperature pyrometallurgical and hydrometallurgical process was proposed for the treatment of EAF dust. This process has considerable commercial potential.

GENERAL INTRODUCTION

An intensive review on the presently available pyrometallurgical and hydrometallurgical processes for the treatment of electric arc furnace (EAF) dust will be presented in Chapter One. There is a growing interest in hybrid pyrometallurgical and hydrometallurgical processes for the treatment of EAF dust. The high temperature requirements of a pyrometallurgical process for EAF dust are a disadvantage and the low-value products usually require hydrometallurgical treatment in order to produce metals which have marcket value. The hydrometallurgical processing of EAF dust is thus a major component of the research in this project.

Zinc ferrite, which is present in EAF dust as a major constituent, is insoluble in the conventional leaching processes and thus the zinc recovery is usually low in the hydrometallurgical process. Consequently, the recovery of the zinc from the zinc ferrite is a major problem in any hydrometallurgical treatment process and is therefore the major focus in this research.

Since zinc ferrite is not commercially available, it was synthesized for the present research. In Appendix, the research on the kinetics of zinc ferrite formation will be presented and discussed. Also, using the method described in this chapter, zinc ferrite was synthesized for the subsequent research. This research improves the understanding of the formation mechanism of zinc ferrite during roasting and in dust formation in pyrometallurgical processes.

Because EAF dust has high iron content and the iron oxides do not dissolve in the alkaline media, caustic soda is usually employed as a lixiviant to avoid the troublesome iron removal process which is usually encountered in the acidic hydrometallurgical treatment processes. However, there is no information available on the leaching behaviour of zinc ferrite in caustic media. Thus, a systematic

research study was performed on the leaching of synthetic zinc ferrite in caustic media and this research will be presented and discussed in Chapter Two.

Although intensive research has been carried out on the caustic leaching of EAF dust, more research is still needed in order to better understand the leaching behaviour of the various elements in EAF dust. Research on the leaching kinetics of EAF dust was thus performed and this work will be presented and discussed in Chapter Three. The data from this research also serves as a baseline for comparison purposes with the results in Chapter Four and Five.

The research results from Chapters Two and Three showed that the zinc dissolution rate increased with increasing time, caustic concentration and temperature. For economic reasons, the leaching time must be reasonable and the increase in zinc recovery with caustic concentration was found to be limited by the viscosity of the solution at high concentrations. Consequently, increasing the temperature becomes the major factor which can be considered for increasing the zinc recovery. On the other hand, some results from the published literature indicated that zinc ferrite was still mostly not dissolved in caustic media under high pressures at temperatures up to 553K(280^0 C). Thus, new technologies have to be sought to completely decompose the zinc ferrite. Microwaves as an energy source for leaching has many advantages over the conventional energy sources, such as rapid and internal heating rates and possible catalysis of reactions. Then research on the microwave leaching of EAF dust was therefore explored and this research will be presented and discussed in Chapter Four.

By using microwave leaching, the dissolution rate can be very rapid and the zinc ferrite in the EAF dust can be further decomposed. However, even under microwave irradiation, the zinc ferrite was

not very soluble. Traditionally, a hybrid pyrometallurgical and hydrometallurgical process is employed to achieve a high zinc recovery. Such a hybrid process usually consists of a high temperature roasting process and a conventional leaching process followed by zinc cementation and electrowinning. During the roasting process, the zinc ferrite can be decomposed at high temperatures under a reducing atmosphere which is achieved by the addition of carbon or coke fines as a reducing agent and source of energy. In addition to the high energy consumption and carbon oxide emissions, lead oxide is readily reduced into the metallic lead form which is insoluble in caustic media, resulting in a low recovery of lead. Ideally, however, a hybrid process should have the following features: (i) lower energy consumption, i.e. a low roasting temperature; (ii) high recovery of both zinc and lead in the subsequent leaching process.

Based on the unique properties of caustic soda (i.e. low melting point), the research involved a low temperature caustic roasting process for both the synthetic zinc ferrite and the zinc ferrite in the EAF dust followed by dilute caustic leaching of the roasted residues. This process will be discussed in Chapter Five. Finally, based on the experimental findings in this research, a hybrid low temperature roasting and a dilute caustic leaching process followed by zinc cementation and electrowinning was proposed for the treatment of EAF dust. In this process, the zinc ferrite in the EAF dust can be easily decomposed in a low temperature roasting process and high zinc and lead recoveries can be achieved in the following dilute caustic leaching process. The difficulties associated with iron removal are reduced and the product from the electrowinning process is fairly pure.

ACKNOWLEDGMENTS

Sincere thanks are due to Dr. Christopher Adrian Pickles, my supervisor, for his guidance, encouragement and constant support. Thanks are also due to Dr. J. Cameron, Professor and Head of the Materials and Metallurgical Engineering Department, Dr. M. Shirkhanzadeh, Professor in the same department, and Dr. W. T. Yen, Professor in the Mining Engineering Department, for their support, valuable discussion and advice during the course of my study.

For me, family is always a source of strength and enjoyment. Words can not express my thanks to my dear Mom, Dad, my dear wife, and my sisters. For all of them I am always indebted.

I would like to thank all the staff at Nicol Hall who are always available. In particular, thanks go to Ms. Shirley Donnelly, Ms. Chris Fowler, Mr. Rod Berndt, and Mr. Charlie Cooney.

I would also like to thank Mary of the Chemical Department for her unselfish assistance in performing the AAS analysis which was done during a busy time of year.

Finally, the financial support of the School of Graduate Studies and the Natural Sciences and Engineering Research Council of Canada (NSERC) is most gratefully acknowledged.

TABLE OF CONTENTS

LIST OF TABLES

LIST OF FIGURES

Chapter One

A REVIEW OF PYROMETALLURGICAL AND HYDROMETALLURGICAL TREATMENT OF EAF DUST

SUMMARY

In this chapter, research and development work on the treatment of electric arc furnace dust (EAFD) is discussed. Pyrometallurgical and hydrometallurgical treatment processes are reviewed. Due to the complicated nature of the dust, the treatment processes tend to be elaborate. Furthermore, the processes are becoming more complex as the environmental regulations become more stringent. In the past, considerable research on the pyrometallurgical treatment of dust has been performed. However, more recently, there has been an increased interest in hydrometallurgical processes. This is due to the potential advantages of hydrometallurgical processes which include: the possibility of small-scale, on-site processes, the ability to separate the halide salts and the byproduct metals, and the byproduct metals can be produced in pure metallic form. The major disadvantages of the hydrometallurgical processes are that, in many cases, the zinc in the zinc ferrite can not be recovered and some residues and waste solutions are produced which require treatment. On the other hand, in the pyrometallurgical processes, the zinc in the zinc ferrite can be reduced, but there are a number of problems associated with the condensation of the volatile metals, particularly, if metals halides are present. Furthermore, at the high temperatures and gas flowrates employed in the pyrometallurgical processes, the zinc can become contaminated with iron. Also, waste residues

and dusts are generated which require further treatment. It is likely that, in the future, considerable research effort will be directed at hybrid processes, which are combinations of pyrometallurgical and hydrometallurgical processes.

1-1. INTRODUCTION

1-1-1. GENERAL

Electric arc furnace (EAF) flue dust is considered a hazardous waste in most industrialized countries. It is generated during EAF steelmaking from iron-containing steel scrap. Currently, the EAF steelmaking process accounts for about 31% of world's annual steel production [1-2]. The EAF's share of total steel output has been increasing at the expense of integrated iron and steel production for the last two decades and this trend will likely continue, particularly in North America [3], Europe [4] and Japan [5]. For example, about 35% of the total steel output is produced presently by melting iron-containing scrap in EAFs in America [6], and this number will grow to 50% by the turn of the century [3]. While in Japan, about 33% of the total steel or about 33 million metric tonnes were produced in EAFs in 1989, and it was forecast that the capacity of EAFs in Japan would increase by 10 million tonnes per year by 1995 [5]. This phenomenon has been brought about by an ever-increasing concern over environmental issues, resource conservation and the economic benefits associated with EAF steelmaking have resulted in an increased recycling rate of scrap. As a result, there has been an increasing volume of EAF dusts to be treated. Traditionally, the dust has been stockpiled. However, this treatment is no longer viable for most EAF steelmakers, since, the sites available for stockpiling are being depleted and, also the valuable metal values are lost, but, most importantly, more stringent environmental regulations have been put into effect. Although great efforts have been made over the last decade and various treatment technologies and processes have been developed, none of them is thought to be satisfactory. Thus, new technologies and processes are still emerging.

1-1-2. GENERATION AND QUANTITY OF EAF DUST

The formation of EAF dust has been considered by a number of authors [7-15]. It is believed that the generation of EAF dust is associated with nearly all phases of normal furnace operation. During charging, particulate matter and volatile matter are liberated by agitation and heat. As the melting and refining processes continue, more particulates and volatile substances are carried out of the furnace, due to the high operating temperatures of above 1873K(1600^0 C) and the atomization of liquid steel by "boiling" gas evolution. Volatile elements, such as zinc, lead and cadmium in the charge are mostly evaporated at the early stages of the operation, and eventually all of them enter the gas phase. Other elements, such as iron, chromium, nickel and manganese are carried out of the furnace during the refining period, mainly, due to the injection of oxygen. Particulates are also evolved during tapping, particularly, if alloys or additions are made during the tapping of the molten steel into the ladle.

The discharged volatile components quickly convert themselves into their respective oxides upon contact with air. Then, they physically and chemically combine with the atomizing liquid steel and other particulate emissions, such as slag-forming substances (mainly, calcium oxide), and iron oxides and silica, which are present in the charge. Interactions of these constituents make the final dust complicated in terms of both its chemistry and physics.

The dust is separated from the gaseous phase using de-dusting units, such as scrubbers, baghouses and elecrostatic precipitators so that the off-gas meets the environmental standards before it is vented to the atmosphere. Due to its complex nature, the management and the treatment of dust, have always presented significant challenges for both environmentalists and metallurgists.

It was widely reported that about 10 to 20 kilograms of EAF dust are generated per tonne of steel produced [16-19]. In North America, the quantity of dust generated is approximately 700,000 tonnes per year. In the U.S.A., there are about eighty EAF steelmaking plants producing roughly a total of 600,000 tonnes of EAF dust per year [3,20], while in Canada, a total of twelve mini-mill plants produced 100,100 tonnes of EAF dust in 1995 and most of the EAF dust produced was generated in Ontario [21]. The average amount of EAF dust generated per plant is approximately 7,500 tonnes and 8,342 tonnes per year in the U. S. and Canada, respectively. According to a survey [21], the average amount of dust produced in the U.S. was slightly over 8,000 tonnes per year per plant in 1992 as compared with 6,000 tonnes in 1985. About 86% of the dust was produced at plants at rates of 2,000 to 20,000 tonnes per year per plant which was comparable to the 1985 results. In the Western European countries, around 480,000 tonnes of EAF dust have been generated yearly [4], while in Japan this amount was about 300,00 to 450,000 tonnes per year from about fifty electric steelmaking facilities [5,22].

1-1-3. PHYSICAL AND CHEMICAL PROPERTIES OF EAF DUST

1-1-3-1. PARTICLE SIZE AND DISTRIBUTION

The particles in EAF dusts tend to exist as aggregates consisting of very fine individual particles. As reported, most of the individual particles are less than 1 μm [16,23]. The average particle size is 1.0-1.2 μm as measured using a Fisher Sub-Sieve instrument [24], or 1.0-4.3 μm using a Microtrac instrument [24]. In most cases, similar results were obtained [25-27]. However, in one case, the

results were significantly different [28]. Table I [24] shows some typical results for the average particle size and some other physical properties of EAF dusts. Another study on EAF dusts which were sampled from eighteen Spanish steekmaking facilities showed that the dusts consisted of spherical particles, which had sizes ranging from a few microns to three hundred microns [25]. About 50% and 80% of the particles studied had diameters of between 2.5 μm and 5 μm, respectively. Recently, A. Hagni and R. Hagni [27] extended their previous research and used the concept of Stoke's Law to study the particle size distribution [29]. They employed a hydro-cyclosizer to separate the dusts in the sub-sieve size range. Three different samples were sized in order to verify repeatability. The determination of particle size distribution was dependent on water temperature, particle density, elutriation flowrate and elutriation time. The densities of ten dust samples were determined using a gas pycnometer and varied within a range from 3.50 g/cm^3 to 4.74 g/cm^3, with a mean density of 4.05 g/cm^3 . These EAF dust densities are consistent with those reported earlier by Themelis and Wu [24]. The average range of the five cyclones and overflows were as follows: -53+28 μm, -28+21μm, -21+14 μm, -14+10 μm, -10+8 μm, and <8 μm. Each sample studied was dry sieved to separate >150 μm, -150/+53 μm, and <53 μm size fractions. The minus 53 μm dust was further separated using a hydro-cyclone. The results of the hydro-cyclosizer are given in Figure 1[27]. It is shown that more than 60% of the minus 53 μm size fraction are less than 8 μm in diameter. On the other hand, reflected light microscopy showed that many of the minus 28 μm particles remained in the -53+28μm cyclone which could account for the abnormal results in sample two. Using the same method as Hagni [29], Cruells [28] found that 12 wt% of the dust fraction was greater than 100 micron and 48 wt% of the fraction between 100 and 56 microns

was silica. He also reported that only one third of the dust fraction was in the range of less than 100 μm and zinc was rich in particle sizes less than 36 μm.

Table I. Characterization of EAF Dust [24]

Property	Single Particle	Aggregates
Moisture (%)	0.1	0.1
Density (g/Cm^3)	3.66-4.53	1.85-2.45
Diameter (μm)	1	>4
Porosity (%)	—	38-79

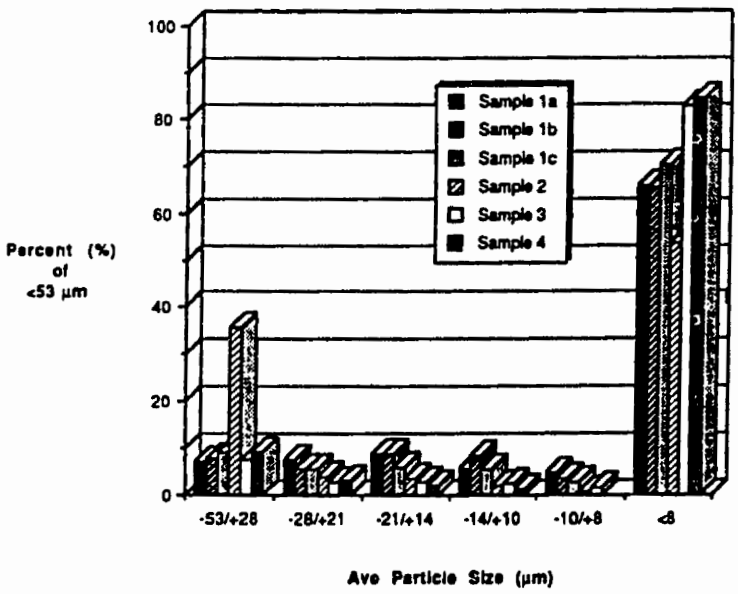

Figure 1. EAF Dust Hydrocyclone Particle Size Distribution [27]

1-1-3-2. CHEMICAL COMPOSITION

The composition of EAF dust varies considerably. It is dependent not only on the scrap used and the type of steel being made, but also the operating conditions and procedures. Even a minor change in the operating procedures from heat-to-heat could result in a variation in the composition of the dust. However, some general trends have been noted. For example, the dusts from carbon steelmaking are all rich in zinc and lead, while the dusts from stainless steelmaking are relatively low in lead and zinc, but richer in alloying elements, such as chromium, nickel, manganese, etc. Since the ratio of galvanized steel scrap used has been increasing, the composition of zinc and lead in the dusts has also been increasing and this trend will likely continue [4]. According to a survey of fifty two EAF steel mills in the U.S.[30], the concentration of zinc in the dusts varied from 0.18% to 32.0% in 1992 compared to 1.5 % to 42.2 % in 1985 [31]. About 67% of the plants have dusts containing between 15 % and 30 % zinc which accounts for about 78 % of the total zinc available. This compares to 40 % of the plants with dusts containing between 15 % and 25 % zinc in 1985, which accounted for about 55 % of the zinc available. In addition to zinc , the dust also contains a considerable percentage of iron and a lesser percentage of lead, manganese, calcium, sodium and potassium as well as trace amounts of other elements, such as cadmium, chromium, nickel, coppper, magnesium, silicon, and chlorine. Table II [25,30,32-33] shows the typical compositions of EAF dusts from the U. S., Spain and France. Since the major component of the feed in EAF steelmaking is the steel from iron-containing scrap, then the composition of the dust would not be expected to vary significantly from country to country. For example, a study of thirteen Taiwanese steelmaking plants showed that the Taiwanese EAF dusts were comparable in chemical composition to those from American plants [34].

Table II. Mean Composition of EAF Dusts

Element	U. S.[30]	France [32]	Spain [25]
Fe	28.5	21.8	25.90
Zn	19.0	21.2	18.6
Pb	2.1	3.6	3.63
Cd	<0.01	NA	0.10
Cr	0.39	0.37	0.31
Ca	1.85-10.0 [a)]	12. 8	3.50
Ni	0.01-0.02 [a)]	0.10	0.07
Mo	<0.02-0.08 [a)]	NA	NA
Mn	2.46-4.60 [a)]	2.5	2.81
Mg	0.77-2.93 [a)]	NA	1.53
Cu	0.06-2.32 [a)]	0.25	0.54
Si	1.35-2.49 [a)]	NA	1.65
Cl	0.51-2.36 [a)]	1.75	3.43
F	0.01-0.88 [a)]	NA	NA
K	0.06-1.12 [a)]	2.06	1.23
Na	0.29-2.31 [a)]	2.23	1.27
Al	NA [b)]	NA	0.44

[a)]: After Keyser, N. H. et al. [33]: [b)]: data not available.

1-1-3-3. MINERALOGICAL DISTRIBUTION OF ELEMENTS PRESENT IN EAF DUSTS

1-1-3-3-1. X-Ray Diffraction Analysis

Significant studies have been performed on the mineralogical phase distribution of elements present in EAF dust [25-28,32-40]. As shown by X-ray diffraction (XRD), the mineralogy of EAF dust

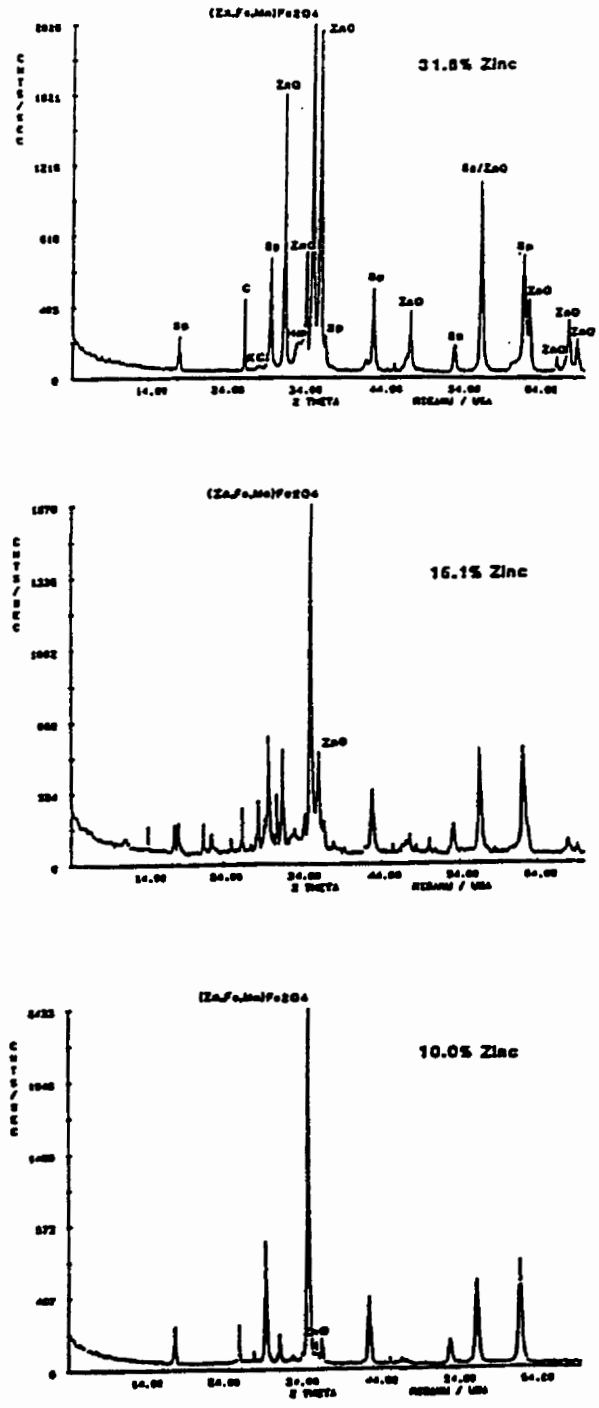

Figure 2. X-Ray Diffraction Patterns of Three EAF Dust Samples with High, Medium, and Low Zinc Percentage Showing Correspondingly Lower Zincite (ZnO) Percentage [27]

Sp=$(Zn,Fe,Mn)Fe_2O_4$; Hm=Fe_2O_3; C=coke.

consists of a predominant magnetite-franklinite-jacobsite solid solution, (Fe, Zn, Mn)Fe_2O_4, with lesser zincite, ZnO, hematite, Fe_2O_3, and minor sylvite, KCl, carbon (coke) [27] and calcia, CaO, as well as silica, SiO_2, calcium and aluminium silicates, (Ca,Al)SiO_3 [25,28]. New phases, such as $Ca[Zn(OH)_3]_2 \cdot 2H_2O$ [28] and $ZnCl_2 \cdot 4Zn(OH)_2 \cdot H_2O$ [34] were also determined in some EAF dust samples by XRD. The typical XRD patterns for EAF dusts are given in Figure 2 [27]. As can be seen, the amount of zincite varies with the percentage of the zinc present in the sample. The amount of zincite in the dust increases with the zinc content. The dust containing 31.8 % zinc has a primary zincite peak almost as great as the (Zn,Fe,Mn)Fe_2O_4 primary peak, while the dust containing 16.1 % zinc had much less zincite and only a trace of zincite had formed in the dust containing 10 % zinc.

1-1-3-3-2. Reflected Light Microscopy

Below is a summary of the results of a reflected light microscopy study on a selected size fraction of EAF dust [27].

+ 150 μm Size Fraction: Most of the particles in EAF dust were spheres and broken spheres. The largest size fraction (>150 μm) also contained large, irregularly shaped coke particles. In this size fraction, seven phases and phase combinations have been identified: magnetite-franklinite-jacobsite solid solution crystals in a Ca-Fe-Si glass, the pure end member magnetite, magnetite oxidizing to hematite along its octahedral planes, metallic iron, metallic iron with an oxidation rim of magnetite, spheres of Ca-Fe-Si glass, and coke. Zincite was not evident in this particle size fraction. About 5 wt% chromium was present in magnetite-franklinite-jacobsite spinels, as determined by scanning electron microscopy-energy dispersive spectroscopy [29].

−150/+53 μm Size Fraction: The same phases were present in this size fraction. However, the (Fe,Zn,Mn) Fe_2O_4 had crystallized out of the Ca-Fe-Si glass. Also, abundant porosity was observed in many of the spheres. This porosity was thought to be attributed to CO and CO_2 gases leaving the system [41].

Sub-Sieve Size Fraction: The crystal morphology of the iron spinel solid solution varied from a dendritic texture to well developed rhombohedrons throughout all the particle sizes. Magnetite is present as individual spheres, while franklinite and jacobsite were not observed in this size fraction of EAF dust. Solid solution spinel containing zinc and/or manganese was present as crystals in spheres of Ca-Fe-Si glass. Zincite was observed in the −28/+21μm size fraction and also smaller size fractions. Many of the minus 1 μm particles were attracted to one another due to their magnetic and electrostatic properties and formed halos around the larger particles. These finer particles were found to contain zincite.

1-1-3-3-3. Transmission Electron Microscopy

The EAF dust particles less than 8 μm in diameter were observed using the transmission electron microscope. Agglomeration of the dust particles was evident even down to 2100 A^0. As was found in the larger particles with reflected light microscopy and scanning electron microscopy-energy dispersive spectroscopy, many of the fine dust particles had crystallized in the form of a magnetite-franklinite-jacobsite solid solution within a Ca-Fe-Si glass sphere. Zincite was present as individual spheres in the smaller size fractions.

The mineralogical phase distributions of the elements present in EAF dust are summarized in Table III.

Table III. Mineralogical Phase Distribution of Elements Present in EAF Dust [2,25,27]

Element	Phase Distribution
Fe	Main: $(Fe,Zn,Mn)Fe_2O_4$; minor: Fe_3O_4; trace: α-Fe_2O_3 and Fe; Fe cations are replaced partially by other metals such as Mg, Cr and Si, etc.
Zn	Main: $(Fe,Zn,Mn)Fe_2O_4$, and ZnO; minor: $Ca[Zn(OH)_3]_2 \cdot 2H_2O$ [28] and $ZnCl_2 \cdot 4Zn(OH)_2 \cdot H_2O$ [34]; sulphide,silicate and aluminate.
Pb	Main: PbO; minor: $PbCl_2$ and $PbSO_4$.
Cd	Distribution not well established, but possibly the same as for Zn considering the similarities in most properties of the two elements.
Cr, Ni	Replace iron in ferrite solid solution and are associated with Fe_3O_4 in spinel type phase.
Ca	Main: CaO, $CaCO_3$; minor: $CaO \cdot Fe_2O_3$, CaF_2 and various silicates.
Mn	$(Fe,Zn,Mn)Fe_2O_4$.
Mg	Replaces Ca in ferrite.
Si	SiO_2 and silicates.

1-1-4. TOXIC NATURE OF EAF DUSTS

EAF dust is a listed hazardous waste, since it fails the EPA toxic test based on its lead, cadmium, and chromium contents. Table IV gives the soluble limit of EAF dust following the toxicity characteristic leaching procedure (TCLP) [10,42]. Some samples of EAF dust which were tested by following the TCLP are shown in Table V [10,25]. These tests were perfomed under the following conditions [10]:

Procedure:	EPA
Sample Size:	100 g
Weight of Distilled Water:	1500 g
Extractor:	3L Glass Beaker
Agitation:	Electric Stirrer
Time:	27 hours
Temperature:	Room Temperature
pH:	5.2
Volume of 0.5m Acetic Acid Used:	400 ml
Solid Liquid Separation:	Physical Decantation
Metal Analysis Done by:	Atomic Absorption Spectrophotometer

Table IV. Leachability Limit (ppm) for EAF Dust [4,10,42]

Element	Pb	Cd	Cr	As	Ag	B	Hg	Se	U
US EPA	5	1	5	5	5	N/A	0.2	1	N/A
Ontario*	0.5	0.5	0.5	0.5	0.5	50	0.01	0.1	200
Italy	0.2	0.02	2	0.5	N/A	N/A	N/A	N/A	N/A
German	2.0	0.5	10.0	1	N/A	N/A	N/A	N/A	N/A

*: Ontario Regulation 347/309.

Table V. TCLP Toxicity Test Results (ppm) on EAF Dusts [10,25]

Element	Pb	Cd	Cr	As	Hg	Se	Ag
U. S. Samples			Carbon Steel				
A	674	38	<1.0	<0.1	<0.001	<0.01	<1.0
B	714	35	<1.0	<0.1	<0.001	<0.01	<1.0
C	491	38	<1.0	<0.1	<0.001	<0.01	<1.0
Spanish Samples			Carbon Steel				
Range	30-320	6-110					
Mean	121.0	31.1					
		Stainless Steel					
Range	<0.5	1-6	4.0-26.3				
Mean	<0.5	3.5	18.1				
Italy	620	27	0.8	0.5			

It is clear that all samples tested failed the toxicity test. This was mainly due to the presence of lead and cadmium in the dust from carbon steelmaking and, due to the chromium content in the dust from stainless steelmaking.

1-1-5. REGULATIONS GOVERNING EAF DUST MANAGEMENT AND TREATMENT

Unlike well-defined air or water standards, solid waste regulations vary widely from country to country, and even differ from province to province [7,21]. However, due to its toxic nature, EAF

dust is classified as hazardous waste in North America, Western Europe and Japan.

Currently, although there are no Federal regulations that regulate steel mill dust in Canada, each province has its own environmental regulations and the TCLP procedure is the same for all the provinces [21].

In Alberta, the disposal of EAF dusts is regulated by Waste Control Regulation 129/93 under the Environmental Protection and Enhancement Act. If the dust does not meet the TCLP criteria, it is deemed to be a hazardous waste and is regulated.

In Saskatchewan, the dust is regulated under the Environmental Management and Protection Act, Dangerous Goods Transportation Act and Dangerous Goods Transportation Regulations.

In Manitoba, hazardous waste must go to a licensed secure facility according to the Environmental Management and Protection Act and is subject to the leachate criteria of the Dangerous Goods Handling and Transportation Act.

In Quebec, the Environmental Quality Act and Hazardous Waste Regulation Q-2, r.3.01 apply to all steel mill dusts.

In Nova Scotia, all steel mill dusts are regulated under the Environmental Assessment Act, Dangerous Goods and Hazardous Waste Management Act, Dangerous Goods Storage Regulations and N.S. Regulation 97/89.

In Ontario, waste Management Regulation 347 of the Environmental Protection Act regulates steel mill dusts. If the dust fails the TCLP test, it must go to a secure landfill; otherwise, an ordinary

landfill can be used.

In the U.S., EAF dust was considered to be a hazardous waste (K061) by the Environmental Protection Agency (EPA) under the 1980 Resource Conservation and Recovery Act (RCRA) regulations [3]. The disposal of the dust has been limited to designated hazardous waste landfills since 1980. Legislation was further enacted prohibiting the further disposal of K061 in any landfill site after August 8, 1988 [43]. Based on an appeal from the steel producers, this ruling was subsequently modified and an extension was granted to allow for further development of process technologies until August 8, 1990. However, this revised regulation required that High Temperature Metal Recovery (HTMR) technology as the Best Demonstrated Available Technology (BDAT) be employed for those dusts with zinc contents of 15 % or more, while stabilisation and landfill disposal were permitted for those dusts with zinc contents less than 15 % [20,43,44]. Later in 1992, the EPA proposed to abolish HTMR as BDAT for all K061 wastes, regardless of the zinc content. The management and the treatment procedures for the dust were as described below [20]:

- It was permitted to sell the dust to the fertilizer industries as a source of zinc for micro-nutrients.

•• Any dust treatment technology could be used if it met the revised treatment standards for the following fourteen elements:

Antimony	Arsenic	Barium	Beryllium	Cadmium	Chromium	Lead
Mercury	Nickel	Selenium	Silver	Thallium	Vanadium	Zinc

These rules allowed hydrometallurgical processing of dust as long as the final residues, if any, met the TCLP requirements. Then, surprisingly, the EPA ruled in July, 1995 that stabilisation and

subsequent disposal in conventional landfills was permissible for all EAF dust regardless of site specifity, as long as the stabilised product met appropriate requirements for the fourteen elements for which the TCLP leachate standards existed [45].

The 1995 ruling was obviously favorable for the steelmakers, since it allowed them to pursue potential less costly EAF dust management methods. However, the dust processors using metal recovery processes were concerned, since their business was significantly affected. Litigation is still underway regarding the 1995 ruling. In the future, it could be concluded that whatever the final direction of EAF dust management, only those technologies which are not only cost-effective, but profitable, will survive, and the development of such technologies will be the trend for the future in EAF dust management and treatment.

1-2. EAF DUST MANAGEMENT METHODS AND TREATMENT TECHNOLOGIES

1-2-1. GENERAL

Perhaps the most logical use of EAF dust would be in the iron and steelmaking process in which it is generated. Its iron rich nature has resulted in attempts to directly recycle the dust to the various iron and steelmaking processes. However, its content of zinc, lead and other tramp elements such as copper, sulphur, sodium, potassium as well as halides makes it impossible to recycle into the ironmaking process. Zinc has been found to be the cause of many troubles in blast furnace operation [46], such as refractory failure, scaffold formation in the stack, and complete filling of the gas off-take. Consequently, the feed to an iron blast furnace must have a very low zinc content. For

example, the requirement for zinc content in iron ore, according to most specifications is usually less than 0.01 % [47]. Similarly, other tramp constituents are unwanted even at low concentration levels, since they either reduce furnace life and efficiency [16], or are difficult to remove from the steel bath and lead to the production of poor quality steel. EAF dusts have been recycled to the steelmaking process to recover portions of the iron and to minimize the quantity of dust which eventually has to exit from the process. Due to a larger proportion of the very fine dust particles in the feed, the amount of dust to be collected increases with each recycle. As the amount of recycled dust increases, the energy consumption also increases for reducing and melting the iron and the other constituents in the dust. Another negative factor influencing the recycling of dust is that the non-ferrous metals will build up with repeated recycling to such a point that they adversely affect the steel melting operation and the steel quality. As oxides present in the slag, they may attack the refractory lining of the furnace. In reduced form, these metals may enter the molten steel at concentrations higher than permissible to meet the specifications for the proper mechanical and physical properties of the steel. At this point, the dust has to be removed from the system. Traditionally, the dust has been disposed of in landfill sites.

As ever more stringent environmental regulations come into effect, landfilling is becoming a less viable option for steelmakers. Landfilling sites are costly, and the future liabilities of landfilled dusts are far from certain. With a depletion of the number of landfill sites, the total costs for landfill of the dust including pretreatment, transportation and disposal could exceed $200 per ton [3]. In 1992, only 11.2 % of the EAF dust in the U.S. was landfilled, while in 1985, this number was as high as 73.0 % [20]. It is likely that the landfill option may disappear in the near future [20]. The options currently available for steelmakers could be comprehensively classified as follows:pyrometallurgical,

hydrometallurgical, stabilization or vitrification processes as well as other miscellaneous processes. Some of these processes have either been commercialized, or commercialized for a period and then abandoned; Many of these have only reached the pilot scale. The status of the pyrometallurgical and hydrometallurgical processes will be described in the following sections.

1-2-2. PYROMETALLURGICAL PROCESSES

Most of the commercially available processes, such as the rotary kiln processes, for the treatment of EAF dusts can be considered as pyrometallurgical. However, since rotary kiln processes usually require large tonnages of EAF dust to be treated in order to be economically competitive, other technologies have also been developed, particularly those which aim at the development of a small scale, on-site treatment process. Unfortunately, some of these processes have proven to be too elaborate and energy-intensive, such as most plasma processes. Normally, they all require a very well-designed condenser for the recovery of zinc, lead, cadmium and salts such as sodium and potassium chlorides. However, even if the elaborate operation regulations are strictly followed, the efficiency of metal recovery is low. Therefore, it is not surprising that some of these processes have been abandoned. As for the development of small scale, on-site technologies, however, it remains to be seen if such efforts will provide a competitive option for dust treatment. The major rotary kiln processes, plasma processes and other High Temperature Metal Recovery (HTMR) processes are discussed in the following sections.

1-2-2-1. HTMR-ROTARY KILN PROCESS

The HTMR rotary kiln processes are summarized in Table VI.

Table VI. Rotary Kiln Reduction Processes for EAF Dust

Process	Developer/Owner	Status	Location	Capacity (t/y)	Products	Ref.
Waelzing & Calcining	Horsehead Resource Development Company (HRD)	Commercial (1980)	HRD (Palmerton, PA)	270,000	Zinc calcine lead/cadmium oxide iron-rich slag	3,48
Waelzing	(as above)	Commercial (1988)	HRD (Calumet, IL)	82,000	Crude zinc oxide iron-rich slag	3,48
(as above)	(as above)	Commercial (1990)	HRD (Rockwood, TN)	82,000	Crude zinc oxide ron-rich slag	3,48
(as above)	Zinc Nacional	Commercial	Zinc Nacional (Monterry, Mexico)	110,000	Crude zinc oxide iron-rich slag	49
(as above)	Berzelius Umwelt-Service AG	Commercial (1975)	Berzelius (Duisburg, German)	65,000	Crude zinc oxide iron-rich slag	50
(as above)	Berzelius Umwelt-Service AG	Commercial (1987)	Aser SA (Bilbao, Spain)	80,000	Crude zinc oxide iron-rich slag	4,50
(as above)	Berzelius Umwelt-Service AG/Metaleurop SA	Commercial (1993)	Recytech SA (Fouquieres, France)	80,000	Crude zinc oxide iron-rich slag	49
(as above)	Nuova Samim	Commercial	Nuova Samim (Ponte Nossa, Italy)	50,000	Crude zinc oxide iron-rich slag	4,49
(as above)	Sumitomo Metal Mining Co. Ltd.	Commercial (1977)	Shisaka Works (Hisaka, Japan)	60,000	Crude zinc oxide iron-rich slag	5,22
(as above)	Sotetsu	Commercial	Sotetsu (Japan)	60,000	(as above)	5
(as above)	Kaneko	Commercial	Kaneko (Japan)	40,000	(as above)	
HTR	Himeji	Commercial (1978)	Himeji (Japan)	45,000	(as above)	51
Inclined Rotary Kiln Reduction Process	ZZT Minerals	Commissioning (1994)	ZTT Minerals (Caldwell, TX)	20,000	Crude zinc oxide Salt, Slag(ferrolime)	49,52

1-2-2-1-1. WAELZ KILN PROCESS [3,48]

Essentially, a Waelz kiln is a rotary kiln. The name Waelz is derived from the German verb "Walzen", meaning to trundle or roll, the words which accurately describe the movement of the charge through the rotary kiln. As a leading resource recycling company, Horsehead Resource Development (HRD) Co., Inc. now has its Waelz kiln facilities in Palmerton, PA, Calumet, IL, and Rockwood, TN., which treat about 80-85% of the dust from carbon steelmakers in the U. S. The specifications of HRD's rotary kilns are summarized in Table VII. A typical process flowsheet is given in Figure 3 [48].

Table VII. HRD Rotary Kiln Specifications [48]

Rotary Kiln	Location	Process	Length (Ft.)	Shell Diameter (Ft.)	Drive (HP)	Slope	Rotation (RPM)
1	Palmerton	Calcining	142	10	75	3%	0.5
2	Palmerton	Waelzing	160	11.25	100	3%	0.9
3	Palmerton	Waelzing	160	11.25	75	3%	0.9
5	Palmerton	Waelzing or Calcining	160	12	125	3%	0.9
6	Palmerton	Calcining	160	12	125	3%	0.8
7	Chicago	Waelzing	180	10.5	125	6%	0.6
8	Rockwood	Waelzing	148	11.5	200 (DC)	3%	0.8

The received EAF dusts and/or other zinc bearing materials are conditioned to about 8-12% moisture and the $(CaO+MgO):SiO_2$ ratio is maintained above 1.35. Before being fed to the kiln, the conditioned materials are blended with a carefully sized carbon source, typically anthracite coal

(Palmerton), petroleum coke (Chicago), or metallurgical coke fines (Rockwood); or a combination of these sources. About one tonne of coal (dry basis) is needed for every five tonnes of zinc bearing feed. Several distinct reaction zones are observed within the kiln as follows:

i). drying and preheating of feeds; ii). decomposition of limestone, if added; iii). volatilization of the halide compounds; iv). partial reduction of iron oxides, and v). reduction/volatilization and reoxidation of lead, zinc and cadmium.

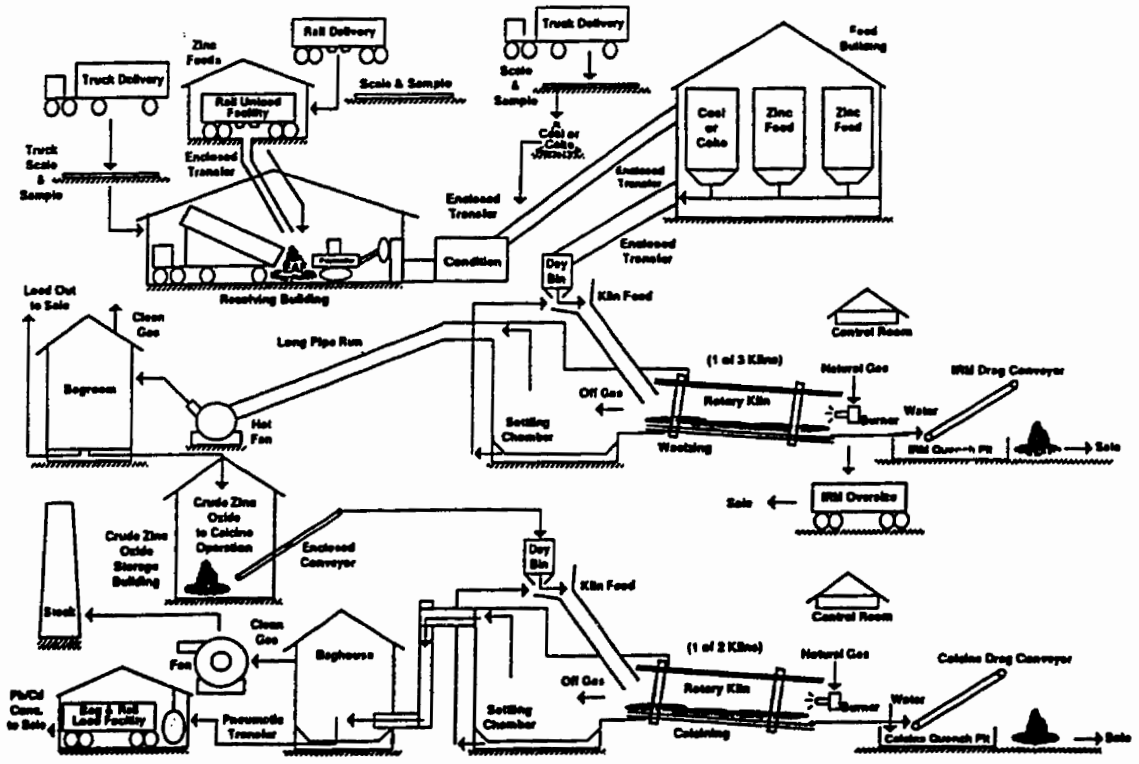

Figure 3. Schematic Flow Diagram of Palmerton, PA Plant[48]

Efficient kiln operation is achieved with a steady kiln temperature profile. This is accomplished by controlling kiln pressure through remotely operated louvers on the suction side of the hot fan (Palmerlton), or outlet dampers on the suction fan (Chicago and Rockwood). Figure 4 shows a typical temperature profile along the process.

The kiln can be viewed as two reaction zones, as shown in Figure 5 [3]: the solid material charge zone (bed) and the free gas zone (freeboard). In the bed, the anthracite coal is oxidized, largely by the Bouduard reaction as follows $CO_2 + C = 2CO$. This generates carbon monoxide which reduces

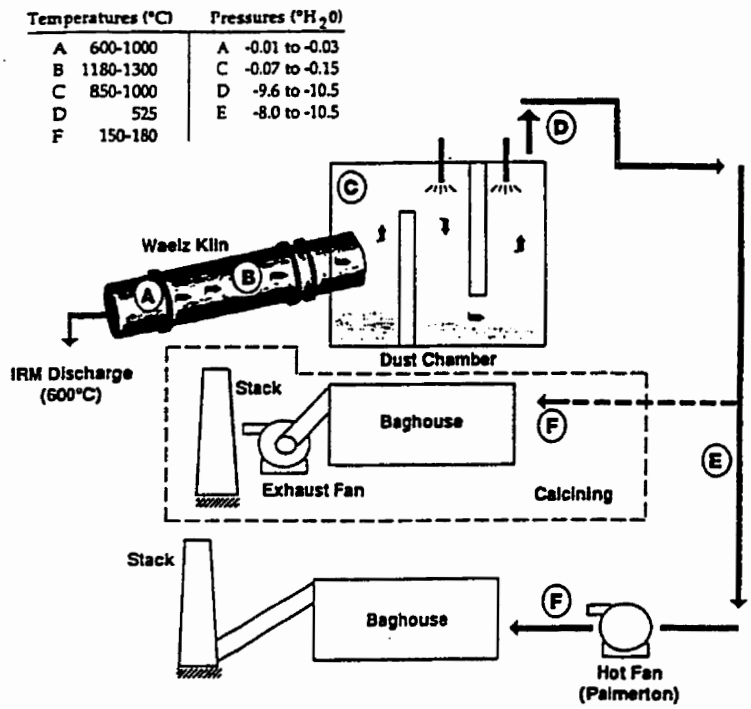

Figure 4. Waelzing Operation Condition [48]

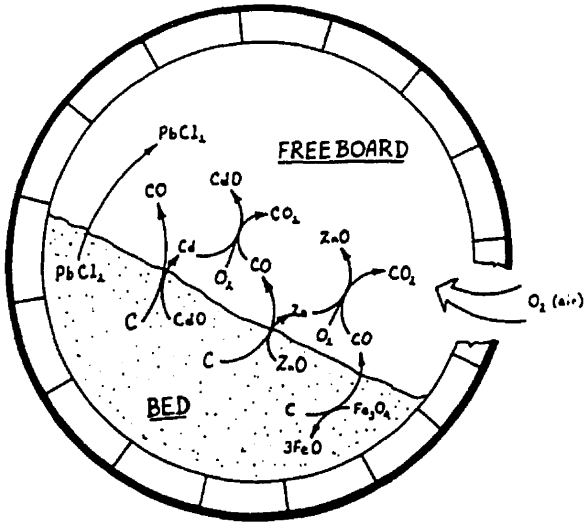

Figure 5. Waelz Kiln Schematic Cross Section [3]

the metal oxides. The reduced metals evaporate into the freeboard area and then are reoxidized. Generally, the reactions are completed within ten feet of the discharge end of the kiln. The Waelz kiln has a natural gas burner at the Iron Rich Materials (IRM) discharge end of the unit. The burner is only used intermittently for temperature control, since the anthracite coal combustion provides the thermal requirement. Some typical reactions in the kiln are given in Table VIII [3].

Two products result from the Waelzing process: Crude Zinc Oxide and IRM. The Crude Zinc Oxide is collected in individually operated baghouses. The temperature of the exit gas from the kiln

Table VIII. Typical Reactions in Waelz Kiln [3]

Combustion of Carbon:
$C + 0.5O_2 = CO$ $C + O_2 = CO_2$ $C + CO_2 = 2CO$
Reduction:
$Fe_3O_4 + CO = 3FeO + CO_2$ $ZnO + CO = Zn + CO_2$
$CdO + CO = Cd + CO_2$
Oxidation:
$CO + 0.5O_2 = CO_2$ $Zn + 0.5O_2 = ZnO$ $Cd + 0.5O_2 = CdO$
$PbS + 2O_2 = PbSO_4$

is reduced to approximately 423-453K(150-180^0 C) by means of evaporative cooling, dilution, and convective/radiant cooling. The evaporative cooling sprays are also automatically activated by sensors in the baghouse to prevent bag damage from excessive temperatures. Nomex bags are used at all facilities. Clean furnace off-gas streams are maintained well within air permit specifications at all sites.

IRM is collected at the discharge end of the kiln, where it passes through a 3" trommel. At Palmerton, the IRM drops into a quench tank equipped with an inclined drag conveyor. At both Chicago and Rockwood, the -3" IRM passes directly into rotary coolers before discharge. Plus 3" coarse material discharges separately. The IRM production typically amounts to 50-60% of the feed rate of the zinc bearing feed. At all locations, the IRM product is evaluated by the TCLP test, and after passing is marketed as a variety of construction materials, for example, as iron units to the cement industry, as aggregate for use in asphalt production, and as highway anti-skid material.

Typical Waelzing feed and product compositions are given in Table IX. Crude zinc oxide produced at Chicago and Rockwood is discharged from the product baghouses directly to rail cars for delivery to customers or transferred to Palmerton. Crude Zinc Oxide produced at Palmerton is loaded directly into rail cars for sale or transferred to the calcining kiln feed bins for calcining.

Table IX. Typical Waelz Kiln Feed and Products [48]

Element	EAF Dust (%)	Crude Zinc Oxide (%)	IRM (%)
Zn	17.5	52.4	0.8
Fe	23.1	4.2	37.1
Ca	9.1	1.4	14.7
Si	1.7	NA	6.2
Na	0.64	1.2	0.8
K	0.47	0.48	NA
Mn	2.9	0.56	3.5
Mg	1.9	0.39	2.6
Al	0.46	0.12	1.7
Pb	2.6	8.0	0.12
Cd	0.66	0.76	0.01
Cu	0.23	0.087	0.39
Cr	0.12	0.026	0.2
Ni	0.03	0.01	0.1
Sn	0.04	0.09	0.03
Cl	1.03	3.58	0.01

1-2-2-1-2 CALCINING KILN PROCESS [3,48]

To effect further metal separation, a separate rotary kiln is used to selectively volatilize cadmium, lead, chlorine and fluorine from the zinc oxide. Historically, rotary kilns employed in such a process were referred to as calcining or clinkering kilns [69-70]. Calcining kilns are essencially identical to the Waelz kilns, as evidenced by the dual capability of Number 5 kiln to perform either Waelzing or calcining in Palmerton PA. However, the processing conditions are different. In contrast with the reducing conditions required for the Waelzing process, calcining is performed under an oxidizing atmosphere. Crude Zinc Oxide received from the Palmerton Waelzing process or from the Chicago and/or the Rockwood operations, is conditioned with water for material handling purposes and conveyed to the kiln feed bin. Then the Crude Zinc Oxide is fed directly to the kiln without any reducing agent. Temperature profiles in the calcining kiln are also different from those employed for Waelzing. The temperature of cold charge rises as it proceeds downkiln towards the discharge-end burner, where the maximum temperatures are reached in the neighborhood of 1523K(1250^0 C). At

Table X. Composition (%) of Products from the Calcining Kiln [48]

Element	Zinc Calcine	Pb/Cd Concentrate
Zn	55-66	5-10
Pb	0.5-1.5	35-50
Cd	0.05-0.15	1.2
Fe	4-9	0.5-1.5
Cl	0.15	15-25

such high temperatures, the lead and cadmium are fumed as oxides, suphides, and halides. These materials condense in the exit gas stream and are collected in a fabric filter bag collector. This lead/cadmium concentrate is transferred and bagged for shipment in fully enclosed facilities. Zinc Calcine, the remaining solid phase, is discharged from the kiln to a water quench and further transferred via a drag conveyer and loader for shipment. Table X gives the typical composition for the Zinc Calcine and the Lead/Cadmium Concentrate.

1-2-2-1-3 OTHER ROTARY KILN PROCESSES

All rotary kiln processes for the treatment of EAF dusts are basically the same in terms of process physics and chemistry. However, some differences exist, such as feed preparation and Crude Zinc Oxide treatment. As discussed previously, burdened and mixed EAF dust feed is introduced directly into the Waelz kiln in America, while it is fed into the kiln in the form of pellets or briquettes in Europe and Japan [4,22]. Since no Imperial Smelting Furnace (ISF) plants exist in America, then most Crude Zinc Oxide is further treated in rotary kilns to generate Zinc Calcine, which is sold to an electrothermic zinc smelter. While in Europe, Crude Zinc Oxide from the Waelz processes is either sold to ISP smelters directly [4] or dehalogenated in a hydrometallurgical process before it is sold to ISP smelters in Japan [22]. Another example of a modification of the Waelz kiln process is the Inclined Rotary Reduction Process (IRRP) [49,52]. The major difference between the Waelz process and the IRRP is that the mixed oxide recovered in the bag filters is pelletized with high quality coal powder and binder, and then fed to a retort which is heated externally by kiln off-gases. Zinc, lead and cadmium are fumed in the retort and recovered as zinc alloy (containing less than 1.5 % Pb) and lead alloy (containing about 10 % Zn and 1 % Cd) in an ISP condenser. The balance of

zinc, lead and cadmium is recovered from the off-gas as a mixed oxide in a baghouse and is recycled to the retort. An oxy-gas (CH_4/O_2) burner is employed in the kiln in order to reduce the volume of off-gas.

1-2-2-2. HTMR-PLASMA PROCESS

These processes are shown in Table XI. Intensive efforts have been made on the development of plasma technologies for the treatment of electric arc furnace dusts. They have involved both pilot scale and commercial production processes [21,45,49,53-62,71-78]. However, the majority of these processes did not survive, due mainly to the problems which were encountered with the operation of the condensers. The high content of alkali and halide elements in the EAF dusts led to the formation of a dross, which reduced the efficiency of the condensers. The existence of copper and sulfur in the dust made the iron-rich slag unacceptable for direct reuse in steelmaking processes. Also the metallic zinc which was obtained was usually below Prime Western (PW) grade, and thus the processes were uneconomical. Furthermore, with the carry-over of slag forming materials and EAF dust into the off-gases as well as the evaporation of iron and/or iron oxides under the high operating temperatures (around 1873K/1600^0 C), hard zinc was inevitably formed, which also reduced the efficiency of the condensers. The Tetronics Plasma Process is an example of a process which expecienced some of these problems. It evolved into commercial use for a while, but eventually had to be abandoned. The ScanDust Process, on the contrary, is relatively elaborate and more complex, and attempted to solve the commonly encountered problems with plasma technology. These two processes will be discussed in more detail in the following paragraphs.

Table XI. Plasma Reduction Processes for EAF Dust

Process	Developer/Owner	Status	Location	Capacity (t/y)	Products	Ref.
Plasmadust	Scan Arc Plasa Technologies AB	Commercial (1984)	ScanDust AB (Landskrona, Sweden)	41,000	Crude zinc oxide Iron alloy, slag, fuel gas	53-55
Enviroplas Plasma Arc Process	Pyromet-Mintek	Pilot (1993)	Mintek (Randburg, SA)	2,000 kg/h	Zinc metal, crude lead condenser dross, iron alloy & slag	45,49
Hi-Plas Process	Davy International Ltd.	Pilot (1989)	Davy International (Stockton-on-Tees, UK)	400 kg/h	(as above)	56,57
Extended Plasma Arc Process	Ticron Ecological Corporation	Pilot (1987)	Ontario Research Foundation (now ORTECH) (Mississauga, ON)	500 kg/h	(as above)	58
IMS/Tetronics Plasma Furnace	International Mill Service, Inc./Tetronics Research and Development Co. Ltd.	Commercial (currently shut down)	Nucor-Yamato (Blytheville, AR)	14,000	Zinc metal (below PWG) Crude lead, Condenser dross, slag, iron alloy	59-62
(as above)	(as above)	(as above)	Florida Steel (Jackson, TN)	8,000	(as above)	(as above)
IBDR-ZIPP Process	Phillips Environmental Inc.	to be commercial 1997	Hamilton Canada	77,000	Pig iron, Zinc oxide Vetrified slag	21,45

The Tetronics Plasma Process was developed jointly by International Mill Service, Inc. and Tetronics Research and Development Co. Ltd. Two commercial plants (the plant at Jackson, TN and the plant at Blytheville, AR) were in operation in United States for a number of years, but both plants were shut down for various technical and/or economic reasons [59-62]. This process is no longer being offered for sale.

A schematic diagram of the Tetronics Plasma Process is shown in Figure 6 [61]. The cylindrical furnace is made of mild steel and lined with carbon-impregnated magnesia bricks. The sealed

furnace roof is cooled with water and is lined with a high-grade alumina castable refractory. The argon-stabilised plasma arc is transferred from the plasma torch to the furnace melt which is in electrical contact with the mild steel anodes in the furnace hearth.

In operation, the pre-blended EAF dust, reductant and flux materials were dried and introduced through feed ports in the roof, and as they descended through the furnace atmosphere they were heated and then rapidly dissolved in the melt. Metal oxides were selectively reduced carbothermically in the furnace slag, and the zinc, lead and cadmium present were volatilized, leaving an iron-rich slag for disposal.

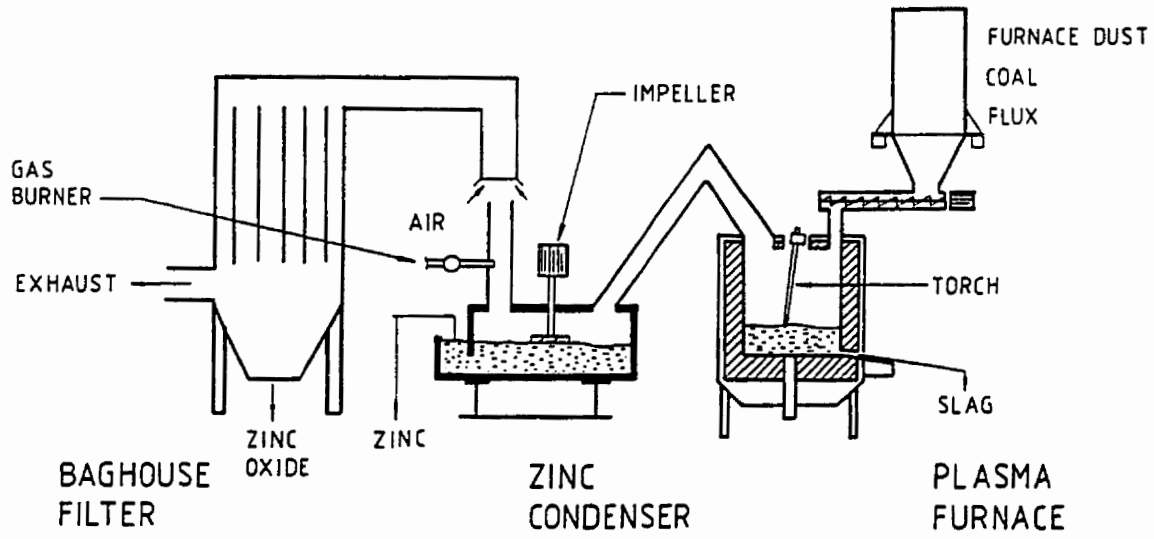

Figure 6. Schematic Diagram of Tetronics Plasma Process [61]

An Imperial Smelting Process (ISP) zinc splash condenser was used to recover the zinc, lead and cadmium from the gas mixture produced in the furnace. A mechanically rotated graphite impeller generated a spray of metal droplets of large surface area, to promote efficient condensation. The heat load in the condenser, produced by the exhaust gases and zinc condensation, was controlled by an immersed water cooling coil. All the metal vapors present were condensed by this mechanism, and the liquid in the condenser consisted of two layers, zinc and lead, with the cadmium partitioned between them.

The gases from the outlet of the condenser were burned in a combustion chamber with an excess of air being employed to cool the gas stream entering the baghouse to below the specified baghouse temperature rating. A proportion of the zinc rich baghouse fume may be recycled to the furnace to increase the zinc yield. The cleaned exhaust gases were vented to the atmosphere.

The Tetronics Plasma Process was simple, since the pelletizing or the agglomeration of the feed materials was not required. Flux materials were needed to make a high fluidity slag, which had a $CaO:SiO_2$ basicity ratio of 1.0-1.2. The temperature was maintained at 1773K(1500^0C) during the treatment process. The major problems of this process were as follows [59]:

(1) Condenser efficiency was only about 75% for zinc;

(2) Metals dispersion: dross (due to alkali and halide constituents present in the dusts), hard zinc (due to volatilization of iron and iron oxides), new baghouse dust;

(3) High operating temperatures: 1773-1873K (1500^0 C-1600^0 C).

(4) Zinc metal produced was below PWG. New dust contained 60 % zinc and other impurities.

Compared with the Tetronics Plasma Process, the Plasmadust Process developed by ScanArc Plasma Technologies AB was very elaborate in terms of process flowsheet and the requirement for the preparation of materials to be treated. This technology resulted in a commercial plant, which started operations in April 1984. Three MW plasma generators from SKF Steel were used. Figure 7 shows the ScanDust flowsheet [53-55].

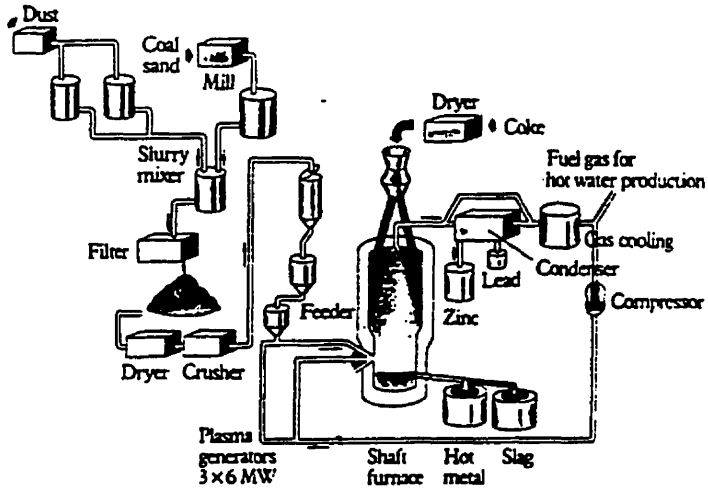

Figure 7 ScanDust Flowsheet [54]

The plant consisted of a material-handling system for dust, coal, coke and slag former, a shaft furnace, plasma generators, condensers for cooling and condensing zinc and lead, gas-cleaning units and tapping and casting equipment for zinc, lead, hot metal and slag.

As-received dust was mixed with water to form a slurry with a solids content of about 50 percent. The slurry was pumped to two slurry mixers, each with a volume of 400 m^3 (14,000 cu.ft.), which were fitted with agitators to ensure satisfactory homogenization.

The slurry was then pumped to a 40 m^3 (1,400 cu.ft.) mixing tank, to which coal and slag former were added. The mixture then contained 50 percent solids and 50 percent water. After homogenization, it was pumped to a mechanical filter press, where the water content was reduced from 50 percent to between 15 and 20 percent. The filter cakes were stored for an interim period, during which the water content was further reduced, and were subsequently dried and crushed to a maximum of 2 mm (0.08"). The drying unit used some of the excess process gas. The dried and crushed material was then stored in a silo from which it was fed into three transfer hoppers. The material was blown from the hoppers to injection feeders near the shaft furnace, from where it was injected into the shaft's reaction zone.

Coal and sand were ball milled to a grain size less than 0.1 mm (0.004") for 80 percent of the product. Then they were water mixed and the mixed slurry was pumped to a 30 m^3 (1,060 cu.ft.) slurry mixer for storage and was later added to the mixing tank in the correct quantities.

Commercial coke, with a grain size of 20 to 60 mm (0.8-2.4") was used. The coke was charged to a silo and was then dried and screened before being fed to a conveyer for transport to the top of the shaft furnace. Coke fines were returned to the ball mill. The coke was charged at the shaft furnace top via a gas-tight valve system.

The mixture of EAF dust, coal and slag former was fed via three tuyeres with a total capacity of 8-12 tonnes per hour. A 6 MW plasma generator was mounted in each tuyere.

The amount of hot metal produced varied from 200 to 600 kg (440-1,325 lbs.) per tonne of dust. The tapping temperature was approximately 1673K(1400^0 C). The hot metal was cast into pigs in a casting machine, and the liquid slag was tapped and cooled prior to disposal at a dump or delivery to a user. The amount of slag was 200 to 500 kg (440-1100 lbs.) per tonne of dust.

It was estimated that the furnace could be operated for 7,600 hours per year. Operating time was based on a 1-1.5 month round-the-clock operating cycle, before changing the feed material. The plant would be shut down for four weeks per year for maintenance. Plant availability was estimated at 95 percent.

The exit gas, a valuable form of energy, was cleaned and cooled after leaving the shaft. When smelting baghouse dust with a low zinc content, the exhaust gas contained approximately 75 percent carbon monoxide, 24 percent hydrogen and 1 percent nitrogen. The temperature of the exhaust gas from the shaft furnace was approximately 1473K(1200^0 C). The gas passed through a venturi scrubber, where it was cleaned, and the temperature fell to approximately 313K(40^0 C). The venturi water was first led to a thickener and a cooling tower, and was then recirculated. The thickener sludge was returned to the process.

For a dust with high zinc and lead levels, three condensers were employed. The temperature of the gas entering the condensers was approximately 1473K(1200^0 C). This gas had a zinc content between 4 and 20 percent. The exhaust gas from the condensers had a low zinc content and a temperature of 773-873K(500^0- 600^0 C). The gas then passed through the venturi scrubber and the exhaust ventilation system.

Zinc and lead, at a temperature of approximately 773K(500^0 C), flowed continuously from the condensers to a holding furnace. The amount of zinc normally contained in one tonne of dust varied from 200 to 400 kilograms (440-880 lbs.). Lead and zinc were cast into jumbo ingots or 25 kilogram (55 lbs.) slabs, according to customer requirements.

Some of the cleaned and cooled gas was recirculated as process gas after passing through a gas compressor. The excess gas was used as fuel for raw material drying, ladle preheating and a hot water boiler, connected to the local municipal district heating network. The hot water boiler also utilized energy in the cooling water from the shaft furnace, the plasma generators and the condensers. The annual quantity of thermal energy recovered amounts to approximately 65 GWh (220 billion Btu), which is equivalent to 6,500 m^3 (1.7 million gallons) of oil.

From 70,000 tonnes of dust, 9,000 tonnes of coal, 3,600 tonnes of coke and 6,000 tonnes of sand which were to be processed annually, a total materials input of almost 90,000 tonnes, the following quantities of metals would be recovered:

Recovered metals	Quantities (tonne)
Zinc	15,000
Lead	2,800
Hot metal	13,800
Alloyed hot metal	3,700

The zinc was of Prime Western Grade, permitting it to be registered and sold on the London Metal Exchange. In addition to the recovery of metals, ScanDust also generated 30,000 tonnes of slag which was used as filling material for construction projects, and generated an excess energy equivalent to 65 GWh (220 billion Btu) per year.

1-2-2-3 HTMR-OTHER PROCESSES

The use of other HTMR processes is quite limited, since they are mostly adapted from primary metal production processes, such as the Electrothermic Process [65], the Half-Shaft furnace process [66] and the Elkem Multi-Purpose EAF process [68]. These processes are shown in Table XII. As examples, the Electrothermic Process and the Half-Shaft furnace process would only be economic within certain regions, as the equipment and/or facilities were modified from those previously used for primary smelting. Although the Elkem Multi-Purpose EAF process was developed from the former Elkem sealed electric arc furnace process and eliminated a number of troublesome features which lead to abandonment of the initial Elkem process, its marketability is still unknown at this time [45]. In addition, all these processes share those problems which are common to the other HTMR processes, as discussed in Chapter 1, Section 2-2-2.

Some of these HTMR processes were particularly designed for the treatment of EAF dusts. Of these processes, the Flame Reactor Process, which was developed by Horsehead Resource Develpoment Company (HRD), is one example [48,63]. The Flame Reactor process is a patented flash smelting technology developed to meet a market demand for a small-scale, site-specific waste processing facility. It achieves processing results similar to Waelzing technology for zinc-bearing

feeds. However, its high specific throughput makes possible economic operation at the 10,000-50,000 tpy level, rather than the much higher feed rates needed for the Waelz kiln operation to be cost-effective [48].

Table XII. Other HTMR Processes for EAF Dust

Process	Developer/Owner	Status	Location	Capacity (t/y)	Products	Ref.
Flame Reactor	Horsehead Resource Development Co. (HRD)	Commercial (1988)	HRD (Monaca, PA)	20,000	Crude zinc oxide iron-rich slag	48,63
(as above)	(as above)	Commercial (1993)	North Star Steel (Beaumont, TX)	30,000	(as above)	(as above)
INMETCO Direct Reduction process	INMETCO	Commercial (1978)	INMETEO (Ellwood City, PA)	55,000	Crude zinc oxide alloy ingots slag	64
Electrothermic Process	Toho Zinc Co.	Commercial (1974)	Ryoho Recycle Co. (Japan)	42,000	Zinc oxide Slag	65
Half-Shaft Furnace Process	Mitsui M & S	Commercial	Mitsui M & S (Miike, Japan)	90,000	Crude zinc oxid slag	66
Ausmelt Process	Ausmelt Pty. Ltd.	Pilot (1993)	Ausmelt Technology Corp., (Denver, CO)	400 kg/h	(as above)	49
Shaft Induction Furnace	Sumitomo Heavy Industries, Ltd.	Pilot (1990)	Niihama Technical Research Lab. (Niihama, Japan)	100 kg/h	Zinc metal pig iron Slag	67
Elkem Multi-Purpose EAF	Elkem Technology	Commercial (currently shut down)	Laclede Steel (Alton, IL)	36,000	Zinc Metal (below PWG) crude lead, slag	68

Intensive work had been done on the development of the Flame Reactor technology since the 1980s by St. Joe Minerals Corp. and it was acquired by HRD in 1987 [48]. Since then, significant

resources have been invested in a successful burner development, process and equipment testing at commercial levels, and the important demonstration that the process reliably produces an environmentally safe IRM product. Development work on new materials and applications continues at HRD's 20,000 tpy Flame Reactor plant at Monaca, PA.

Figure 8 [48] shows a cutaway view of the Monaca Flame Reactor plant. This process has been thoroughly described in the technical literature [79-81], and consists of the following four basic steps:

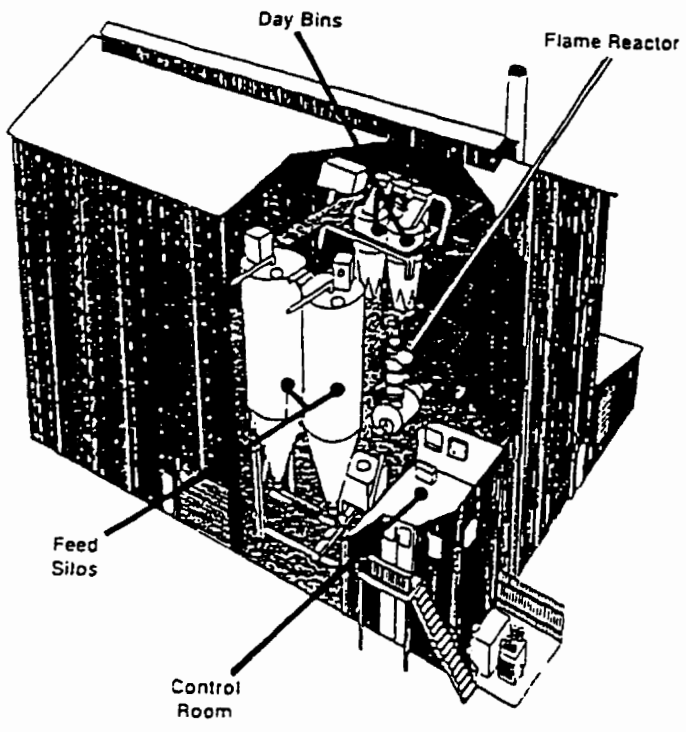

Figure 8. Flame Reactor Plant Cutaway [48]

- Natural gas (or solid carbon fuel) is intensively mixed and reacted with oxygen-enriched air under fuel-rich conditions at flame temperatures over 2473K(2200^{0}C), to produce a hot, reducing gas.

- Zinc-bearing feed (or other fine, dry solids) is injected into the hot gases in a second, larger water-cooled furnace downstream of the burner; refractory compounds fuse to form molten slag at the >1873K(1600^{0}C) temperatures in the particle-flame suspension.

- The molten slag is conveyed with the combustion gases through the reactor and flows down into a horizontal gas/liquid separator; the slag is recovered as IRM by continuous tapping, then crushed/sized and sold.

- The separator off-gases are post-combusted to reoxidize and condense metal oxides; the gases are then cooled before recovering the zinc, lead, and cadmium, along with halides, alkali metals and a small amount of dust/slag carryover report to the Crude Zinc Oxide product.

The Flame Reactor process has been operated at a commercial scale at Beaumont, TX since 1993. This process treats about 30,000 tonnes of EAF dust per year. Figures 9 and 10 show a schematic process flow diagram of this plant and the diagram of the Flame Reactor, respectively.

At the Beaumont Flame Reactor plant, EAF dust is received in bulk via trucks from either the baghouse holding bin or from outside suppliers, weighed, sampled and then pneumatically transferred to the process blending bins. Dust is discharged from the blending bins by metered feeders, to maintain feed mix composition within acceptable ranges, to a blending pipe and pneumatically conveyed to two dust feed bins above the reactor. The entire receiving, blending, and

transfer system is fully enclosed. Each feed bin has a dedicated feeder to provide a carefully controlled solids feed rate to the two reactor feed injection tubes. Feed bins are sized to be topped-up once per shift.

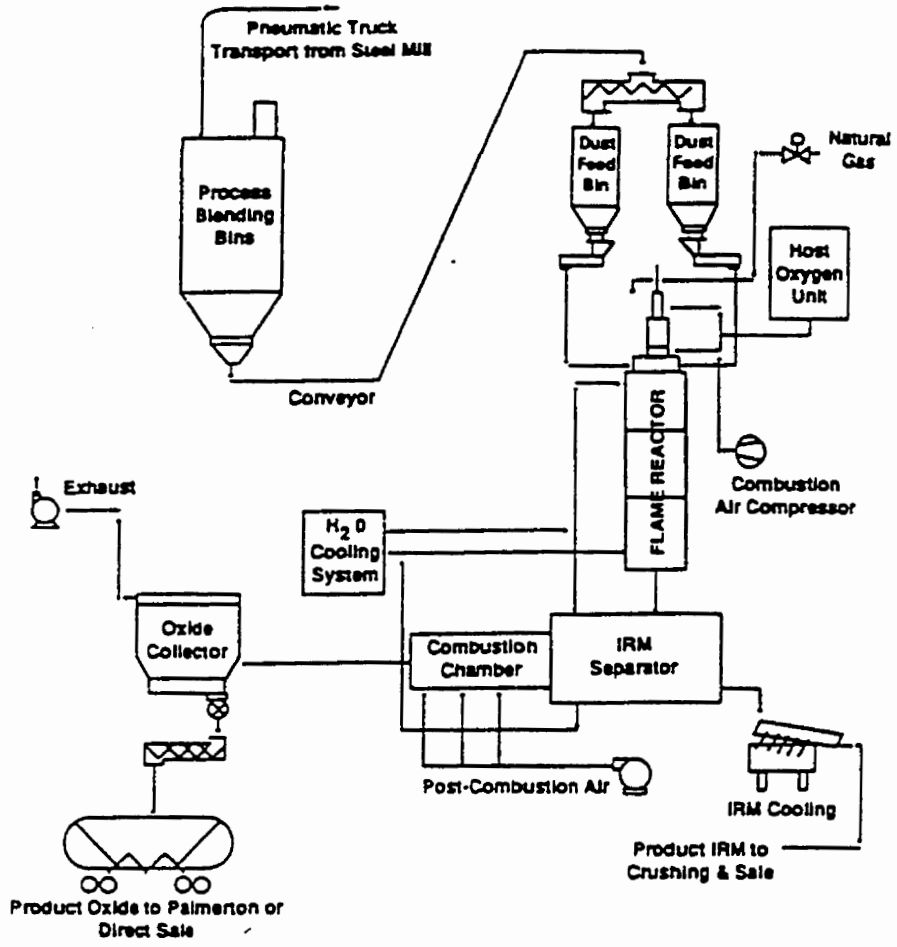

Figure 9. Beaumont Flame Reactor Plant Process Flow Diagram [48]

The Flame Reactor itself consists of two stages: the burner and the reaction shaft. The burner is situated on top of the reaction shaft, and receives natural gas and oxygen enriched air into its mixing section. A mixture of 90% O_2 and 10% air is required for the process. The feed injection system introduces solids radially at the top of the reaction shaft and portions of the burner are not refractory-lined, but they are water-cooled. During start-up ignition, preheat of the unit takes 15-20 minutes. The absence of refractories provides the rapid start-up and shut-down capability, a very

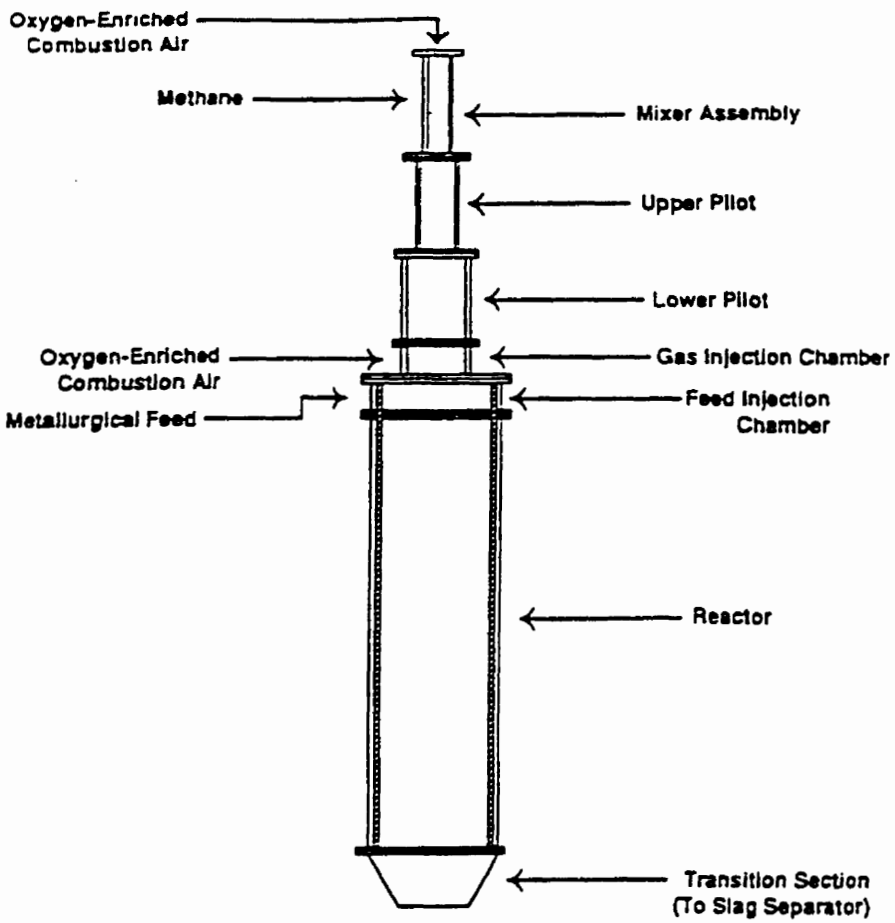

Figure 10. Flame Reactor [48]

practical advantage of the process over classical pyrometallurgical technologies. Once at temperature, dust feed is initiated and the flows are increased to full throughput. During operation, a layer of frozen slag coats the inside wall of the reactor shaft.

Dust reacts in the hot flame and the volatiles are removed, while the remaining materials fuse. Linear velocities of the downward gas-particle stream are controlled at 15-31 mps (50-100 fps). At the bottom of the reaction shaft, reactor gases are sampled and analyzed for CO/CO_2 ratio to maintain desired operating conditions. The Beaumont unit typically operates at 60-70% oxygen-enriched air, and a CO/CO_2 ratio of 0.2-0.4. The operating temperature is about 1923K(1650^0C) at the exit of the shaft. Pressure measurements at the bottom of the reaction shaft are used to control the baghouse fan damper to yield a slight suction at the slag discharge.

At the base of the reaction shaft, the gas-particle stream passes into a refractory-lined horizontal cyclone which effectively separates the molten slag from the gas stream. Slag is then tapped continuously at approximately 1473-1673K(1200-1400^0C), while the hot gas stream proceeds to a vertical, refractory-lined combustion chamber. The slag is cooled, sized if necessary, and sold as IRM product after undergoing the TCLP analysis. Enclosed IRM storage/handling facilities are provided. The gas is post-combusted to fully oxidize the metal vapors and incomplete combustion products. Excess combustion air and radiative losses also provide some gas cooling at this point.

Fully combusted off-gas is further cooled by dilution and radiant transfer to about 443K(170^0C) prior to entry to the product baghouse. The baghouse uses Goretex bags and is of the reverse-pulse type with an air:cloth ratio of about 3-4:1. Crude Zinc Oxide is discharged from the baghouse and delivered directly to rail cars for sale or shipment to Palmerton for calcining.

As desired, this process is aimed at economic operation on a small scale, on-site plant for EAF dust treatment [48]. To some degree, it is successful as is evidenced by the Beaumont Flame Reactor. Similar to most other HTMR processes, the Flame Reactor process produces an Iron-Rich Material (IRM), which meets EPA disposal requirements, but the Crude Zinc Oxide produced needs further treatment. The process requires fine, dry EAF dust and oxygen to react with coke or coal reductant and reportedly has very high operating costs. Thus, its widespread application could be limited.

1-2-3. HYDROMETALLURGICAL PROCESSES

The major impetus for the development of hydrometallurgical processes for the treatment of EAF dust is that, a small scale, on-site process could be economic, because of its low capital and operating costs as well as the recovery of the valuable metal containing products. Also, there may be some environmental benefits of hydrometallurgical processes in comparison to pyrometallurgical processes. Although today's commercial EAF dust treatment processes are predominantly pyrometallurgical, hydrometallurgical processes are gradually replacing these pyrometallurgical counterparts for the treatment of EAF dust. Table XIII shows the hydrometallurgical processes which now have been developed either commercially or to a pilot plant scale. These processes are to be discussed according to the information which is available in the literature. Some other experimental and bench scale research activities will also be discussed later.

Table XIII. Hydrometallurgical Processes for the Treatment of EAF Dust

PROCESS	DEVELOPER	STATUS	LOCATION	CAPACITY	PRODUCT	REF.
MRT Process	Metals Recycling Technologies Corp. (MRT)	Commissioning (1995)	Nucor Steel (Darlington, SC)		Zinc Oxide (99.9%) Lead/Cadmium Iron	45
EZINEX Process	Engitec Impianti	Commissioning (1996)	Ferriere Nord (Osoppo, Italy)	10,000 t/y	Zinc Cathodes Cement Lead Iron Oxide Cake	45,82
Modified ZINCEX Process	Tecnicas Reunidas S.A.	Pilot	(Bilbao, Spain)		Zinc Cathodes Cement Cadmium Salable Lead Disposable Residue	45, 83
Cashman Process	American Metals Recovery Corp.	Pilot	(U.S.A.)		Zinc Oxide Cadmium and Lead Iron Oxide/Iron	45
Cebedeau Process	Cebedeau Research Center/U. of Liege/ SERH	Commisioning (1986) Now Shut Down	(Saint Florentin, France)	12,000t/y	Zinc Powder Lead Cement Iron Oxide Cake	85-88
Cardiff Process	U. of Wales College of Cardiff	Pilot (1979-1983)	(Cardiff, Wales)		Zinc Powder Lead Cement Iron Oxide Cake	89

1-2-3-1. COMMERCIAL AND PILOT HYDROMETALLURGICAL PROCESSES

1-2-3-1-1. MRT PROCESS [45]

The MRT process is the first commercial-use hydrometallurgical process for the treatment of EAF dust in North America. In 1995, MRT started operating a plant at Nucor Corporation's minimill in

Darlington, South Carolina on a contract basis. Dust is leached with hot ammonium chloride to dissolve most of the zinc, lead and cadmium oxides in the dust. Leach slurry is filtered and the unleached iron oxide, containing zinc ferrite, is filtered, washed, and recycled to the steel mill or stockpiled. Leach solution is treated with zinc dust to precipitate the dissolved lead and cadmium as cement which is further separated into metallic lead and cadmium which can be sold. Clean solution passes to a crystalliser where high purity zinc oxide crystals are produced for sale. Ammonium chloride solution is concentrated and recycled to the leach process.

The plant has been operating reasonably since the start-up problems were corrected. Improvements have been made and patented to increase zinc recovery and produce a value-added metallised iron product for recycle or sale using a pyrometallurgical rotary hearth pre-reduction step prior to leaching. A 30,000t/y plant, incorporating these improvements, is under construction at Ameristeel in Jackson, Tennessee. A third plant is also being developed in the United States.

According to Burrows [90], the chemistry of this process is shown in Table XIV.

Table XIV. Chemistry for MRT Process [90]

$ZnO + 2NH_4Cl \rightarrow Zn(NH_3)_2Cl_2 + H_2O$
$Pb(NH_3)_2Cl_2 + Zn \rightarrow Zn(NH_3)_2Cl_2 + Pb$
$Cd(NH_3)_2Cl_2 + Zn \rightarrow Zn(NH_3)_2Cl_2 + Cd$
$Zn(NH_3)_2Cl_2 + H_2O \rightarrow 2NH_4Cl + ZnO$

1-2-3-1-2. EZINEX PROCESS [45,82]

A 10,000t/y EAF dust plant was constructed at Ferriere Nord in Osoppo, Italy and was commissioned in early 1996. This plant was reported to be operating in a satisfactory manner. Worldwide opportunities to marketing this process are being sought. In this process, dust is leached in ammonium chloride solution to solubilize the zinc, lead and cadmium oxides. Leach solution is filtered and treated with zinc powder to cement the lead and cadmium which can be sold. Unlike the MRT process in which the zinc is recovered as zinc oxide by crystallizing the cemented solution, zinc is electrowon from the purified solution in the EZINEX process. The spent electrolyte is recycled to the leaching stage. The iron-rich, zinc ferrite containing leach residue is dried, pelletised with coal, and recycled to the EAF. No other by-products are produced which require further disposal. A mixed NaCl-KCl salt is recovered by crystallisation and can be sold as a flux.

1-2-3-1-3. MODIFIED ZINCEX PROCESS [45,83]

The Modified Zincex process was developed from the original Zincex process. This process consists of atmospheric leaching, solvent extraction and conventional electrowinning, to produce 99.99% purity zinc cathodes or zinc ingots. Pilot plant testing and the engineering design of a 80,000t/y dust treatment plant have been completed. However, approval of this plant has been deferred.

Figures 11 and 12 show the process flowsheet. In this process, the zinc and cadmium oxides are dissolved in a dilute sufuric acid solution under atmosphere. Leached liquor is purified by precipitation to remove aluminium and iron prior to introducing it to the solvent extraction process. Zinc is extracted selectively from the pregnant liquor by a liquid cationic exchanger (D_2EHPA). Impurities such as cadmium, chlorine, fluorine, and magnesium remain in the aqueous phase. A

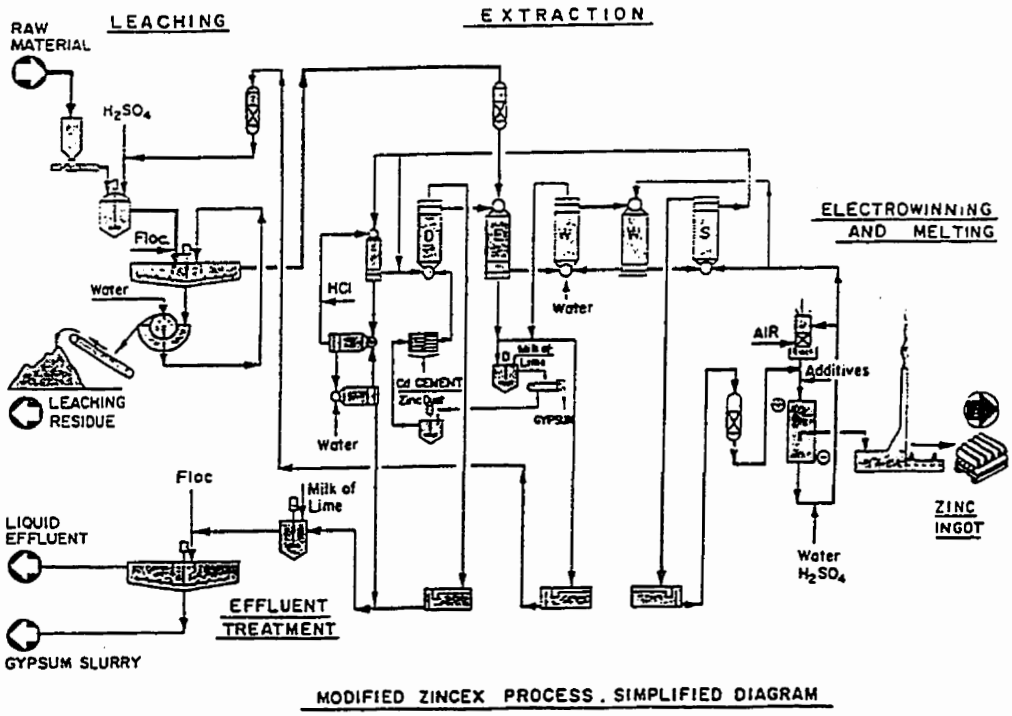

Figure 11. Modified Zincex Process Flowsheet [83]

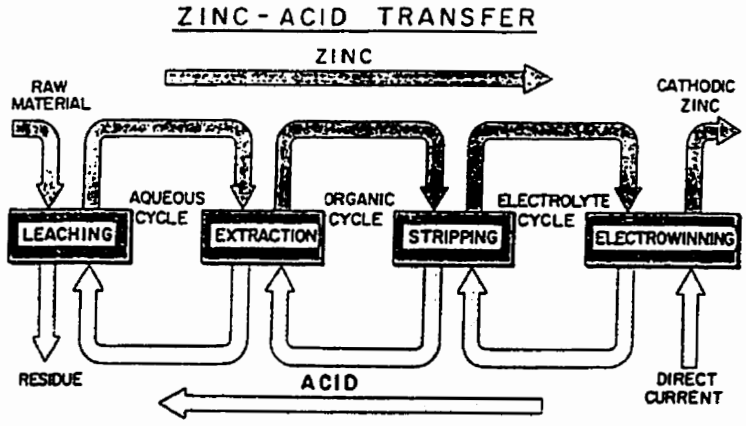

Figure 12. Conceptual Process Diagram for the Modified Zincex Process [83]

small fraction of this aqueous phase is bled-off in order to remove the above-mentioned impurities, while most of this aqueous solution is recycled back to the leaching step. Stripping of the zinc from the organic phase back to the aqueous phase is achieved by increasing the acidity of the zinc spent electrolyte. In this step, a loaded high purity electrolyte and an organic raffinate are produced. The organic raffinate is returned back to the previous extraction step. Finally, zinc is electrowon on aluminium cathodes from the loaded electrolyte.

Table XV. Results from the Pilot Plant Test [83]

Zinc Leaching Yield	70-91 *	Gypsum (kg)	100-80
Zinc Solvent-Extraction Recovery	>99	Iron Residue (kg)	300-210
Current Efficiency at 4.2 A/dm^2	93	Liquid Effluent (m^3)	3.1-2.0
Global Zinc Recovery	67-90 *		
Zinc Metal Quality	SHG (99.99)	H_2SO_4 (kg)	0.8-1.7
Wastes (ecological risk)	Nil	$Ca(OH)_2$ (kg)	0.6-0.7
		NaOH (kg)	0.02-0.03
Leaching Residue (kg)	420-700	Electric Power (KWh) (DC)	2.9
		Process Water (L)	11-15

* Depending on the zinc ferrite in the feed.

The major reactions which occur in this process are as follows:

Leaching: $ZnO + 2H^+ = Zn^{2+} + H_2O$

Solvent extraction: $2RH + Zn^{2+} = R_2Zn + 2H^+$

Stripping: $R_2Zn + 2H^- = 2RH + Zn^{2+}$

Electrowinning: $Zn^{2+} + H_2O = Zn + 2H^- + 1/2O_2$

Some results from the pilot plant test are summarized in Table XV [83]

Although great efforts have been made to increase the zinc recovery, the yield of zinc is still low, and depends on the amount of zinc ferrite in the EAF dust. The iron residue contains most of the lead which was present in the EAFD; thus further treatment to remove lead is needed. The gypsum produced in the purification process, in most cases, is a waste, which, like other waste effluents, requires careful treatment before it is released into the environment.

1-2-3-1-4. CASHMAN PROCESS [45]

This process was originally used for the treatment of arsenic-bearing ores and copper smelter dusts, and then was adapted for the treatment of EAFD by American Metals Recovery Corp. Laboratory and small scale pilot plant tests were conducted.

In this process, zinc, which is not in the zinc ferrite, along with lead and cadmium in the EAFD are pressure leached in a calcium chloride solution. The leached solution is purified by precipitation using zinc dust in order to remove the lead and cadmium. The cemented lead and cadmium mixture is separated and treated to produce metallic lead and cadmium using conventional procedures. High purity zinc oxide is precipitated from the purified solution. The leach residue is treated in order to recover residual zinc and to produce an iron-rich residue which is suitable for recycle or disposal in a landfill.

This process employs pressure leaching, but the zinc recovery is not very high. Although the leachant is comparatively cheap, there can be some corrosion problems.

1-2-3-1-5. CAUSTIC LEACH PROCESS [85-89]

The chemistry of the caustic leach process can be described by the following reactions:

Leaching reactions: $ZnO + 2NaOH = Na_2ZnO_2 + H_2O$; $PbO + 2NaOH = Na_2PbO_2 + H_2O$

$$SiO_2 + 2NaOH = Na_2SiO_3 + H_2O$$

Clarification reaction: $Na_2SiO_3 + Ca(OH)_2 = CaSiO_3 + 2NaOH$

Cementation reaction: $Zn\downarrow + PbO_2^{2+} = Pb\downarrow + ZnO_2^{2-}$

Electrolysis reactions: in cathode: $ZnO_2^{2-} + 2H_2O + 2e^- = Zn\downarrow + 4OH^-$

in anode: $2OH^- = 1/2\ O_2 + H_2O + 2e^-$

overall: $ZnO_2^{2-} + H_2O = Zn\downarrow + 1/2\ O_2 + 2OH^-$

Two examples of the caustic leach process are the Cebedeau Process and the Cardiff Process which are described in more detail below.

Cebedeau Process [85-88]

The Cebedeau process was developed into a commercial process in France in 1986 [85]. However, this plant was shut down later for some unspecified reasons [87]. The process flowsheet for this plant is shown in Figure 13 [88].

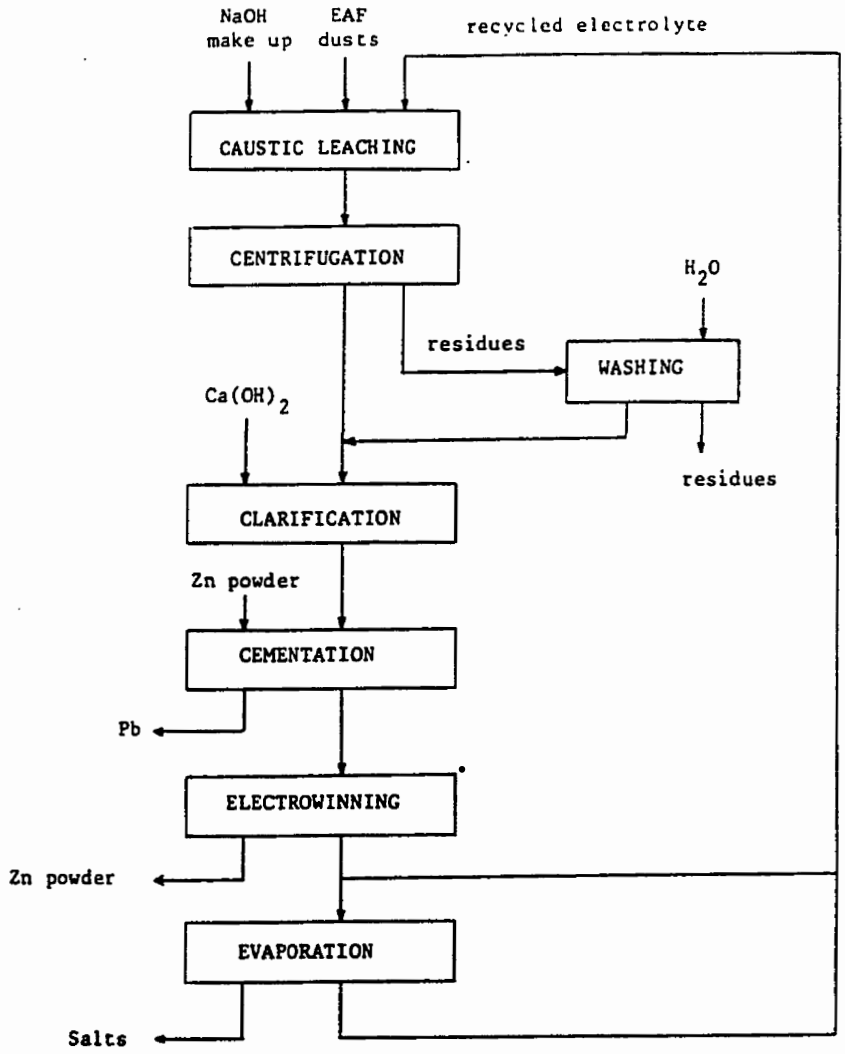

Figure 13. Simplified Flowsheet of the S. E. R. H. Plant [88]

In this process, EAFD is leached in hot concentrated sodium hydroxide solution (368K/95^{0}C, 6-12 M). Zinc, lead and cadmium oxides are dissolved in this step, leaving most of the iron in the leach

residue. The recovery of zinc is mainly dependent on the amount of zinc which is present in the zinc ferrite, since this portion of zinc is not solubilized. For the EAFD tested with the Cebedeau process, 65 to 85% of the zinc and 70-85% of the lead were recovered.

Centrifugation is employed to separate the leached solution, which is precipitated in a thickener with starch (1 kg/t) as flocculant. After washing with water, the residue is ready for disposal.

Clarification, if necessary, is achieved by adding calcium hydroxide to the solution. In this step, a clean solution and a small amount of calcium silicate are produced.

The clarified solution is directed to the cementation step, in which lead is precipitated using zinc powder at about 1.5-2 times the stoichiometric requirement. Lead cement, which contains unreacted zinc, other co-precipitated metals such as cadmium and copper, could be sold as a raw material to a lead smelter, or processed to value-added metallic products by using conventional methods.

The lead-free, purified solution is electrolyzed in order to produce high quality zinc powder for market. A current density of about 250 to 375 A/m^2 and a potential of around 3.2 V are employed in the electrolysis step. During electrolysis, a small amount of sodium stannate (0.24 g/l) is added to increase the current efficiency by about 6-7%. Most of the spent electrolyte is recirculated back to the leaching step, while a portion of the electrolyte is bled off and the saleable halide salts are separated by evaporation.

Cardiff Process [89]

Over the period of 1979-1983, a pilot facility for the treatment of EAFD was operated in Cardiff.

Later, outside the college of Cardiff, a larger scale pilot plant was tested in order to solve some problems relating to the engineering of a full scale plant.

As shown in Figures 14 and 15[89], this process is essentially similar to the Cebedeau process. However, unlike the Cebedeau process which utilized centrifugal filtration to achieve solid-liquid separation, the Cardiff process employed a magnetic separator. The researchers found that the settling of the solids after the leaching step was very slow and could take many days. Centrifugal separation was disappointing, while chemical flocculants and conventional filters were unsuccessful. Another distinctive difference from the Cebedeau process was that the Cardiff process employed a reduction roasting process to break down the zinc ferrite which was present in the leach residue. Thus, metal recoveries by the Cardiff process were claimed to be over 80 and 90%, respectively for zinc and lead.

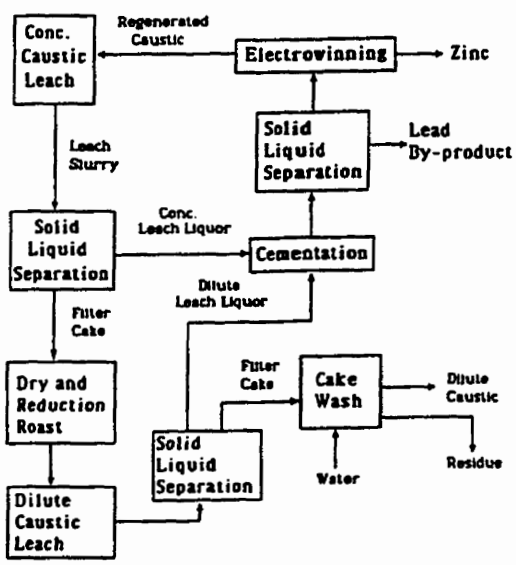

Figure 14. Cardiff Process Flowsheet [89]

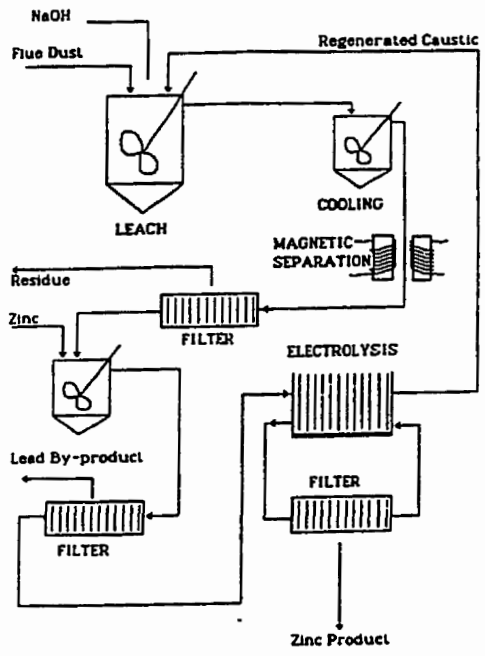

Figure 15. Pilot Plant Layout for Treatment of EAF Dust by the Cardiff Process[89]

1-2-3-2. OTHER HYDROMETALLURGICAL PROCESSES

1-2-3-2-1. SULFURIC ACID LEACH PROCESSES

As early as 1981, some exploratory work on the sulfuric acid leaching of EAFD was performed at Warren Spring Laboratory in the U. K. [91]. The main findings of this work were that about 85 to 90% of the zinc could be extracted by sulfuric acid at pH 2 and 80% at pH 3 to 4. The major problems reported were filtering and a high iron concentration in the solution (20 to 22 g/l).

Later, AMAX Extractive Research & Development, Inc. proposed an acid leach process [15], which is based on some results conducted on the leaching of laterite ores with sulfuric acid [92].

These results showed that iron can be rejected from sulfate solutions as hematite at higher temperatures. In Japan, the Iijima Refinery of the Akita Zinc Company employs an autoclave process on a zinc-iron sulfate solution to precipitate iron as hematite [93].

The AMAX two stage sulfuric acid leach process is shown in Figure 16 [15]. In the first stage, EAFD is leached with mild sulfuric acid solution at atmospheric pressure below the boiling point.

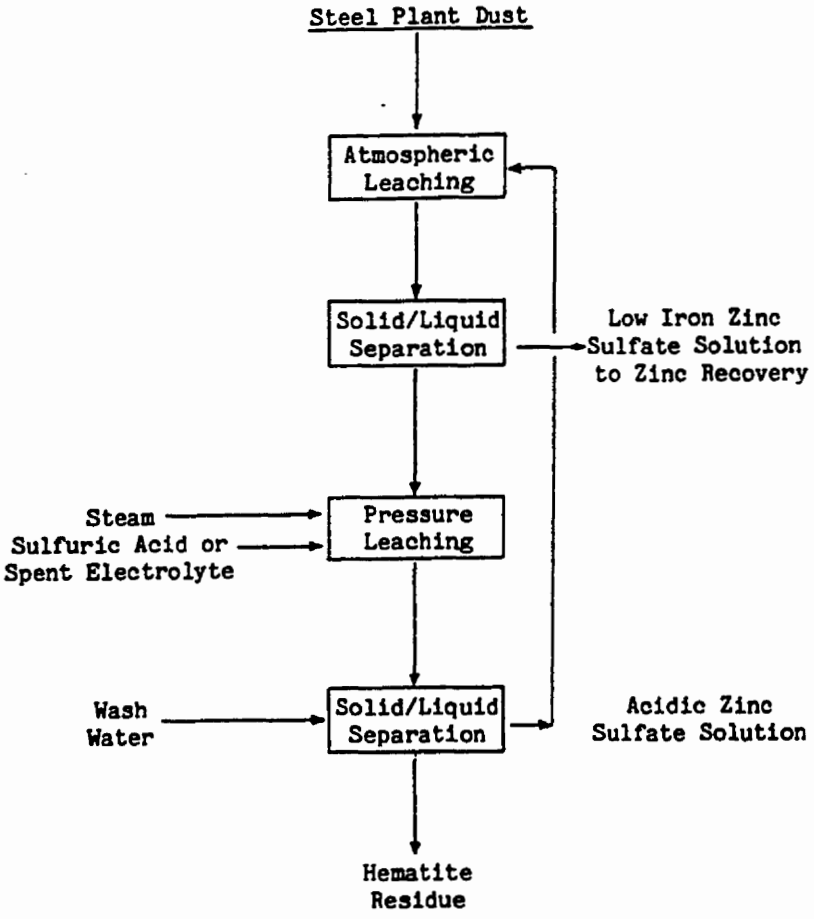

Figure 16. Conceptual Flowsheet of a Two-Stage Leaching Process for Steel Plant Dust [15].

The leachate, a low-iron, high-pH zinc sulfate solution, is sent to purification and then the zinc is recovered. The solids are pressure leached in an autoclave to completely dissolve the residual zinc, leaving iron as an easy-settling hematite residue. After solid-liquid separation, the solids are washed to recover zinc sulfate, while the solution goes to the first-stage leach step. The washed residue can be recycled back to the steel plant or it can be further treated. Caustic or brine can be used to leach any lead present in the residue. The solids can be pelletized and recycled to the steel plant. AMAX had filed patent applications for these processes.

The chemistry for this process could be expressed as follows [94]:

Atmospheric leaching (pH 2.5-3.5, 343K/70^{0}C): $ZnO + H_2SO_4 = ZnSO_4 + H_2O$

$$PbO + H_2SO_4 = PbSO_4 + H_2O$$

$$Fe^{3+} + 2H_2O = FeOOH + 3H^+$$

Pressure leaching (pH 1-1.5, 473-543K/200-270^{0}C): $ZnFe_2O_4 + H_2SO_4 = ZnSO_4 + H_2O + Fe_2O_3$

Recently, Cruells and Nunez [28] conducted a bench scale study on the leaching of EAF dust using sulfuric acid solution. They also did an extensive study on the characterization of the dust. Under the following optimum leaching conditions: 1 M H_2SO_4, a solid/liquid ratio 1:10, a leaching time 3 hours, at room temperature and a stirring speed 1000 min^{-1}, they obtained 80% zinc recovery from the non-magnetic portion of EAFD and 40% of iron dissolved in the acid solution. Lead was not leached and was retained in the residue, while the iron was easily solubilized as shown in Figure 17 [28].

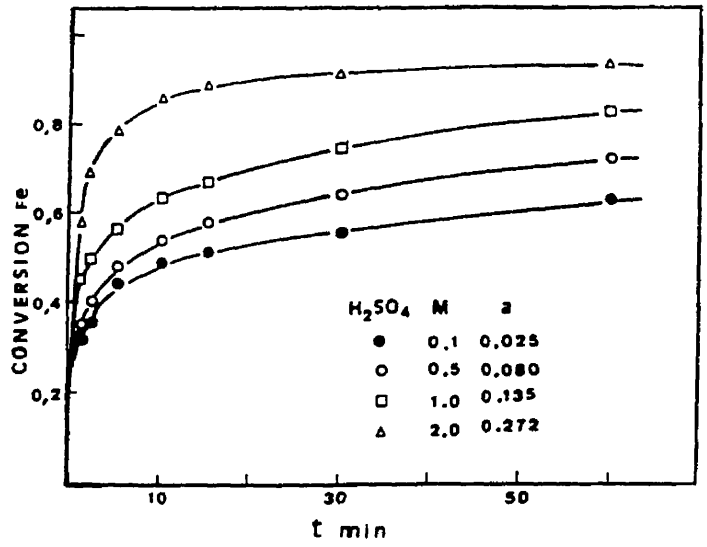

Figure 17. Effect of Sulfuric Acid Activity on Fe Conversion [28]

1-2-3-2-2. THE UBC-CHAPARRAL PROCESS

The aim of this process, in a similar manner to the other processses, was to recover the metal values and to produce a non-toxic residue from EAFD. However, great care has to be taken to ensure that the process residue will meet the more stringent environmental regulations in the future. The process is very elaborate, as shown in Figure 18 [11].

The process consists of the following steps [11]: i). selectively remove chlorides by water wash; ii). selectively remove calcium in an acetate lixiviant; iii). selectively leach zinc in an ammoniacal solution; iv). clean up the solids to render the dust residue non-toxic; v). precipitate final products in a high purity and in a saleable form.

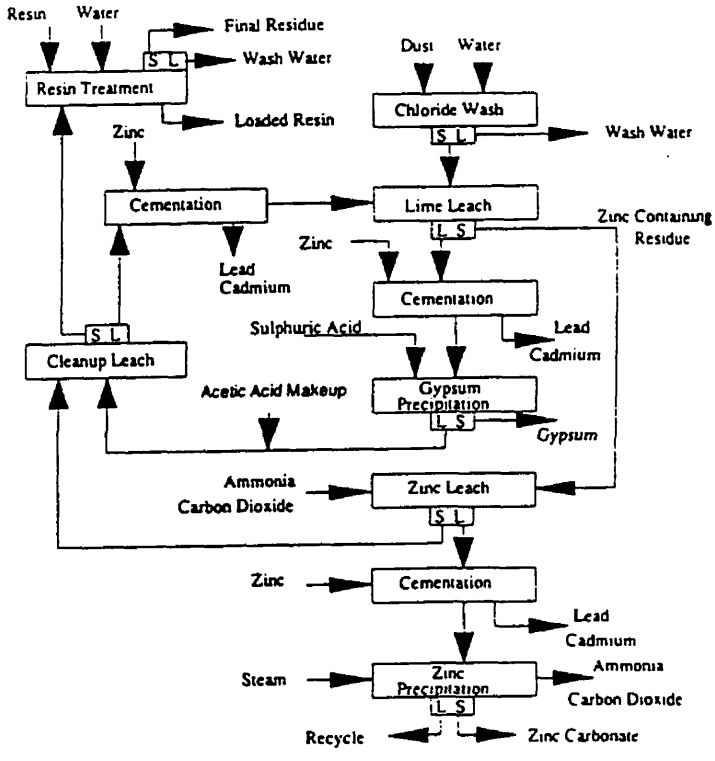

Figure 18. General Flowsheet of UBC-Chaparral Process [11]

Some chemical reactions which are involved in this process are as follows:

Calcium leach (pH 7-8, boiling point): $2HAc + CaO = CaAc_2 + H_2O$, where $Ac=CH_3COO$ radical

$$ZnAc_2 + CaO = CaAc_2 + ZnO$$

Zinc leach: $ZnCO_3 + 4NH_3 = Zn(NH_3)_4^{2+} + CO_3^{2-}$

$$ZnO + 2NH^{4+} + 2NH_3 = Zn(NH_3)_4^{2+} + H_2O$$

Solids clean up: $CaCO_3 + 2HAc = CaAc_2 + CO_2 + H_2O$

$PbCO_3 + 2HAc = PbAc_2 + CO_2 + H_2O$

Zinc precipitation: $Zn(NH_3)_4CO_3 + yH_2O = xZnCO_3 \cdot yZn(OH)2 + 4NH_3 + CO_2$

Entrained metals in the final residue are removed by a cation exchange resin. The mixed zinc carbonate-hydroxide is suitable for introducing into a conventional zinc plant circuit, or it could be sold as a chemical. Other byproducts, such as lead and calcium sulfate are also said to be suitable for market. The final residue meets the present toxicity standards.

Metal recoveries are of the order of 60% for zinc and lead, 85% for cadmium, and 100% for calcium for the treatment of EAFD which contains 20.5%Zn, 4.0%Pb, 0.18%Cd and 12.5%Ca.

1-2-3-2-3. HATCH ACETIC ACID LEACH PROCESS

This process was developed by Hatch Associates on the basis of the UBC-Chaparral process [95], and thus the two processes have many similarities. The Hatch process is a simplified UBC-Chaparral process. Most of the heavy metals are recovered in one step, which consists of a strong acetic acid leaching stage, while the iron rich residue which contains insoluble zinc ferrite, is recycled back to the steelmaking process. The heavy metals in solution, such as zinc, lead, copper and cadmium, are precipitated as a bulk sulfide product for delivery to a zinc plant. The acetic acid is regenerated by the ion exchange treatment of the acetic solution to remove calcium and magnesium and the concentration is adjusted before returning it to the leaching process. Figure 19 shows this process [95].

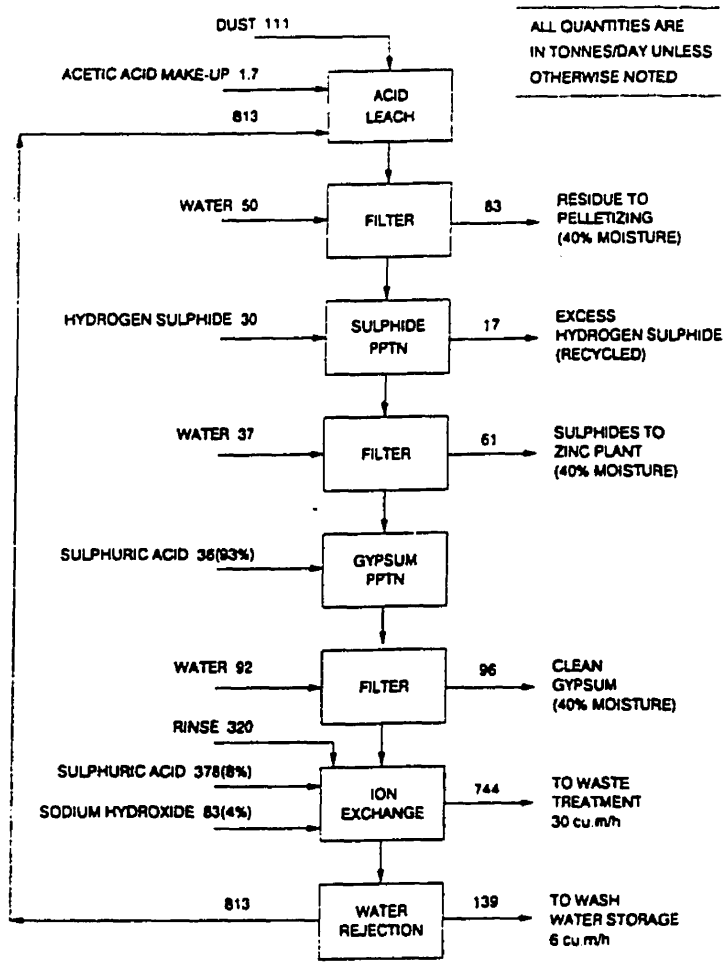

Figure 19. Acetic Acid Leach Process [95]

Metal extractions for both leaching and precipitation are shown in Tables XVI and XVII, respectively [95]. The leaching conditions were: solids concentration 150 g/l, 3 M acetic acid, residence time 30 minutes.

Table XVI. Summary of Metal Extractions During Acid Leaching of Water-Leached Dust [95]

Element	Feed (wt.%) (water-leached dust)	Extraction (%)	Element	Feed (wt.%) (water-leached dust)	Extraction (%)
Zn	17.33	70.5	Fe	23.07	13.5
Pb	2.09	76.3	Cd	0.083	85.2
Cu	0.24	46.6	Ni	0.029	18.2
Mn	2.49	16.8	Ca	13.73	92.9
Mg	3.58	76.4	Na	0.12	83.0
K	0.033	83.6			

Table XVII. Summary of Metal Extractions by Precipitation with Hydrogen Sulphide [95]

Element	Concentration in head liquor (g/l)	Extraction %	Element	Concentration in head liquor (g/l)	Extraction %
Zn	14.4	99.96	Fe	3.06	99.47
Pb	1.88	99.85	Cd	0.1	99.90
Cu	0.135	99.69	Mn	0.49	22.35
Mg	3.04	16.70	Ca	16.5	15.35
Ca	15.6	15.35	Al	0.102	27.28
SiO_2	0.369	63.31			

1-2-3-2-4. THE VERSATIC ACID LEACH PROCESS

The major feature of this process is that the leachant itself also serves as the extractant[96]. Thus, in the same operation, leaching and solvent extraction take place according to the following equations:

$$ZnO + 2HR_{org} = ZnR_{2_{org}} + H_2O$$

$$ZnO + HR_{org} = ZnOHR_{org}$$

Where HR represents the extractant or leaching reagent and org the organic phase. The versatic acid is a mixture of tertiary monocarboxylic acids with the simplified formula $R_1R_2C_2H_3COOH$, where R_1 and R_2 are alkyls with 3 or 4 carbon atoms. In leaching applications, versatic acid is dissolved to 30 vol % in a paraffinic fraction, such as kerosene.

Zinc is recovered from the organic phase by stripping with sulfuric acid.

$$ZnR_{2_{org}} + H_2SO_{4\ aq} = ZnSO_{4\ aq} + 2HR_{org}$$

This reaction generates leachant, which is returned to the previous leaching step. Zinc is finally recovered by electrolysis.

$$ZnSO_4 + H_2O = ZnO + H_2SO_4 + 1/2O_2$$

The leach residue contains most of the lead present in the dust and also the zinc which was present in the ferrite. Thus, the residue needs further treatment.

1-2-3-2-5. THE CHLORIDE LEACH PROCESS [97]

This process uses dilute hydrochloric acid as leachant. The leaching reactions which occur at pH below 1 are as follows:

$$ZnFe_2O_4 + 2HCl = ZnCl_2 + Fe_2O_3 + H_2O$$

$$ZnO + 2HCl = ZnCl_2 + H_2O$$

$$PbO + 2HCl = PbCl_2 + H_2O$$

By increasing the pH to 2-4, dissolved iron and lead are precipitated according to the following reactions:

$$Cl_2 + 2FeCl_2 + H_2O = 2FeOOH + 6HCl$$

$$PbCl_2 \text{ (high temp)} = PbCl_2 \downarrow \text{(low temp)}$$

Zinc is recovered from the solution by solvent extraction, using alkylphosphoric or alkyphosphonic acid as extractants for zinc. Finally, zinc is electrowon as follows:

$$ZnCl_2 = Zn^\circ + Cl_2$$

The process can produce cathode zinc, but the residue needs further treatment for detoxification. Also, goethite needs to be washed in brine to eliminate any co-precipitated lead chloride.

1-2-3-2-6. THE CHLORIDE-SULPHATE PROCESS [98]

In this process, EAFD is leached with hydrochloric and sulfuric acids at pH between 1 and 4:

$$ZnO + 2HCl = ZnCl_2 + H_2O$$

$$PbO + H_2SO_4 = PbSO_4 + H_2O$$

$$CaCO_3 + H_2SO_4 = CaSO_4 + H_2O + CO_2$$

$$CaO + H_2SO_4 = CaSO_4 + H_2O$$

$$ZnFe_2O_4 + 2HCl = ZnCl_2 + Fe_2O_3 + H_2O$$

The residue from the first leaching step is leached again using sodium hydroxide as the leachant:

$$PbSO_4 + 4NaOH = Na_2PbO_2 + Na_2SO_4 + 2H_2O$$

$$CaSO_4 + 2NaOH = CaO + Na_2SO_4 + 2H_2O$$

Dissolved iron and aluminum are removed by precipitation at elevated pHs:

$$Fe^{3+} + 2H_2O = FeOOH + 3H^+$$

$$Al^{3+} + 3H_2O = Al_2O_3 + 6H^+$$

Solvent extraction is employed to recover the zinc from the pregnant solution using phosphoric and phosphonic acids and zinc is then electrowon. The residue needs to be detoxified to remove lead and cadmium before being discharged.

1-2-3-2-7. AMMONIUM CARBONATE PROCESSES

One proposed process is based on the reaction in which EAFD is leached with ammonia and carbon dioxide [99]. This reaction is as follows:

$$ZnO + 2NH^{4+} + 2NH_3 = Zn(NH_3)_4^{2+} + H_2O$$

Zinc is finally recovered as zinc ammonium carbonate in the purified solution:

$$Zn(NH_3)_4CO_3 + yH_2O = xZnCO_3 \cdot yZn(OH)2 + 4NH_3 + CO_2$$

Impurities such as lead, cadmium and copper are recovered using cementation by precipitation with zinc powder. The final residue contains zinc ferrite and lead, and thus, needs post-treatment.

Another process called CENIM-LNETI [100], is similar, in principle, to the above process. However, instead of ammonia and carbon dioxide, ammonium carbonate is used as a lixiviant in this process. Another difference is that the solvent extraction step is incorporated into the process to enhance the efficiency of solution purification. Thus, zinc can be recovered as high-quality electrolytic zinc. The third variation of the process is that the zinc can be recovered as high-purity zinc oxide (>99.9%) [101], which is produced by precipitating zinc carbonate from the leach solution followed by calcining at 1273K(1000^0C).

1-2-3-2-8. LEACHING OF EAF DUST IN VARIOUS MEDIA

Recently, Caravaca, et al have completed some research on the leachability of EAF dust in different leaching reagents [102]. Their results are shown in Tables XVIII-XX [102]. Generally, the zinc recovery is enhanced in acidic media compared to that obtained in alkaline media. However, a relatively clean and iron free leach solution can be achieved by alkaline leaching, which avoids the very complicated iron removal process for most acid leach processes. Except for the case of leaching in very strong acid, zinc ferrite is insoluble and thus the zinc recovery is usually low.

Table XVIII. Leaching with NaOH Solution [102]

Leaching Reagent	L/S Ratio	Temp. K/°C	Time min.	% Leached Zn	Cu	Fe	Pb	Cd
NaOH 5M	10	298/25	120	32.2	0.5	0.02	23.6	3.3
			240	41.6	1.0	0.02	49.1	5.6
	20	298/25	120	47.4	1.0	0.05	29.3	8.9
NaOH 5M	10	298/25	120	32.2	0.48	0.02	23.6	3.3
			240	41.6	1.0	0.02	49.1	5.6
		323/50	120	52.5	1.9	0.04	39.6	8.9
			240	50.0	7.1	0.08	6.4	13.3
		373/100	120	58.8	1.4	n.a.	51.1	6.7
			240	54.6	3.3	n.a.	65.0	8.9

Table XIX. Leaching with Acidic Reagents [102]

Leaching Reagent	L/S Ratio	Time min.	% Leached Zn	Cu	Fe	Pb	Cd	Note
H_2SO_4 5M	10	120	71.7	66.7	14.9	—	88.9	In all cases initial
		240	71.7	66.7	25.0	—	91.1	temperature was 25°C,
	20	120	79.4	71.4	15.7	—	95.6	but the reaction is
		240	80.4	71.4	15.7	—	97.8	exothermic and
HCl 5M	10	120	74.7	80.9	41.5	42.2	95.6	increases the
		240	76.3	83.3	41.5	42.2	95.6	temperature until
	20	120	94.8	95.2	31.5	100	100	60°C-70°C. The
		240	97.6	95.4	27.0	100	100	systems were allowed
HNO_3 5M	10	120	70.6	69.1	14.5	100	94.4	to evolve freely.
		240	71.6	71.4	30.0	100	94.4	
	20	120	71.1	76.2	11.3	100	95.6	
		240	71.1	76.2	11.3	100	95.6	

Table XX. Leaching with Complexing Reagents [102]

Leaching Reagent	L/S Ratio	Time min.	% Leached Zn	Cu	Fe	Pb	Cd
$(NH_4)_2CO_3$ 2M	10	120	44.9	38.1	0.3	17.8	44.4
		240	45.4	40.5	0.3	15.6	44.4
	20	120	47.4	43.8	0.5	32.0	51.1
		240	48.5	44.3	0.5	28.9	48.9
NH_4Cl 5M	10	120	34.5	35.7	—	48.2	71.1
		240	38.7	38.1	—	48.2	71.1
	20	120	43.3	40.9	—	74.7	80.0
		240	43.3	40.9	—	74.7	80.0
NH_4OH 5M	10	120	15.3	22.6	—	0.13	48.9
		240	17.9	26.2	—	0.27	50.0
	20	120	16.5	23.8	—	0.6	46.7
		240	21.7	28.6	—	0.6	51.1
$(NH_4)_2SO_4$ 4M	10	120	30.4	38.1	—	0.2	65.6
		240	30.4	38.1	—	0.2	62.2
	20	120	28.9	38.1	—	0.36	62.2
		240	34.4	38.1	—	0.36	62.2

1-3. CONCLUSIONS

The research and development work on the pyrometallurgical processes for the treatment of electric arc furnace dust is relatively more advanced than that performed on the hydrometallurgical proceses. The pyrometallurgical processes are energy intensive and have high throughput rates. The energy requirements are high, particularly in the plasma processes. Because of the complex nature

of the dust, the condensers tend to be elaborate. This is due in part to the presence of alkali halide salts in the dust, which promote dross formation in the condenser. Although the majority of these salts could be removed by a simple leaching step prior to smelting, this would require that a drying operation be included in the flowsheet which further increases the energy requirements. Furthermore, the off-gas entering the condenser usually contains some iron which contaminates the zinc. Normally, a residue and a dust are produced which require further treatment.

The hydrometallurgical research is less-advanced. However, there is considerable potential for small-scale on-site operations. In some of the processes, there is a problem with the separation of iron. Also, it is difficult to decompose the zinc ferrite and thus, the zinc in the ferrite is not recovered. It appears easier to separate the byproduct metals which can be recovered as relatively pure metals. Waste water solutions and residues can be produced in the hydrometallurgical processes, but it may be shown that the hydrometallurgical processes are more environmentally friendly than the pyrometallurgical processes.

Chapter Two

KINETICS OF ZINC FERRITE LEACHING IN CAUSTIC MEDIA

SUMMARY

The role of zinc ferrite in the hydrometallurgical recovery of zinc from both primary zinc production and zinc-containing-waste treatment processes are discussed. Kinetic experiments on caustic leaching of zinc ferrite were performed in a 500 ml beaker, which was placed into a heated water bath of about ±2K temperature accuracy. Atomic Absorption Spectroscopy (AAS) and X-Ray Diffraction (XRD) analyses were employed to analyze both the leach solutions and the residues.

The effects of time, caustic concentration and temperature were investigated. It was found that the fraction of decomposed zinc ferrite increased linearly with increasing leaching time. Although the decomposition increased with the caustic concentration, the maximum dissolution rates were limited by the viscosity of the leach solution. The maximum fraction of decomposed zinc ferrite was only about 9% under the experimental conditions.

The dissolution rate of zinc ferrite was controlled by the diffusion of zinc ions in the imperfect latttices. With XRD analysis, the dissolution reaction was found to be as follows:

$$ZnFe_2O_4 + 2[OH^-] = ZnO_2^{2-} + Fe_2O_3 + H_2O.$$

2-1. INTRODUCTION

2-1-1. GENERAL

In both pyrometallurgical and hydrometallurgical processes for recovering zinc, sintering of sphalerite concentrates is usually the first step in zinc extraction[103]. During sintering, zinc ferrite is formed, if iron is present in the concentrates[104]. Since iron is one of the most common constituents present in the sphalerite concentrates[103], then the formation of zinc ferrite is unavoidable[105]. However, zinc ferrite is not a problem for pyrometallurgical recovery processes, because it is easy to decompose and can be reduced by carbon monoxide[104]. On the other hand, zinc ferrite is a problem for hydrometallurgical recovery processes, since it is insoluble in dilute suphuric acid. In order to achieve a zinc recovery of over 85%, a hot-acid-leach process is required[104]. In this process, concentrated sulphuric-acid solutions and temperatures of about 373K(100^0C) are used[104,106]. During leaching, a significant amount of iron is also dissolved. The dissolved iron interferes with the removal of Cu^{2+}, Cd^{2+} and Co^{2+} ions by zinc cementation, promotes anode corrosion and the uptake of lead and iron in the cathodic zinc[107]. Therefore, it has to be removed.

Although the jarosite($MFe_3(SO_4)_2(OH)_6$ with $M=Na^+$ or NH_4^+), the geothite(FeOOH) and the hematite(Fe_2O_3) iron-removal processes have been developed and employed in industry for decades, none of them are satisfactory. In these iron-removal processes, there are always difficulties in operation and the iron-rich residues are an environmental problem[104,108].

Similar problems occur in the hydrometallurgical treatment of electric arc furnace(EAF) dust, because the dust contains a significant amount of zinc ferrite[25-28,32-40]. Usually, it is more

difficult to treat EAF dust than other zinc bearing materials due to its high percentage of zinc ferrite.

One possible solution to avoid the troublesome iron removal process in the treatment of EAF dust is to use sodium hydroxide as the lixiviant. During leaching, zinc, lead and cadmium oxides, carbonates and silicates are readily dissolved, while the iron oxides are insoluble[109]. However, similar to acid leaching, the zinc in the ferrite can not be recovered. In order to recover this portion of zinc, leaching processes are usually performed in concentrated sodium hydroxide solutions at high temperatures [86]. The total zinc recovery is still low and is strongly dependent on the amount of zinc in the zinc ferrite, i. e. the more zinc ferrite in the dust, the lower zinc recovery [85-89].

2-1-2. LEACHING IN ACID MEDIA

The behavior of zinc ferrite in acid media has received much attention in the past few decades[108-120]. Recently, Bhat et al.[110] have developed a bench scale sulfuric acid electroleaching process to recover appoximately 18% of the zinc which was present in the leach residues from several zinc plants. They found that reductive dissolution and creation of anion vacancies were responsible for the dissolution of zinc ferrite. While about 97.90% zinc was extracted with 2 M H_2SO_4 after 4 hours, the majority of iron present in the residue was also extracted. Later, Lu et al.[111] employed cyclic voltammetry of carbon paste electrodes to investigate the relative rates of dissolution of copper, zinc, and nickel ferrites in HCl solution. Their research showed that: 1) The relative reactivities in 1M HCl at 298K(25^0C) were in the order: Fe_3O_4 >> $ZnFe_2O_4$ > $CuFe_2O_4$ >Fe_2O_3 >$NiFe_2O_4$; 2) The leaching of metal ferrites and iron oxides with the exception of NiO is enhanced by the presence of some reducing agents, such as Cu^+ and Sn^{2+}; 3) The dissolution of zinc ferrite

was found to follow the chemical reaction control model with an activation energy of about 87 kJ mol^{-1}. Similar results were also reported by many other researchers[112-114]. Recently, Elgersma et al employed a surface-reaction controlled, shrinking core model to describe and analyze the dissolution of zinc ferrite in acid media[117-119]. Their research showed the following results: 1) The dissolution rate was enhanced by increasing the concentration of H^+ and Fe^{2+} ions and it was retarded by Zn^{2+} in HNO_3, H_2SO_4 and $HClO_4$ solutions at temperatures between 348K(75^{0}C) and 368K(95^{0}C)[117]; 2) The activation energies were found to be 74 kJ mol^{-1}, 47 kJ mol^{-1} and 37 kJ mol^{-1}, respectively, for H_2SO_4, $HClO_4$ and HNO_3 media[117]; 3) The dissolution rate was twice as high in 1M $HClO_4$ solution at 363K(90^{0}C) in the presence of 5 g/l Fe^{2+} in H_2O as that in D_2O, and 11% higher in H_2O than in D_2O in 0.5m H_2SO_4 at 363K(90^{0}C) in the absence of Fe^{2+} ions[118]; 4) Zinc ferrite can be converted into ammonium jarosite ($NH_4Fe_3(SO_4)_2(OH)_6$) in a single-step seeded batch process at 368K(95^{0}C) and pH 1.7 or 1.95[119]. It was claimed that all of the zinc ferrite could eventually be converted and the zinc content in the converted residue was below 0.1 wt%[119]. More recently, Filippou et al.[115,120] investigated the effect of the variations in the zinc ferrite formula [(Zn_{1-x} , Fe_x^{2+})Fe_2^{3+} O_4, $x \leq 0.4$] on the dissolution rate in 1 M H_2SO_4 at temperatures between 348 K to 368 K. They found that the samples with high fraction x exhibited higher magnetic susceptibility and dissolved faster. This phenomenon was thought to be attributed to the lattice substitution of Zn^{2+} by Fe^{2+} in the more magnetic ferrite fractions, which created crystal defects and rendered the ferrite more chemically reactive.

2-1-3. LEACHING IN ALKALINE MEDIA

Compared with the acid leaching of zinc ferrite, less work has been performed with alkaline media.

However, a few studies have been reported on the behaviour of oxidized zinc ores and wastes during leaching with caustic media[109, 121-122]. Merrill and Lang[109] carried out a detailed research in 1964. Their results showed that the sodium hydroxide concentration and leaching temperature had significant effects on the dissolution of oxidized zinc ores and minerals, but the agitation speed and the particle size had relatively insignificant effects. Recently, Frenay[121] performed research on oxidized zinc ores in various media. In the caustic leach tests, the results showed that ZnO, $Zn(OH)_2$, PbO, $PbCO_3$ and $2PbCO_3$ $Pb(OH)_2$ dissolved very rapidly and completely, but ores which are rich in iron can only be processed with concentrated caustic soda at high temperatures. Because of the high percentage of iron in galvanizing zinc waste, Nirdosh et al[122] employed a pressure leaching process to recover zinc in caustic media. They achieved a 90% zinc recovery for 6-8 mesh particles at a caustic concentration of about 250 g/l and a pressure of about 345 kPa. In order to improve the zinc recovery, some roasting experiments were performed. However, no significant improvement in zinc recovery was achieved. They postulated that, while some zinc was converted to readily soluble zinc oxide during roasting, an equal fraction of zinc was converted to the insoluble zinc ferrate, zinc ferrite and zinc oxychloride complexes.

2-2. EXPERIMENTAL

Zinc ferrite was prepared using the same method, procedure and raw materials as those discussed in Appendix. The prepared zinc ferrite was crushed and ground into two particle sizes: −100+200 and −200 mesh. Figure 20 shows an XRD pattern for this synthetic zinc ferrite and only zinc ferrite was

detected. Any unreacted zinc oxide in the ferrite was extracted using 4M NaOH solution at about 353K (80^0C) for about 4 hours. The leached solutions were filtered in vacuum and analyzed

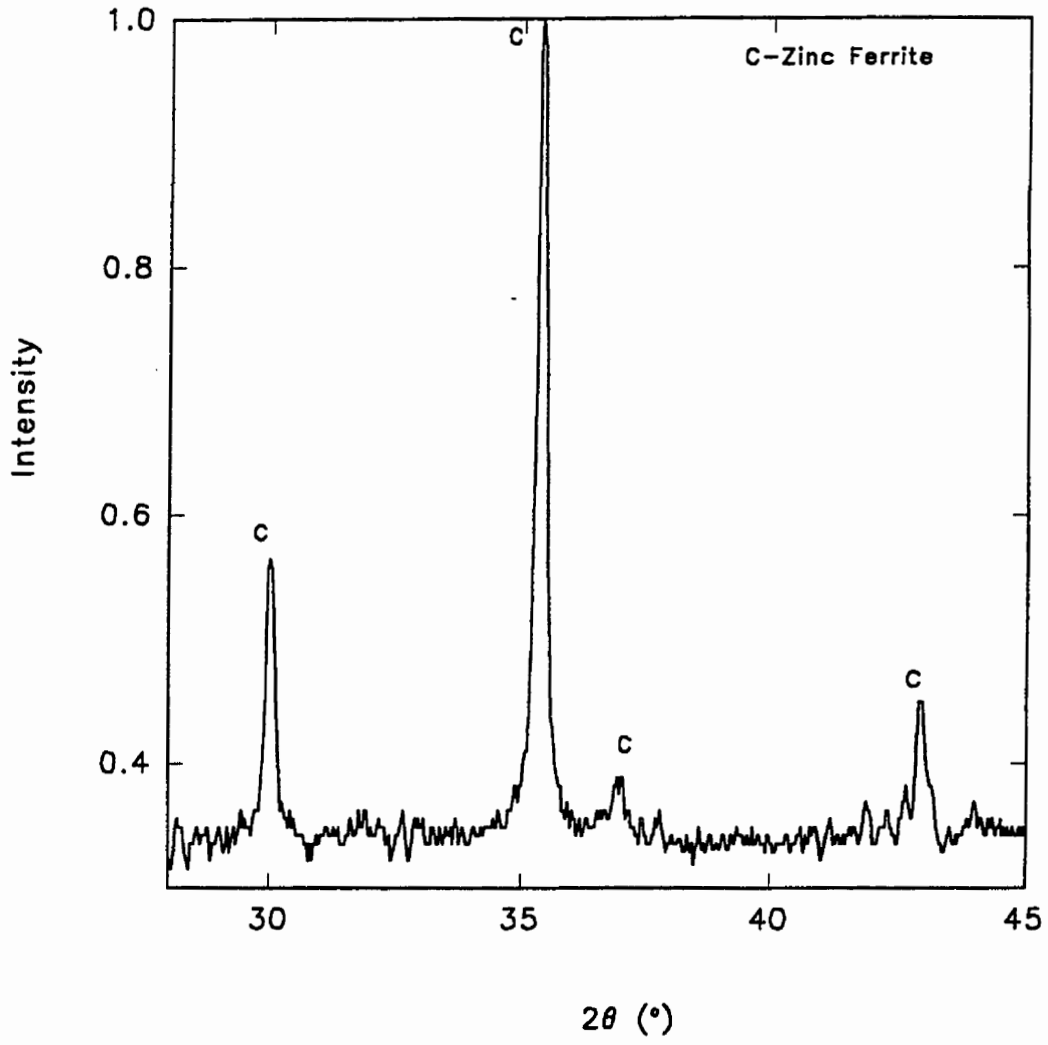

Figure 20. An XRD Pattern of Synthetic Zinc Ferrite

using Atomic Absortion Spectroscopy (AAS). The standards for AAS were prepared by following the same procedures as those described in Appendix. It was found that all the samples contained less than 1% unreacted zinc oxide.

Seven gram samples were employed for each leaching experiment. Samples were leached with 100 ml of 4 M, 8 M, 10 M and 12 M NaOH solutions, respectively, at temperatures between 299K(26^0 C) and 353K(80^0 C) in a 500 ml beaker. The beaker was immersed in a water bath with a temperature accuracy of about ± 2K and covered in order to keep the solid-liquid ratio constant during the experiments. A mechanical stirrer was employed for all the experiments at a speed of 300 rpm.

2-3. RESULTS AND DISCUSSIONS

2-3-1. GENERAL

Experimental conditions and results are shown in Tables XXI, XXII and XXIII, respectively. In

Table XXI. Experimental Conditions and Results for 4 M NaOH

Leaching Time, min		60	120	180	Rate Constant, min^{-1}
Temp., K	Particle Size	Fraction of Decomposed Zinc Ferrite, X			min^{-1}
353	-200 mesh	0.6580	0.6585	0.6585	8.33×10^{-6}
333	-200 mesh	0.1283	0.1381	0.1381	3.33×10^{-7}
299	-200 mesh	0.0790	0.0792	0.0796	5.0×10^{-8}

Table XXII. Experimental Conditions and Results for 8M NaOH

Leaching Time, min		60	120	180	Rate Constant
Temp., K	Particle Size	Fraction of Decomposed Zinc Ferrite, X			min^{-1}
353	-100+200 mesh	6.58	6.82	7.03	3.75×10^{-5}
	-200 mesh	7.11	7.54	7.59	4.0×10^{-5}
333	-100+200 mesh	6.23	6.30	6.32	7.50×10^{-6}
	-200 mesh	6.51	6.54	6.54	2.50×10^{-7}
299	-100+200 mesh	2.30	2.31	2.31	8.33×10^{-7}

Table XXIII. Experimental Conditions and Results for 12M NaOH

Leaching Time (min)		60	120	180	Rate Constant
Temp., K	Particle Size	Fraction of Decomposed Zinc Ferrite, X			min^{-1}
353	-100+200 mesh	7.4988	9.1081	10.5841	2.57×10^{-4}
	-200 mesh	7.8994	9.6090	10.7836	2.40×10^{-4}
333	-100+200 mesh	6.8551	8.5657	9.7589	2.42×10^{-4}
	-200 mesh	7.2429	8.9536	9.8589	2.18×10^{-4}
299	-100+200 mesh	5.0081	5.0724	5.1266	9.88×10^{-6}
	-200 mesh	5.2702	5.3887	5.4345	1.37×10^{-5}

these tables, X is the amount of zinc ferrite which has decomposed. This fraction is defined as follows:

$$X = \frac{\text{amount of zinc ferrite in leach solution}}{\text{amount of zinc ferrite before leaching}}$$

2-3-2. EFFECT OF LEACH TIME ON DECOMPOSED FRACTION OF ZINC FERRITE

As shown in the previous tables, the decomposed fraction of zinc ferrite increased linearly with leaching time. This trend is shown in Figures 21, 22 and 23. The effect was not as significant as expected with the exception of those experiments which were performed at comparatively high temperatures (333-353K) and high caustic concentrations(12m). In most cases (i.e. 299-353K, 4m and 8m), the decomposed fraction reached its maximum very easily, indicating that there was a portion of zinc ferrite which was dissolved readily in the caustic solutions. This maximum dissolution was mainly dependent on the leaching conditions (i.e. temperatures and caustic concentrations). As many authors have indicated[111, 118, 120, 123-126], reverse spinel structures, crystal imperfections and impurities in the zinc ferrite could be responsible for this phenomenon. The rate contants have been calculated and these contants are shown in Tables XXI, XXII and XXVIII.

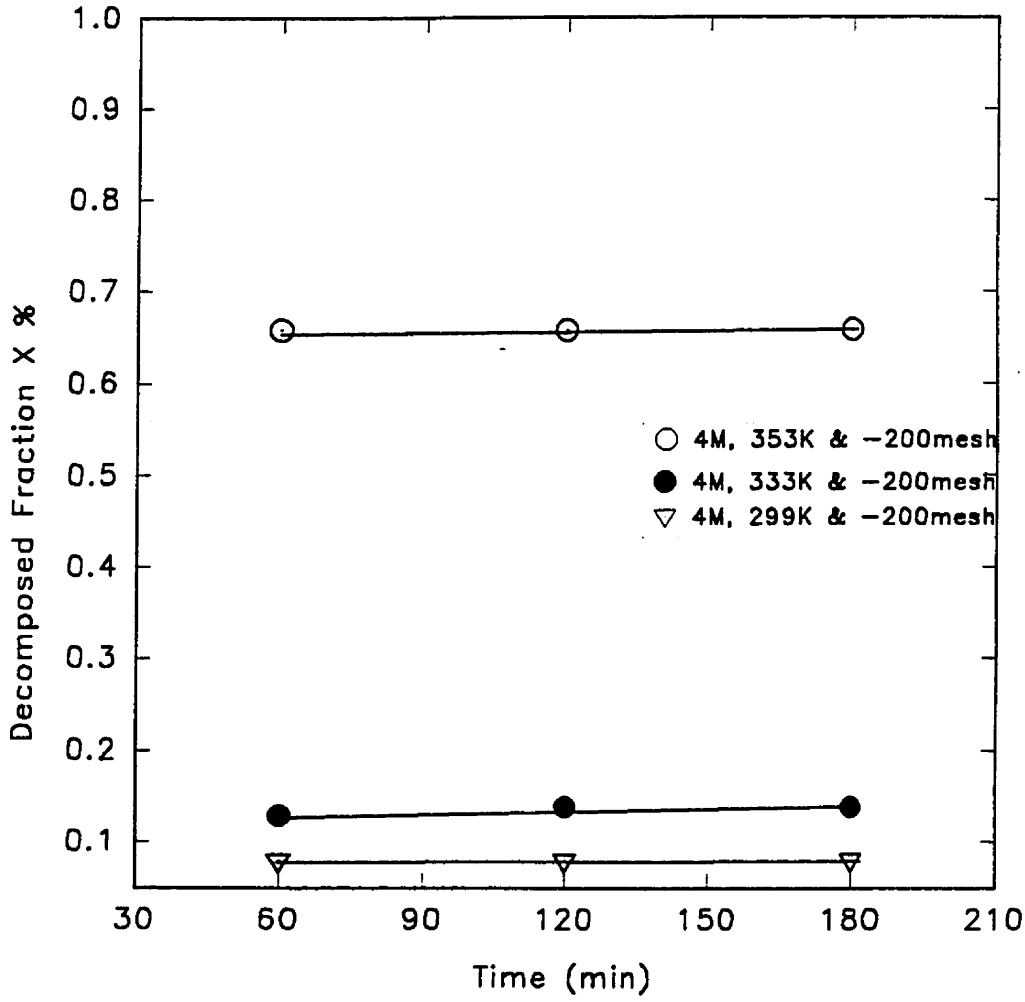

Figure 21. Decomposed Fraction X Versus Leach Time (4 M NaOH)

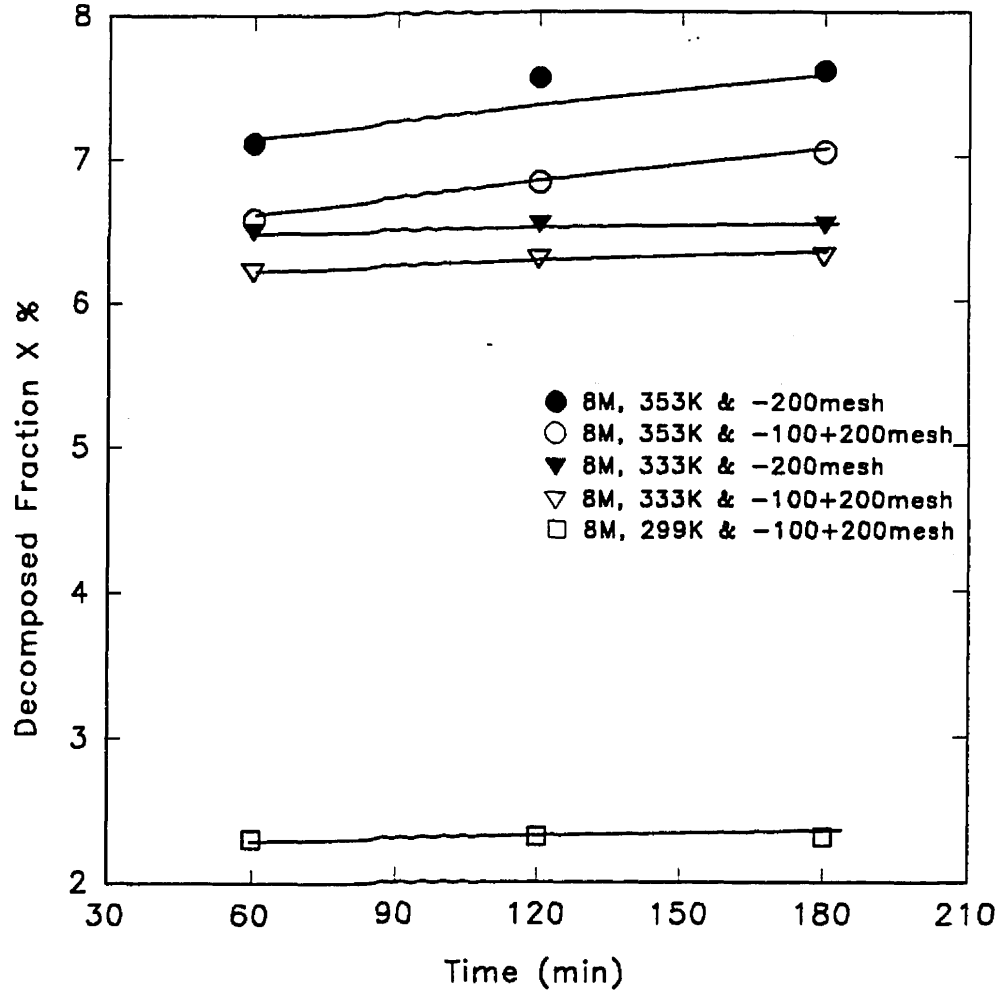

Figure 22. Decomposed Fraction X Versus Leach Time (8 M NaOH)

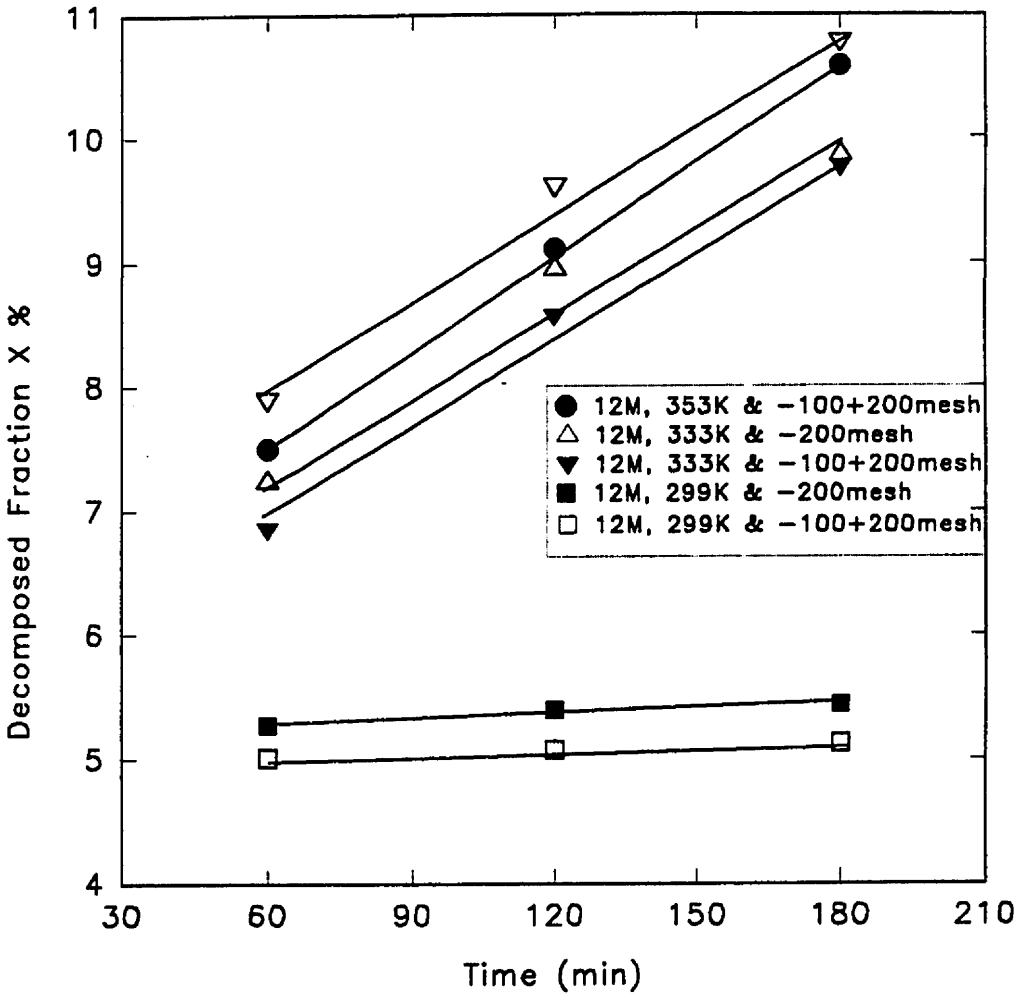

Figure 23. Decomposed Fraction X Versus Leach Time (12 M NaOH)

2-3-3. EFFECT OF CAUSTIC CONCENTRATION ON REACTION RATE

The effect of caustic concentration on the decomposed fraction is shown in Figure 24. As expected, the decomposed fraction increased with increasing caustic concentration. The effect was more significant at lower temperatures than at higher temperatures. It was observed that at a

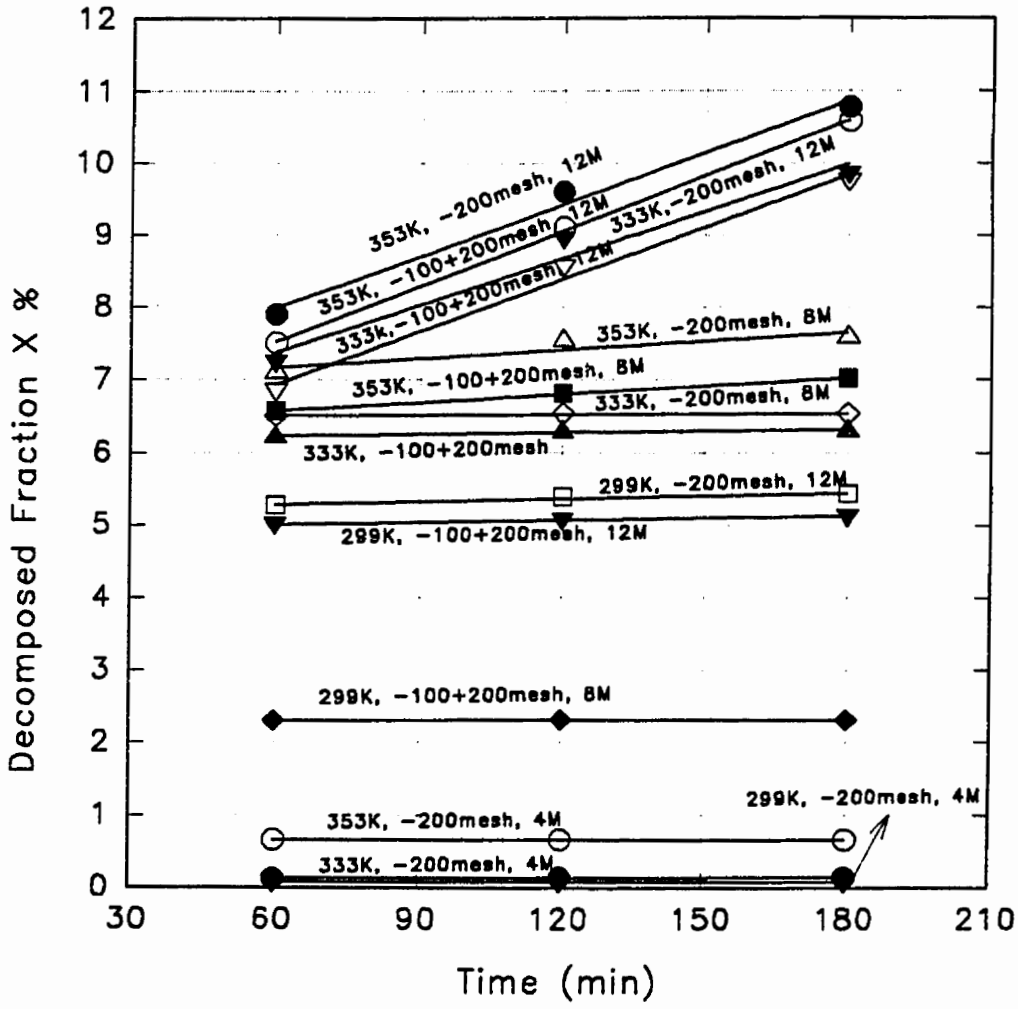

Figure 24. Effect of Caustic Concentration on the Decomposed Fraction X

concentration 12 M there were difficulties in solid-liquid separation. Thus, a caustic solution of 10 M was employed in order to optimize the leaching process. Although still very viscous, the experiments showed that the 10 M solution was managable. However, only 9% of the zinc ferrite was decomposed when it was leached at 366 K for 3 hours. The experiments also showed that there was only an 8.1253% increase in the amount of zinc ferrite decomposed from 30 minutes to 180 minutes, indicating that the dissolution of zinc ferrite could be attributed to the dissolution of a specific fraction of the zinc ferrite in which the atoms were easily activated and hence easily dissolved. Table XXIV shows these experimental results.

Table XXIV. Results for 10 M NaOH Leaching (366K)

Leach Time (min)	30	60	90	120	150	180
Fraction Decomposed (%)	8.0317	8.2178	8.3430	8.4964	8.5418	8.6843

2-3-4. EFFECT OF TEMPERATURES ON THE DISSOLUTION RATE

The experimental data were fitted to the Arrhenius equation. As shown in Figure 25, it can be seen that the dissolution rate increased with increasing temperature, but the effect was not as significant as expected. The experimental data were analysed using linear regression. The calculated activation energies are shown in Figure 25, while the linear equations are as follows:

$$\log k = 4.5187 - 3179.24/T \qquad (8M, -100+200 \text{ mesh}, 299\text{-}353K) \qquad (2\text{-}1)$$

$$\log k = 4.9484 - 2749.26/T \qquad (12M, -100+200 \text{ mesh}, 299\text{-}353K) \qquad (2\text{-}2)$$

$$\log k = 3.9111 - 2600.96/T \qquad (12M, -200 \text{ mesh}, 299\text{-}353K) \qquad (2\text{-}3)$$

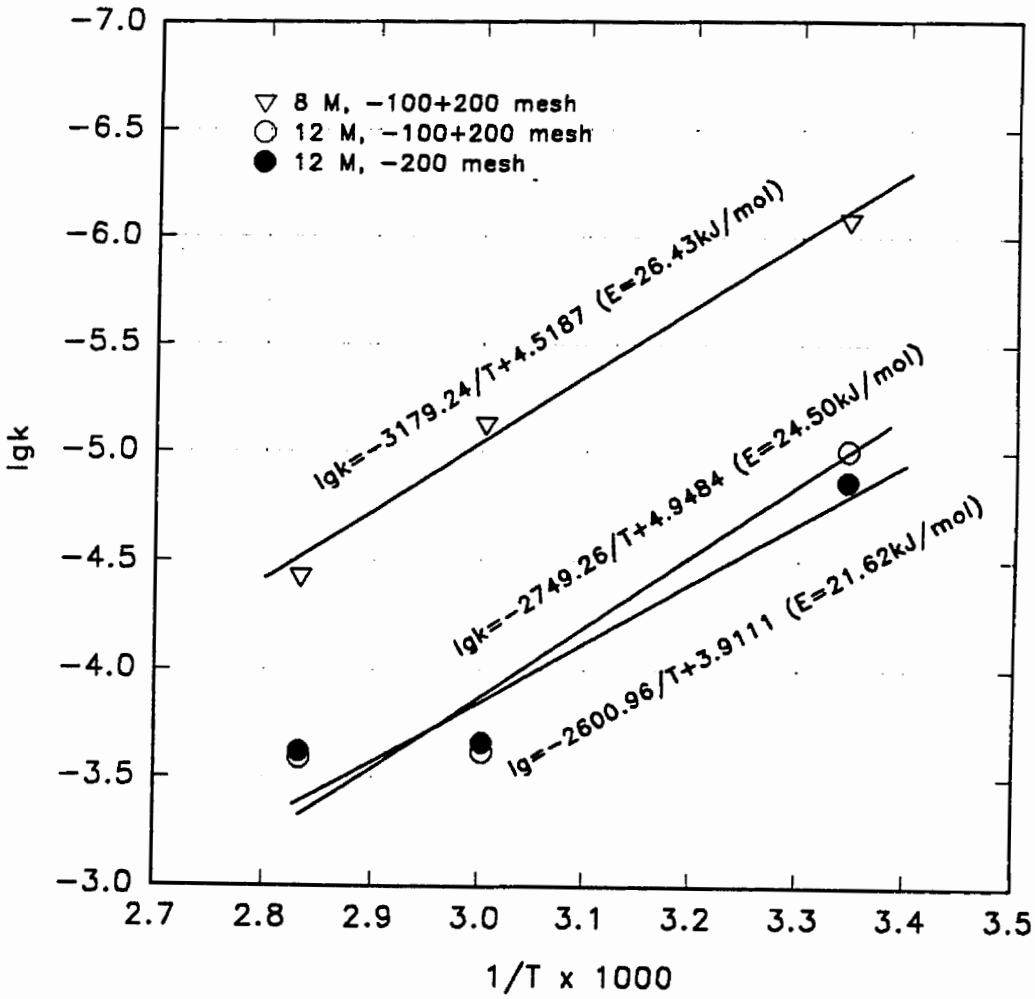

Figure 25. Arrhenius Plots

2-4. MECHANISM OF ZINC FERRITE DISSOLUTION

The observed low zinc ferrite dissolution rates and the low activation energies suggest that the kinetics of zinc ferrite dissolution in caustic media could be related to a solid-state rate controlled process. At the reaction interface, the dissolution reaction occurs preferentially at sites in which the reactants have already been activated. These sites are due to the presence of dislocations or point defects in the zinc ferrite. Severe grinding and the introducing of impurities may increase such the imperfections in the zinc ferrite, and hence may increase the dissolution rate. The dissolution rates may also vary for zinc ferrites which are prepared by different methods and procedures. Figure 26 shows an XRD pattern of the leached residue. The XRD analysis for the residues showed that hematite was present.

The mechanism of zinc ferrite dissolution could be expressed as follows:

(1) Adsorption of [OH^-] on the surface of the zinc ferrite particles;

(2) Diffusion of zinc ions to the zinc ferrite particle surface;

(3) Surface reaction;

(4) Diffusion of reaction product into the solution.

The reactions are as follows:

$$ZnFe_2O_4 + 4H_2O = Zn(OH)_2 + 2Fe(OH)_3 \quad (2\text{-}4)$$

$$Zn(OH)_2 + 2[OH^-] = Zn(OH)_4^{2-} \quad (2\text{-}5)$$

$$2Fe(OH)_3 = Fe_2O_3 + 3H_2O \quad (2\text{-}6)$$

$$Zn(OH)_4^{2-} = ZnO^{2-} + 2H_2O \quad (2\text{-}7)$$

Overall $ZnFe_2O_4 + 2[OH^-] = ZnO^{2-} + Fe_2O_3 + H_2O$ (2-8)

Step (2) is rate controlling.

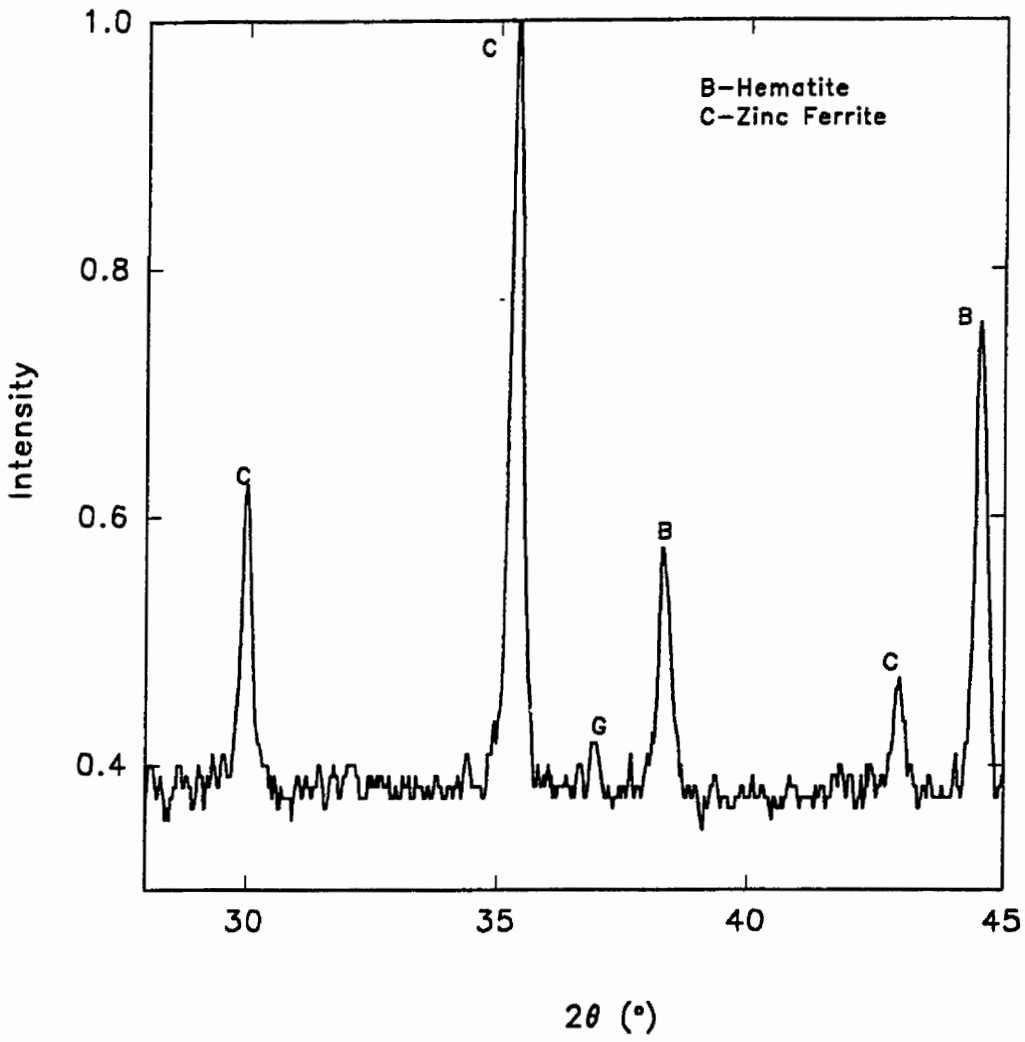

Figure 26. XRD Pattern for a Leach Residue

2-5 CONCLUSIONS

1. The effects of temperature and NaOH concentration were not as significant as expected. This phenomenon could be attributed to the dissolution mechanism in which the diffusion of zinc ions in the imperfect lattices controlled the dissolution rate .

2. According to the XRD analysis with the leach residues, the dissolution reaction was found to be as follows: $ZnFe_2O_4 + 2[OH^-] = ZnO_2^{2-} + Fe_2O_3 + H_2O$

3. The optimum leaching conditions were found to be as follows: 8M-10M NaOH, 333K(60^0 C) to boiling point, and 120-180 minutes.

4. The maximum fraction of the decomposed zinc ferrite was only about 9%.

Chapter Three

LEACHING OF EAF DUST IN CAUSTIC SOLUTIONS

SUMMARY

Experiments were performed on leaching EAF dust in caustic media under various conditions. It was found that temperature, caustic concentration and solid-liquid ratio all had a significant effect on the zinc and the lead recoveries, while leaching time had a less significant effect. Lead was dissolved more rapidly and to a greater extent than zinc. The major factor limiting the zinc recovery was the zinc which was present in the zinc ferrite. As the percentage of zinc, which was present in the zinc ferrite, increased, then the zinc recovery decreased.

3-1. INTRODUCTION

As discussed in the literature review, hydrometallurgical processes have the following advantages over pyrometallurgical processes for the treatment of EAF dust:

(1) A small scale on-site process can be economic.

(2) Potential environmental benefits.

Almost all leach media, including strong mineral acids and bases have been employed to leach EAF dust. However, the following common problems exist.

(1) A low recovery of zinc because of the zinc ferrite present in the dust.

(2) The metal separation methods are expensive.

Considerable research has been performed on caustic leaching because of the following advantages:

(1) Iron can be separated in the leaching step, since, unlike other metal oxides, such as zinc, lead and cadmium oxides which are readily dissolved, iron oxides are insoluble in caustic media. Thus, complex iron removal processes could be eliminated or, at least, simplified.

(2) A wider choice of low cost tank and electrode materials is available[109,122].

In addition to those caustic-base processes which have been discussed in detail in the literature review in Chapter One, Section 1-2-3-1-5, Amax Base Metals Research and Development Inc. in USA[127] has also performed significant research on this topic. All these processes are similar in many aspects, but differ mainly in the solid-liquid separation methods which are employed. In order

to understand and verify the problems which could be encountered, some experiments have been performed on the caustic leaching of EAF dust, which will be discussed in this Chapter. Also, these experiments will serve as a baseline for the microwave leaching of EAF dust and the hybrid process which will be discussed respectively in Chapters 4 and 5.

3-2. EXPERIMENTAL

3-2-1. CHEMICAL COMPOSITION

The EAF dust used in this research was provided by COSTEEL-LASCO. The composition is shown in Table XXV.

Table XXV Composition of COSTEEL-LASCO EAF Dust

Component	ZnO	Fe_2O_3	CaO	Na_2O	SiO_2	MnO	MgO	PbO	Al_2O_3	K_2O	Cr_2O_3	TiO_2	P_2O_5
(%)	31.2	18.3	15.6	3.8	3.41	2.2	1.35	1.02	0.68	0.67	0.19	0.05	0.11

3-2-3. PHASES PRESENT IN EAF DUST

An XRD pattern of the as-received EAF dust is shown in Figure 27. It shows that zincite (ZnO) and zinc ferrite ($ZnFe_2O_4$) are the two most predominant phases.

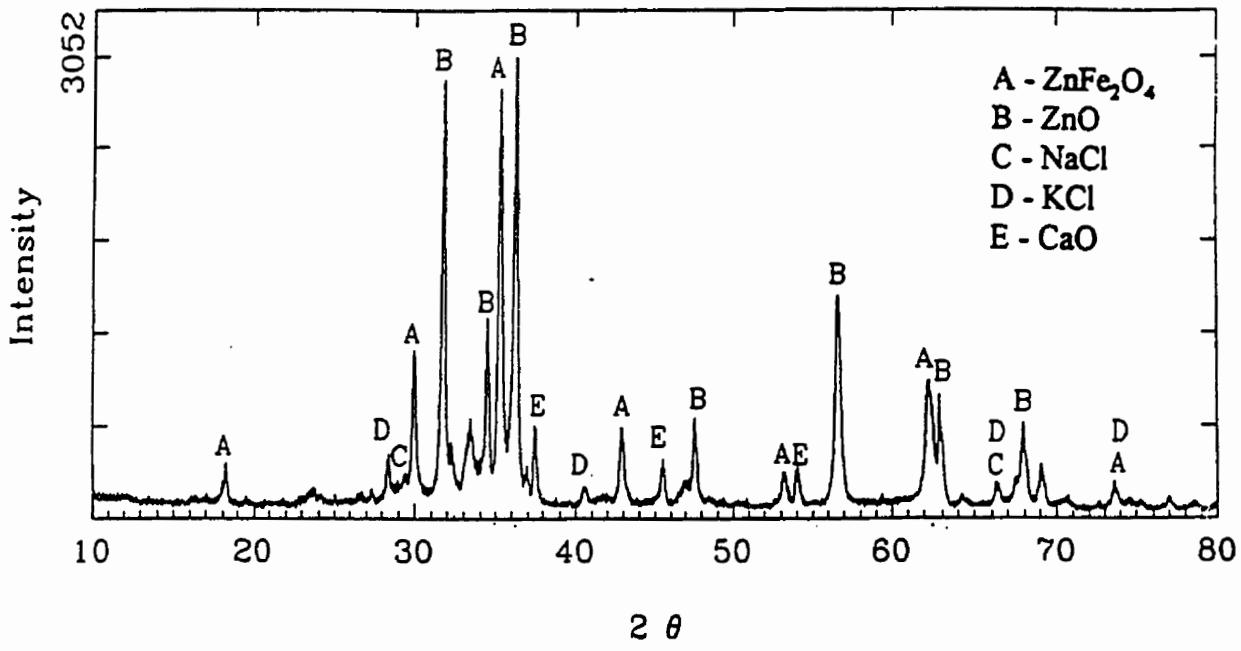

Figure 27 An XRD Pattern for the As-Received EAF Dust

3-2-4. PROCEDURES AND ANALYSIS

The dusts were washed with water at a solid-liquid ratio of about 0.25 at 353K (80^0 C) for two

hours to separate the water soluble materials, such as the sodium and potassium chlorides. The leach slurry was filtered under vacuum and dried at 447K(174^{0}C) for 15 hours. The water content of the dried EAF dust was measured to be less than 0.24 %. A water bath with a temperature accuracy of about ± 2K was employed for the leaching process. A mechanical stirrer was employed and a stirring speed of 300 rpm was used for all the tests. Solid-liquid separation was achieved using a vacuum filter. Titrametric analysis using EDTA was performed to determine the approximate chemical composition of the materials. The actual chemical composition was measured using AAS. All of the zinc in the dust was digested using aqua regia and hydrochloric acid. In the AAS analysis of the leached solutions, it was found that a high caustic concentration interfered with the zinc measurement due to the high solution viscosity and the build-up of caustic on the burner. Thus, similar precautions as have been discussed in Appendix, section A-2-2 were taken in the AAS analysis.

3-3. RESULTS AND DISCUSSION

3-3-1. POURBAIX DIAGRAMS AND ELECTROCHEMICAL MEASUREMENT

Acccording to the Pourbaix diagrams which are shown in Figures 28 and 29[128], potentials of about –0.5 V and higher are required to prevent iron dissolution. A typical measurement of the pH and the potential of solutions which consisted of 10M 100 ml caustic and 7 grams of dust at 366K(93^0 C) are shown in Table XXIX. It is clearly shown that under the pH and potential

conditions of Table XXVI , which are actually the conditions of the experimental system, iron dissolution could be prevented.

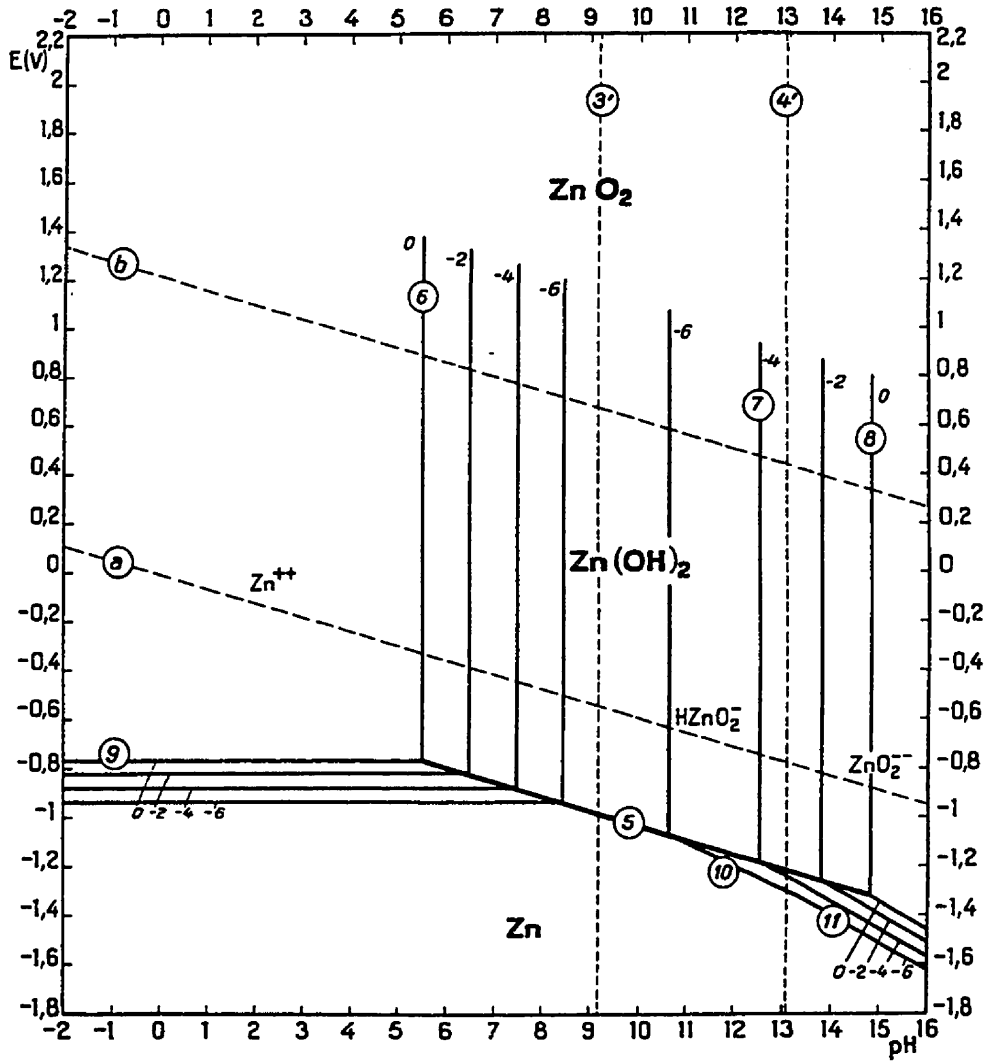

Figure 28. Potential-pH Equilibrium Diagram for the System Zinc-Water, at 25° C[128]

Table XXVI. A Typical Electrochemical Measurement

Time (minute)	0	30	60	90	120
Potential (mV)	–447	–383	–370	–351	–335
pH	14.9	13.8	13.5	13.2	12.9

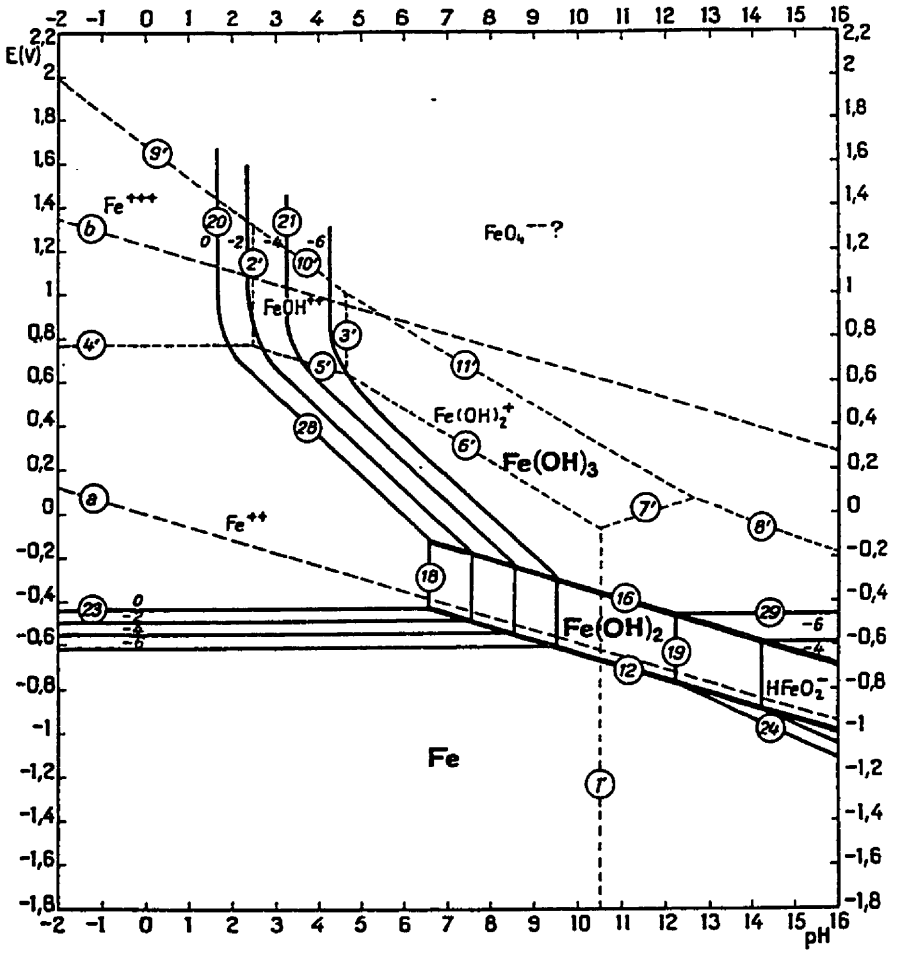

Figure 29. Potential-pH Equilibrium Diagram for the System Iron-Water, at 25^0 C[128]

3-3-2. EXPERIMENTAL RESULTS

Experiments were performed under various leaching conditions. The leaching conditions and the experimental results are shown in Table XXVII, while a typical XRD analysis of the leached residue is shown in Figure 30.

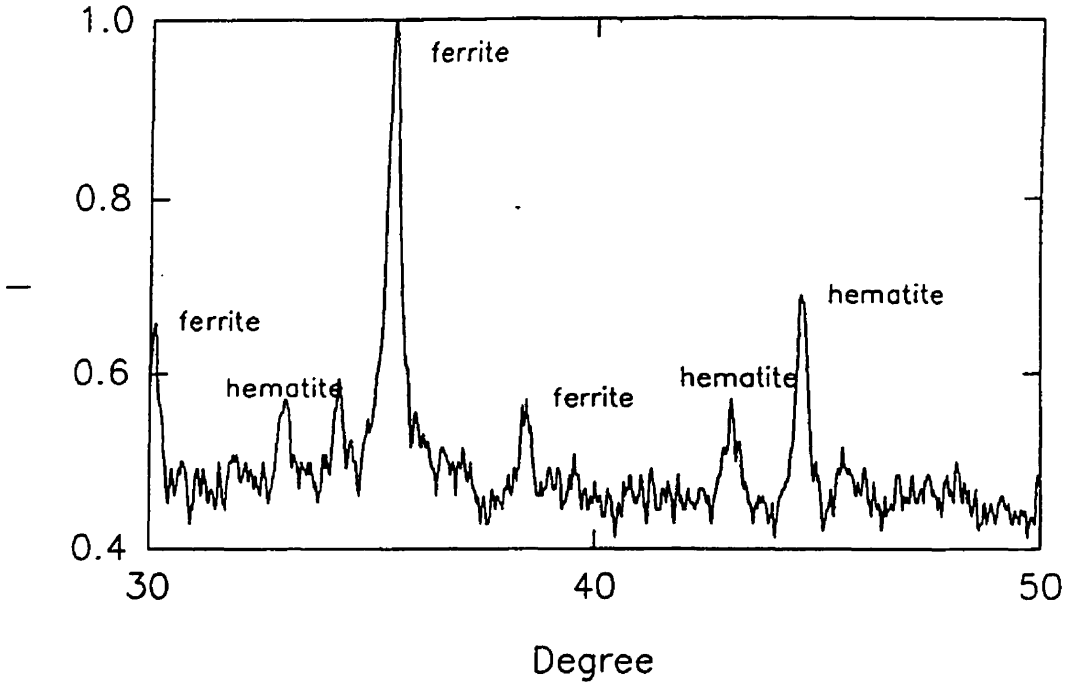

Figure 30. An XRD Pattern for Test L-2-2 Residue

Table XXVII shows that leaching temperature, caustic concentration and solid-liquid ratio all have significant effects on the zinc and lead recoveries, while leaching time has a less significant effect. From Figure 30, it can be seen that all the free zinc oxide had completely dissolved after 30 minutes

Table XXVII. Some Caustic Leaching Results

Experiment No	Temperatur (K)	Time (min)	NaOH (mol)	S/L Ratio (g/l)	Recovery of Zn (%)	Recovery of Pb (%)
L-1-1	293	30	2	16	4.98	17.59
L-1-2	293	30	2	16	5.04	22.24
L-2-1	363	30	6	16	65.93	78.07
L-2-2	363	30	6	16	73.46	78.52
L-3-1	293	240	6	16	31.91	49.45
L-3-2	293	255	6	16	30.55	47.61
L-4-1	363	240	2	16	56.09	73.48
L-4-2	363	240	2	16	69.0	70.0
L-5-1	293	30	6	80	34.29	27.29
L-5-2	293	30	6	80	36.28	28.09
L-6-1	363	30	2	80	11.70	51.56
L-6-2	363	30	2	80	8.19	48.70
L-7-1	293	240	2	80	2.30	32.82
L-7-2	293	255	2	80	4.60	38.00
L-8-1	363	240	6	80	61.74	57.19
L-8-2	363	255	6	80	65.10	58.75
L-9-1	328	135	4	48	45.10	58.07
L-9-2	328	135	4	48	31.73	49.41

of leaching in 6m caustic solution at 363K(90^0 C). In comparison, lead was dissolved more rapidly and to a greater extent than zinc for all experiments. This is in agreement with the results of other researchers[85-89,127].

3-4. CONCLUSIONS

The following conclusions can be made from this research:

(1) Free zinc oxide and lead oxide can be easily dissolved in concentrated caustic solutions at high temperatures.

(2) The final zinc recovery is dependent on the amount of free zinc oxide (i.e. the greater the percentage of free zinc oxide, the higher the final zinc recovery).

(3) Lead oxide is dissolved more rapidly than zinc oxide.

Chapter Four

KINETICS OF MICROWAVE LEACHING OF EAF DUST

SUMMARY

Microwave energy has been widely employed in food processing, rubber and plastics curing, and in ceramic sintering since the 1960s. However, the application of microwaves as an energy source in extractive metallurgy is still in the early stage of development. In this Chapter, some applications of microwaves in extractive metallurgy and analytical laboratories, microwave heating fundamentals, and the interaction of microwaves with materials are reviewed. Then, detailed research results on the microwave leaching of EAF dust to recover metal values are presented. The effects of variables, such as caustic concentration (M), leaching time (min), solids concentration (g/l), and microwave power level (%) were investigated. Finally, a traditional leaching process and a microwave leaching process for EAF dust are compared.

4-1. INTRODUCTION

4-1-1. GENERAL

Microwaves were first used for the heating of materials in 1946, shortly after radar equipment was invented during the second world war. It was evident that microwaves were very effective for heating water and the technology was quickly adopted for drying and cooking. Since the introduction of the first microwave oven by Raytheon in 1952, many millions of domestic microwave ovens have been sold annually[129-130].

In extractive metallurgy, the application of microwaves is in the early stages of development[129-133]. However, there are several reasons for the growing interest in the use of this technology in the field of metals extraction. These include the following potential advantages of microwaves: (1) rapid and selective heating of materials; (2) reactions can be catalyzed since the heating occurs on a molecular or atomic level; (3) clean and controllable energy source; (4) the gas volume is reduced and the atmosphere can be controlled as there are no gaseous combustion products; (5) the material is heated internally in comparison to external heating with conventional methods; (6) the temperature of the refractory can be minimized; (7) the working environment is improved.

4-1-2. APPLICATIONS

The potential applications of microwaves in extractive metallurgy have been discussed in a recent review article [134]. These applications include the following:

(1) Microwave energy in grinding [135];

(2) Microwave treatment of iron ores prior to reduction[136-138];

(3) Microwave reduction of iron ores[139-140];

(4) Microwave processing of electric arc furnace dust[141];

(5) Microwave heating of slags[142];

(6) Microwave preheating of high alumina steelmaking refractories[143];

(7) Microwaves in the extraction of gold from refractory/complex ores[144-146];

(8) Microwaves in the extraction of non-ferrous metals[147-155].

4-1-2-1. MICROWAVE PROCESSING OF EAF DUST[141]

Most of the studies on the application of microwaves in extractive metallurgy are pyrometallurgical. In particular, one of these applications discussed the treatment of EAF dust[141]. In this process, EAF dust was processed in a 900 watt Samsung (2.45 GHz) microwave oven. Twenty grams of EAF dust were used in each test. The EAF dust was mixed mechanically with various amounts of carbon powders, and then, the mixed powders were placed in a fireclay crucible and microwaved for ten to thirty minutes. At the end of the experiment, the crucible was removed from the microwave oven and allowed to cool in air. The zinc oxide which condensed on the top wall of the crucible was carefully collected and weighed.

Figure 31[141] shows an outline of the crucible which was taken from the microwave oven after reduction, while Figure 32 shows the efect of processing time on the temperature of the EAF dust. Figure 31 shows that the zinc oxide condensed in two areas and some metallic zinc was deposited

in the microwaved residue, along with a metallic iron button which was collected from the bottom of the crucible. The coupling between the microwaves and the EAF dust was, in general, very good. A typical analysis of the microwaved residue is given in Table XXVIII[141]. Also, the chemical compositions of the EAF dust and the condensed zinc oxide are shown in Table XXIX[141].

Table XXVIII. Typical Analysis of the Residue[141]

Compound	Fe	SiO_2	Cl	CaO	Zn	MnO	K	Na
Mass (%)	34.23	5.50	7.27	33.1	2.03	5.47	4.03	7.99

Table XXIX. Composition of EAF Dust and Condensed Fume [141]

Materials	Zn	CdO	Fe_2O_3	CaO	Na_2O	K_2O	SiO_2	PbO	Cr_2O_3
EAF Dust	24	0.36	18.3	15.6	3.8	0.67	3.41	1.02	0.19
Area 1 Fume	83.7	0.058	0.01	0.02	0.97	0.60	0.06	0.402	<0.01
Area 2 Fume	79.8	0.077	0.15	0.16	2.03	1.70	0.19	2.5	<0.01

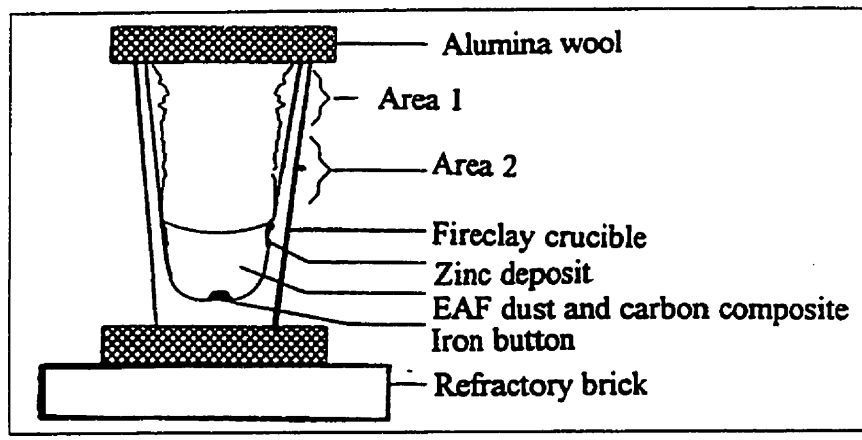

Figure 31. Schematic Diagram of the Crucible after Reduction[141]

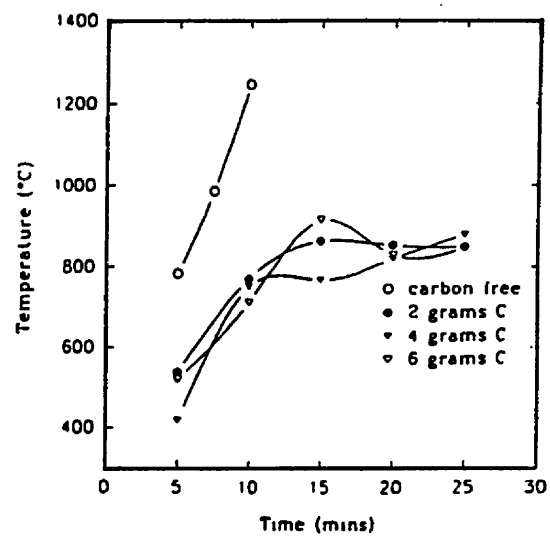

Figure 32. Effect of Processing Time on the Temperature of the EAF Dust [141]

These results show the following:

1) There is excellent coupling between the dust and the microwaves. This can be attributed to the high iron oxide and zinc ferrite contents in the dust. Both oxides readily react with microwave radiation.

2) The extraction rate of zinc is rapid and a relatively pure zinc oxide (low iron oxide) and an iron-rich residue are produced.

However, the zinc is widely distributed in the reactor and thus an elaborately designed reactor could be required. Also, the thermal runaway- which was encountered for some cases in this research needs to be overcome.

4-1-2-2. MICROWAVE ACID DISSOLUTION OF SOLIDS

Microwave heating has been widely used as a replacement for conventional heating techniques in analytical laboratories since the mid-1970s[156-157]. In sample preparation, these applications include drying, extractions, acid dissolution, decomposition and hydrolysis[146-161]. Solids, such as minerals, oxides, glasses, metals, and alloys have been digested with acids under microwave radiation in order to prepare the samples for atomic absorption analysis(AAS) and other instrumental techniques. The main feature of this technique was the fast dissolution rate. Only a few minutes of processing time were required when microwaves were used, while the conventional methods required several hours. This technique was also considered both reliable and cost-effective. Furthermore, relatively simple ovens and controls were generally employed. Currently, most of the development work involves in improving the existing equipment to extend the operating range and

to improve safety and reproducibility. Some of these examples include the improvement of turntables and sample fixtures, pressure vessels fabricated from glass and quartz to allow higher reaction temperatures and pressures than can be achieved in teflon vessels, and optimized pressure relief valves [162]. Consequently, these developments have resulted in a testing standard that is simple, reproducible and can be automated[163].

However, the application of microwaves for the dissolution of samples in alkaline solutions has not been reported in the literature. Only one research study employed microwaves for the leaching of sphalerite minerals using $FeCl_3$/HCl as the lixiviant[155]. Variables such as temperature, particle size, and $FeCl_3$ concentration were investigated. The results demonstrated that the leaching rate increased with temperature in both microwave and conventional heating systems. Under the leaching conditions: 0.1M HCl, 1.0 M $FeCl_3$, 60 minutes and 368^0 K, about 90% of the zinc was recovered in the leaching process with microwave heating, while only about 50% of the zinc was recovered with conventional heating.

4-2. MICROWAVE FUNDAMENTALS

Microwaves are electromagnetic waves with frequencies which range from 0.3 to 300 GHz or wavelengths which range from 1mm to 300 mm. In a similar manner to lasers, but in contrast to visible electromagnetic waves, microwaves are coherent and polarized. They obey the laws of optics and can be transmitted, absorbed, or reflected. Their behaviour depends on the type of materials that they are interacting with[164-165]. As shown in Figure 33, the extent to which a material absorbs microwave energy is primarily determined by its conductivity. Materials with low

conductivities, such as insulators, are effectively transparent to the incident waves and thus, do not store any of the energy in the form of heat. Materials with high conductivities, such as metals, reflect the microwaves, which provides no significant heating effects. Materials, such as semiconductors, with intermediate conductivities, typically from 1 to 10 s m^{-1}, can be effectively heated from room temperature through the interaction of the materials with microwaves. However, as the heating mechanisms in microwave systems are strongly temperature dependent, materials with low conductivities, such as insulators, begin to absorb and even couple more efficiently with microwave radiation when heated above a critical temperature (T_c). The microwave coupling properties of the material can be changed by adding conductive or magnetic phases in the form of fibers, particles, etc. As microwave heating is also dependent on the state of the material, metals can be heated through microarcing phenomena if they are in the form of a powder.

The degree to which any material will absorb microwaves is determined by the complex permittivity as follows[164-165]:

$$\varepsilon = \varepsilon' - j\varepsilon'' = \varepsilon_0(\varepsilon_r' - \varepsilon''_{eff}) \qquad (4\text{-}1)$$

where ε_0 is the permitivity of free space (8.86E−12 F/m); ε_r' is the relative dielectric constant; ε''_{eff} is the relative dielectric loss factor and $j = (-1)^{1/2}$.

When microwaves penetrate and propagate through a dielectric material, an internal electric field (E) is generated within a specific volume. Microwaves induce the transient motions of free or bound charges (e.g., electrons or ions) and also rotating charge complexes such as dipoles are induced. The resistance to these induced motions causes losses and attenuates the electric field due

to inertial, elastic, and frictional forces. As a result of these losses, volumetric heating occurs. For convenience, the loss mechanisms are combined together in the loss parameter, ε''_{eff}. However, the loss tangent is commonly used to describe the losses as follows.

$$\tan \delta = \varepsilon''_{eff} / \varepsilon_r' = \sigma / 2\pi f \varepsilon_0 \varepsilon_r' \qquad (4\text{-}2)$$

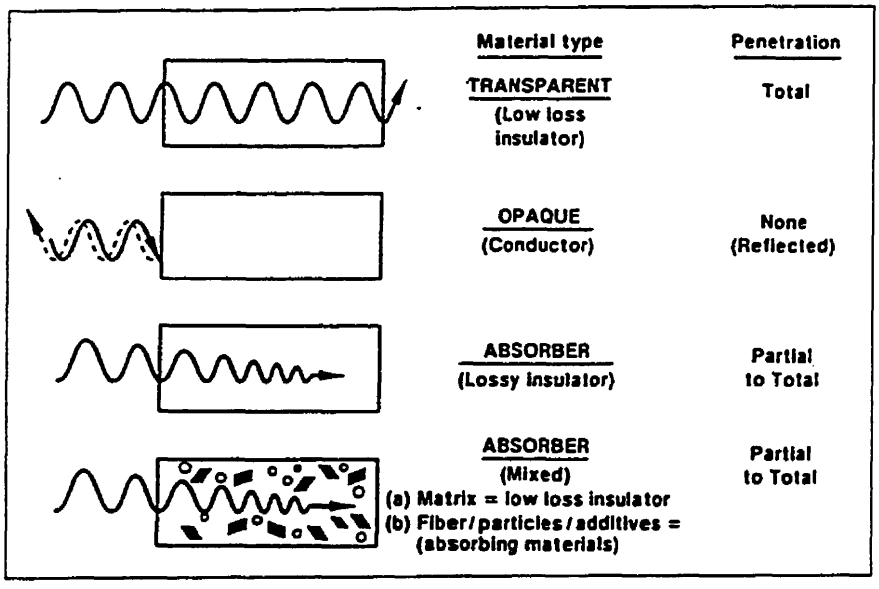

Figure 33. Interaction of Microwaves with Materials[165]

where σ is the conductivity of the material in s/m, and f is the frequency of the incident wave in GHz. This parameter can be related to the penetration depth (D) ,where this is defined as the depth at which the incident power is reduced by one half:

$$D = 3\lambda_0 / 8.868\ \pi \tan \delta\ (\varepsilon_r' / \varepsilon_0)^{1/2} \qquad (4\text{-}3)$$

where λ_0 is the incident or free-space wavelength. It is clear that the penetration depth is inversely proportional to the frequency of the radiation. Although low frequencies result in greater penetration depths, the amount of heating may not significantly increase since the internal field, E, could be low. Again, the effect is strongly dependent on the properties of the material.

The average power absorbed by a material per unit volume P is defined as:

$$P = \sigma\ |E|^2 = 2\pi f \varepsilon_0 \varepsilon_r' \tan \delta\, |E|^2 \qquad (4\text{-}4)$$

This equation shows that the power absorbed varies linearly with the frequency, the relative dielectric constant, tan δ , and varies with the square of the internal electric field.

In a non-homogeneous material, the material may not heat uniformly. Thus, some parts of material heat faster than others, even though some heat is conducted away. This effect is due to the increase in the dielectric loss factor and the loss tangent with increasing temperatures. This phenomenon is referred to as thermal runaway and is one of the major problems with microwave heating[164-167].

Some attempts[166-171] have been made to quantify the conditions under which thermal runaway occurs and also methods of control. In summary, these studies concluded that the temperature distribution was incident power dependent. Stable heating was possible with rapid heat removal (i.e. no insulation) or in cases in which the temperature dependence of the dielectric loss factor was small. There is a critical power level, below which the sample will heat in a stable manner.

4-3. BEHAVIOUR OF MATERIALS UNDER MICROWAVE IRRADIATION

As early as 1967, Ford and Pei[172] studied the high temperature chemical processing of some oxides and sulphides by microwave heating in a resonant, 2.45 GHz cavity with a power level up to 1600 watts. They observed that generally dark coloured compounds heated rapidly to a temperature of about 1273K(1000^0C). Lighter coloured materials required a longer time but were capable of reaching higher temperatures. These results are summarized in Table XXX[172].

Wong [173] and Tinga[174] measured the high temperature properties of some specific oxides in a microwave cavity. Their results were compiled[130]with other data[172]to illustrate the range of cavity heating rates and to attempt to classify the microwave response of various materials (Table XXXI) [130]. This table was useful, since it summarized and defined the different heating behaviours of materials in terms of four categories , i. e. hyperactive, active, difficult to heat and inactive. However, it is difficult to make any comparison of the heating rates and the temperatures achieved in the research reported in the literature, since the surface heat losses and the power coupling factors were different.

In 1984 Chen et al.[175] reported their results of microwave irradiation of 40 minerals in air. The general objective was to determine the behaviour of small samples of minerals (0.5-1.0g) under microwave heating conditions. One of the major problems they encountered was temperature measurement. An AGA thermovision infrared camera system was employed to measure temperatures. However, because this device only measured the surface temperature, the measured temperatures were low, in some cases, by several hundred degrees. Consequently, temperatures were not reported and instead, the microwave power input was given[175]. Despite this problem,

their study was significant because they recorded the heating behaviours of the materials and also performed chemical analysis before and after heating. Two categories of material behaviour were

Table XXX. Heating Rates at 2.45 GHz in a Resonant Cavity. (Sample size varied from 10 g (dark materials) to 200 g (light materials)). (B) signifies a violent reaction. In the case of MnO_2, the reaction could not be recorded [172].

Compound	Colour	Heating Time (min.)	Max. Temp. (K/ ^{0}C)
Al_2O_3	White	24	2173/1900
C (Charcoal)	Black	0.2	1273/1000
CaO	White	40	473/200
Co_2O_3	Black	3(B)	1173/900
CuO	Black	4	1073/800
CuS	Dark blue	5	873/600
Fe_2O_3	Red	6	1273/1000
Fe_3O_4	Black	0.5	773/500
FeS	Black	6	1073/800
MgO	White	40	1573/1300
MnO_2	Black	(B)	—
MoO_3	Pale green	46	1023/750
MoS_2	Black	0.1	1173/900
Ni_2O_3	Black	3(B)	1573/1300
PbO	Yellow	13	1173/900
TiO_2	White	—	—
UO_2	Dark green	0.1	1373/1100
ZnO	White	4	1373/1100

Table XXXI. A Compilation of Microwave Heating Rates at 2.45 GHz and Maximum Temperatures of Various Materials.(reagent grade materials; heating conditions similar but not identical) [130].

Materials Classification	Heating Rate Reported	Maximum Temperature(K/ ^{0}C)	Reference and Notes
(a) Hyperactive Materials	^{0}C/s		
UO_2	200	1373/1100	Note that these MoS_2 materials
MoS_2	150	1173/900	materials tend to be black, with
C (Charcoal)	100	1273/1000	high thermal conductivities.
Fe_3O_4	20[a]	773(1273)	See ahead for mixtures of
		500(1000)	Fe_3O_4/ Fe_2O_3
FeS_2	20	773/500	
CuCl	20	723/450	
MnO_2	—	—	Probably>20 ^{0}C/s [172]
(b) Active	^{0}C/min.		
Ni_2O_3	400	1573/1300	Violent
Co_2O_3	300	1173/900	Violent
CuO	200	1073/800	
Fe_2O_3	170	1273/1000	
FeS	135	1073/800	
CuS	120	873/600	
(c) Difficult to Heat	^{0}C/min.		See also table ahead
Al_2O_3	80	2173/1900	Type unspecified
PbO	70	1173/900	
MgO	33	1573/1300	
ZnO	25	1373/1100	
MoO_3	15	348/75	
(d) Inactive	^{0}C/min.		See also table ahead
CaO	5	473/200	
$CaCO_3$	5	403/130	
SiO_2	2.5	343/70	

[a]: dT/dt probably large enough to mask oxidation effects.

Table XXXII. Mineral Transparent to Microwave Irradiation. (microwave frequency 2.45 GHz; power 150 W; exposure 5 min.)[175]

Mineral Class	Minerals/Compounds
Carbonates	Aragonite, calcite, dolomite, siderite
Jarosite-type compounds	Argentojarosite, synthetic natrojarosite (zinc plant residue, Kidd Creek Mines Ltd.), synthetic plumbojarosite (zinc plant residue, Cominco Ltd.)
Silicates	Almandine, allanite, anorthite, gadolinite,muscovite, potassium feldspar, quartz, titanite, zircon
Sulphates	Barite, gypsum
Others	Fergusonite, monazite, sphalerite (low Fe), stibnite

developed. In the first, little or no heating occurred due to the transparency or surface reflection of the minerals. Thus, the minerals were not affected. In the second, heat was generated in the minerals. These materials were either stable or reacted rapidly and dissociated. They found that the behaviour of minerals in a microwave environment was compositionally dependent (e.g. when Fe was substituted for Zn in sphalerite, the resulting high-Fe sphalerite became microwave sensitive). Mineral deposits of jarosite-type materials could not be decomposed in situ. Their heating results are shown in Tables XXXII to XXXIV[175].

More recently, the U.S. Bureau of Mines has reported data on the microwave heating characteristics of selected minerals and compounds[176-179]. They employed a commercial 1000 watt microwave oven (2.45 GHz) for all the experiments except those in which the fracture

Table XXXIII. Results of Microwave Heating on Ore Minerals (2.45 GHz; exposure 3-5 min.).[178]

Mineral	Power (W)	Heating Response	Product Examination
Arsenopyrite	80	Heats, some sparking	S and As fume; some fusion. Pyrrhotite, As, Fe-arsenide and arsenopyrite
Bornite	20	Heat readily	Some changed to bornite-chalcopyrite-digenite; some unchanged
Chalcopyrite	15	Heats readily with emmision of sulphur fumes	Two Cu-Fe-sulphides or pyrite and Cu-Fe-sulphide
Covellite/anilite (60% vol%	100	Difficult to heat; sulphur fumes emitted	Sintered to single composition of $(Cu,Fe)_9S_5$
Galena	30	Heats readily with much arcing	Sintered mass of galena
Nickeline/cobaltite (3 vol%)	100	Difficult to heat	Some fused; most unsffected
Pyrite	30	Heats readily; emmision of sulphur fumes	Pyrrhotite and S fumes
Pyrrhotite	50	Heats readily with arcing at high temperature	Some fused; most unaffected
Sphalerite (high Fe; Zn 58.9 Fe 7.4, S 33.7%)	100	Difficult to heat when cold	Converted to wurtzite
Sphalerite (low Fe; Zn 67.1% Fe 0.2, S 32.7%)	>100	Does not heat	No change, sphalerite
Stibnite	>100	Does not heat	No Change, stibnite
Tennantite (Cu 42.8, Ag 0.1,Fe 4.8, Zn 1.7, As 12.5, Sb 10.6,S 22.55) (90 vol. % tennanite,6% chalcopyrite, 4% quartz)	100	Difficult to heat when cold	Fussd mass of tennanite-chalcopyrite; arsenic fumes emmitted
Tetrahedrite (Cu 24.9, Ag 18.0, Fe 1.9, Zn 4.8, Sb 25.6, As 13 S 23.4%) (85 vol.% tetrahedrite, 10% quartz, 5% pyargrite, galena, chalcopyrite)	35	Heats readily	Fused mass of Ag-Sb alloy, PbS, tetrahedrite, Cu-Fe-Zn sulphide and Cu-Fe-Pb sulphide

behaviour of the minerals was studied. In these cases, a 3000 watt oven (2.45 GHz) was used. Twenty five gram samples or a constant volume of 18 ml, for low-density materials, were irradiated in a closed system under an inert atmosphere. Temperatures of the samples were continuously monitored and recorded using a sheathed thermocouple which was inserted through the roof of the oven directly into the samples. The accuracy of the thermocouple data was reported to be within ±2% as determined by measurements performed on boiling water. All the solid samples were in the form of powders with some as large as plus 60 mesh, and some were minus 325 mesh. In order to prevent break-down of the thermocouple, tests were terminated as the temperature approached 1373K (1100^{0}C). These data are shown in Tables XXXV to XXXVI [176]. Their temperature

Table XXXIV. Results of Microwave Heating on Oxides and Uranium Minerals(2.45 GHz; 3-5 min.)[178]

Mineral	Power (W)	Heating Response	Product Examination
Allanite	>150	Does not heat	No change, allanite
Cassiterite	40	Heat readily	No change, cassiterite
Columbite (40 vol%- Pyrochlore in silicates (almandine 40%)	60	Difficult to heat when cold	Niobium minerals fused, most silicates unchanged
Fergusonite	>150	Does not heat	No change, fergusonite
Hematite	50	Heats readily; arcing at high temperature	No change, hematite
Magnetite	30	Heats readily	No change, magnetite
Monazite	>150	Does not heat	No change, monazite
Pitchblende (90 vol%) contains chlorite, galena, calcite	50	Heats readily	Some fused to UO_2, U_3O_8, ThO_2 and Fe-Al-Ca-SiO_2 glass; other unchanged

measurement technique is impressive. However, the effect of particle sizes on the heating behaviour of the materials under microwave irradiation should have been considered. The studies of the stress-fracturing behaviour of the different oxide and sulphide ores showed that thermal stress fractures could be induced in some samples. These results are summarized in Figures 34 to 35[176]. However, it is not clear if similar thermal stress fractures could be induced by rapid heating using conventional heating methods.

Table XXXV. Effect of Microwave Heating on the Temperature of Natural Minerals [a,b] [176]

Mineral	Chemical Composition	Temp (K/°C)	Time (min.)	Mineral	Chemical Composition	Temp (K/°C)	Time (min.)
Albite	$NaAlSi_3O_8$	355/82	7	Arizonite	$Fe_2O_3 \bullet 3TiO_2$	563/290	10
Chalcocite	Cu_2S	1019/746	7	Chalcopyrite	$CuFeS_2$	1193/920	1
Chromite	$FeCr_2O_4$	428/155	7	Cinnabar	HgS	417/144	8
Galena	PbS	1229/956	7	Hematite	Fe_2O_3	455/182	7
Magnetite	Fe_3O_4	1531/1258	2.75	Marble	$CaCO_3$	347/74	4.25
Molybdenite	MoS_2	465/192	7	Orpiment	As_2S_3	365/92	4.5
Orthoclase	$KAlSi_3O_8$	340/67	7	Pyrite	FeS_2	1292/1019	6.75
Pyrrhotite	$Fe_{1-x}S$	1159/886	1.75	Quartz	SiO_2	352/79	7
Sphalerite	ZnS	360/87	7	Tetrahedrite	$Cu_{12}Sb_4S_{13}$	158/151	7
Zircon	$ZrSiO_4$	325/52	7				

[a]: Maximum temperature obtained in the indicated time interval. [b] :High purity as identified by X-ray diffraction.

They also conducted studies on the effect of power input on the heating rates of some oxides and sulphides. In general, an increase in the power input accelerated the heating rates, except for those very low and very high loss materials which were sensitive to the power input. As a general

Table XXXVI. Effect of Microwave Heating on the Temperature of Reagent Grade Elements and Compounds [a][176].

Chemical	Temp.(K/°C)	Time (min.)	Chemical	Temp.(K/°C)	Time (min.)
Al	850/577	6	Mo	933/660	4
$AlCl_3$	314/41	4	MoS_3	1379/1106	7
C	1556/1283	1	NaCl	356/83	7
$CaCl_2$	305/32	1.75	Nb	631/358	6
Co	970/697	3	NH_4Cl	304/31	3.5
Co_2O_3	1563/1290	3	Ni	657/384	1
CoS	431/158	7	NiCl	324/51	2.75
Cu	501/228	7	NiO	1598/1305	6.25
CuCl	892/619	13	NiS	524/251	7
$CuCl_2 \cdot 2H_2O$	444/171	2.75	Pb	550/277	7
CuO	1285/1012	6.25	$PbCl_2$	324/51	2
CuS	713/440	4.75	S	436/163	6
Fe	1041/768	7	Sb	663/390	1
$FeCl_2$	306/33	1.5	$SbCl_3$	497/224	1.75
$FeCl_3$	314/41	4	Sn	570/297	6
$FeCl_3 \cdot 6H_2O$	493/220	4.5	$SnCl_2$	749/476	2
Fe_2O_3	407/134	7	$SnCl_4$	322/49	8
$Fe_2(SO_4)_3 \cdot 9H_2O$	427/154	6	Ta	450/177	7
Hg	313/40	6	$TiCl_4$	304/31	4
$HgCl_2$	385/112	7	V	830/557	1
HgS	378/105	7	YCl_3	313/40	1.75
KCl	304/31	1	W	963/690	6.25
Mg	393120	7	WO_3	1543/1270	6
$MgCl_2 \cdot 6H_2O$	527/254	4	Zn	854/581	3
$MnCl_2$	326/53	1.75	$ZnCl_2$	882/609	7
MnO_2	1560/1287	6	Zr	735/462	6
$MnSO_4 \cdot H_2O$	320/47	5			

[a]: Maximum temperature obtained in the indicated time interval.

conclusion, some metal oxides, most metal sulphides, most minerals and amorphous carbon heat rapidly, while the gangue minerals do not readily heat.

Figure 34. Nonmicrowaved Pyrite Ore (light phase is pyrite; dark phase is quartz matrix, ×100) [176]

Figure 35. Microwaved Pyrite Ore Showing Stress Cracking (×100) ([176]

4-4. TEMPERATURE MEASUREMENT

Temperature measurement under microwave irradiation has been one of the major problems encountered in the microwave processing of materials. Thermocouples and optical pyrometers are the two most commonly employed instruments for temperature measurement. If pyrometers are used, serious error in the measured accuracy of temperatures can occur. Because the heat is being rapidly generated internally, the internal sample temperature will likely be higher than the surface. In some cases, errors as great as several hundred degrees are possible[175]. If thermocouples are used, the arcing between the sample and the thermocouple can occur, which leads to thermal runaway and ultimately failure of the thermocouple. According to Walkiewicz[176], Type K thermocouples can be employed with an ungrounded tip that is sheathed in Inconel 702 and stainless 440 to measure the temperature of the oxide and the sulphide samples, respectively. This technique was used to continuously measure the temperature of selected minerals and compounds. The accuracy of the thermocouple data was within ±2 % for samples that absorb microwaves. However errors of greater than ±2 % would be expected for samples that are transparent to microwaves, since microwaves would penetrate the samples and heat the surface of the thermocouple sheath. Another simple solution is to simply turn off the power during temperature measurement. This is perhaps the most widely used method, but it is obvious some decrease in temperature would be expected during the measurement period. Finally, another solution is to estimate the temperatures by identifying and analyzing the phases which are present in the samples and relate these to the thermal history of the sample. However, this is not a reliable method, because the phase composition also depends on a number of other factors.

Thus, it is clear that considerable work needs to be performed on developing accurate and reliable temperature measurement methods. This could involve the development of materials to eliminate the arcing problems which are encountered when thermocouples are employed.

4-5. EXPERIMENTAL

4-5-1. RAW MATERIAL AND PREPARATION

The EAF dust which was employed was from the same plant as that described in Chapter 3. Similar procedures and conditions were employed in order to remove any water-soluble species, such as sodium chloride and potassium chloride. The water content after drying was measured as less than 1%. The washed and dried EAF dust had the chemical composition as shown in Table XXXVII.

Table XXXVII. Chemical Composition of Water Washed and Dried EAF Dust

Element	Zn	Pb	Fe	Cd	Cr
%	24.93	2.28	12.81	0.32	0.13

4-5-2. APPARATUS AND PROCEDURES

A schematic diagram of the microwave-leach system is shown in Figure 36. A Samsung 900 W

(2.45 GHz) microwave oven was employed for this research. The reactor for leaching was constructed of teflon and had a diameter of 64 mm and a height of 64 mm.

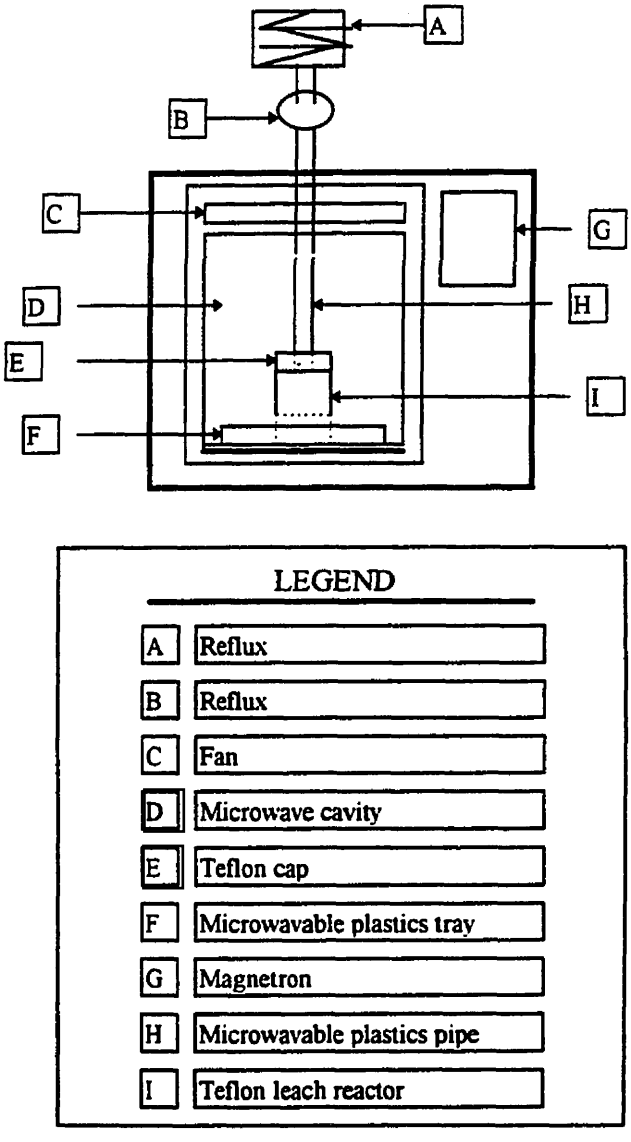

Figure 36. Schematic Diagram of the Microwave-Leaching Appratus

In each experiment, a 50 ml sodium hydroxide solution was employed to leach the EAF dust. The amount of dust was varied. The mixed dust and NaOH solution were sealed in the teflon container and placed in a plastic tray in the microwave oven. Before the power was turned on, all piples were collected and sealed except that which was from the reflux and open to the atmophere. After the desired leaching time, the oven was shut off and the temperature of the solution was immediately measured. A conventional vacuum filtering system was used to separate the leached solution. The leached residue was washed with water and dried to remove any water. AAS and XRD were employed respectively for the chemical and mineralogical analysis. The leaching reactions in the microwave oven were very violent and thus stirring was not required.

4-6. RESULTS AND DISCUSSION

4-6-1. GENERAL

In all the experiments, the zinc recovery (%) was calculated according to the following equation:

$$\text{Zinc recovery (\%)} = \frac{\text{Zinc in EAF Dust (g)-Zinc in Residue (g)}}{\text{Zinc in EAF Dust (g)}} \times 100 \qquad (4\text{-}5)$$

The observation that the reactions were so violent indicates that they likely occur at temperatures which were much higher than those actually measured for the solution. The reason for this phenomenon could be that under microwave irradiation, not only the water absorbs microwaves, but also the EAF dust. According to research by Ghoreshy and Pickles[141], EAF dust reached a temperature of 1073K(800^0 C) after only 5 minutes and 1473K(1200^0 C) after only 10 minutes in

the same microwave oven as used in this research. It was also observed that sparkling occured during all the leaching experiments. It is believed that the oxidation or burning of the sodium ions in the solution comes this phenomenon.

4-6-2. EFFECT OF LEACHING TIME ON ZINC RECOVERY (%)

Some experimental results are shown in Figure 37. It shows that the zinc recovery increases with the increasing of leaching time. Within minutes, the zinc recoveries have reached their maximum

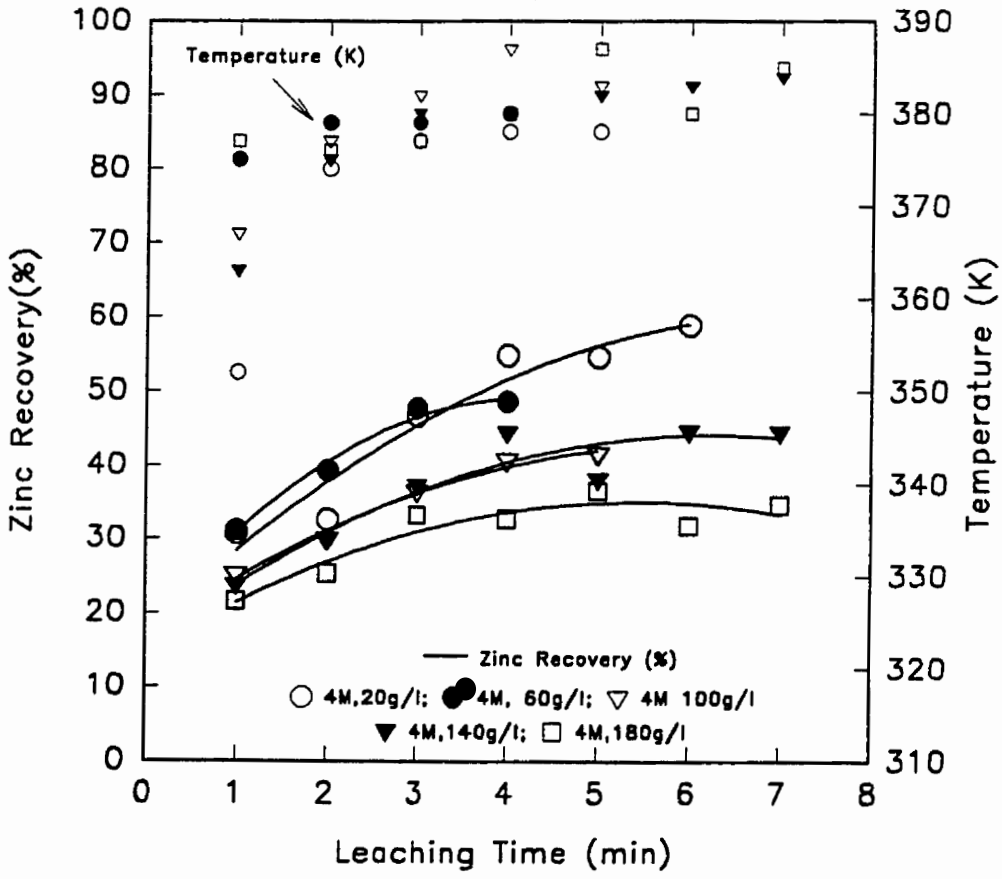

Figure 37. Effect of Leaching Time (min.) and Solids Concentration (%) on Zinc Recovery (%)

values. During leaching, the solution temperatures increase and reach the boiling points(bps) usually after two minutes. After reaching the bps, the temperatures increase slightly, which could be attributed to the phase changes within both the solution and the solids. Also, a slightly reduced volume of the solution during leaching could have an influence on this phenomenon.

4-6-3. EFFECT OF POWER LEVEL (%) ON ZINC RECOVERY (%)

The experiment data for the effect of power level are plotted in Figure 38. Generally, it can be

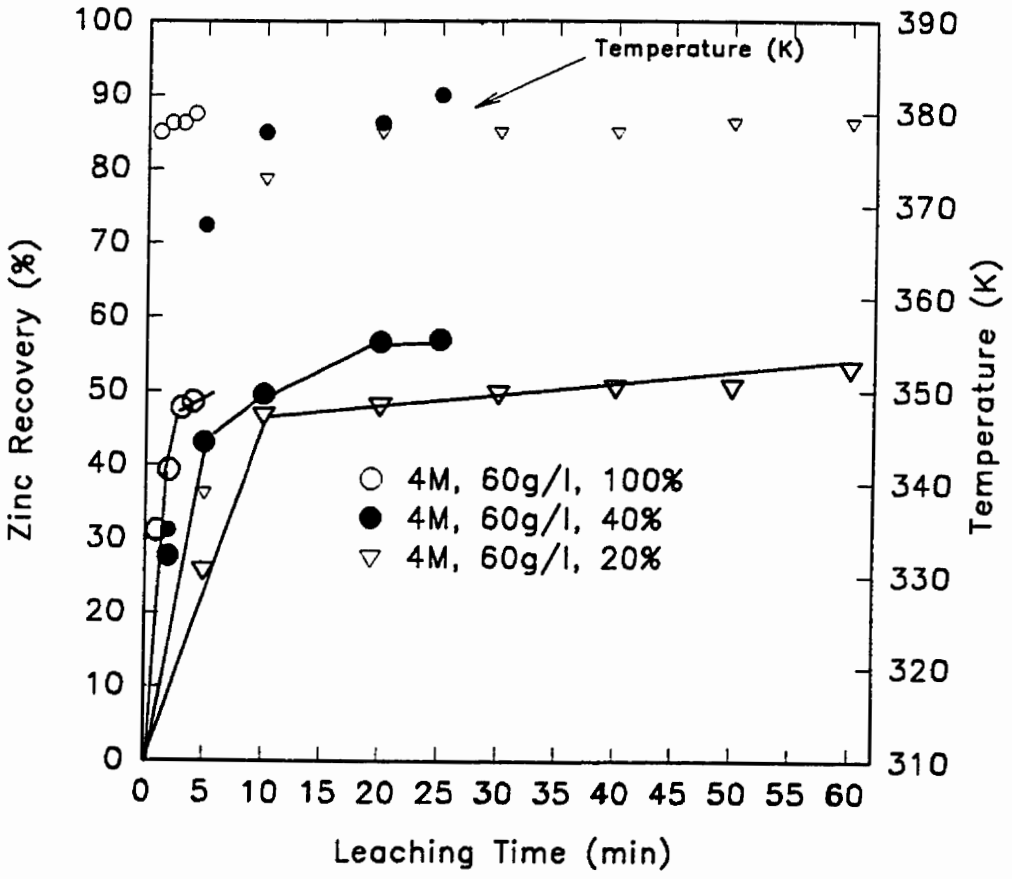

Figure 38. Effect of Power Level (%) on Zinc Recovery (%)

seen that higher power levels resulted in more rapid zinc dissolution. Also, the final zinc recovery increased with power. This phenomenon is attributed to the following facts: at higher power levels, the more intensive microwaves are generated, and the longer irradiation is exerted on the leaching materials.

4-6-4. EFFECT OF SOLIDS CONCENTRATION (%) ON ZINC RECOVERY (%)

As shown in Figure 37, five solids concentrations (20g/l, 60g/l, 100g/l, 140g/l, and 180g/l) were investigated. The results show that the zinc recovery increases with the decrease in solids concentration. As the concentration decreases below about 60g/l, no significant increase of the zinc recovery is noted.

4-6-5. EFFECT OF CAUSTIC CONCENTRATION (M) ON ZINC AND LEAD RECOVERIES (%)

The effect of caustic concentration on the zinc and the lead recoveries was investigated at solids concentration of 60 g/l and the results are shown in Figure 39. It can be seen that both the lead and the zinc recoveries increased with the increase in caustic concentration. The increase is more significant at concentrations above 6M for zinc and 8M for lead. On the contrary, for conventional leaching which was discussed in Chapter 3, the amount of lead which dissolved was less than that of zinc. This phenomenon could be attributed to the different coulping behaviour of the microwaves with the different solids. In the EAF dust, the zinc is present mainly as zinc ferrite and zinc oxide, while lead is present in the oxide and sulfate forms. Because the zinc oxide and the zinc ferrite absorb microwaves more readily than the lead oxide and the lead sulfate, then the actual leaching

temperature at the interface between the solids and the liquid solution must be higher at the interface with the zinc compounds than with the lead compounds. Thus, zinc may be easier to leach than lead under microwave irradiation.

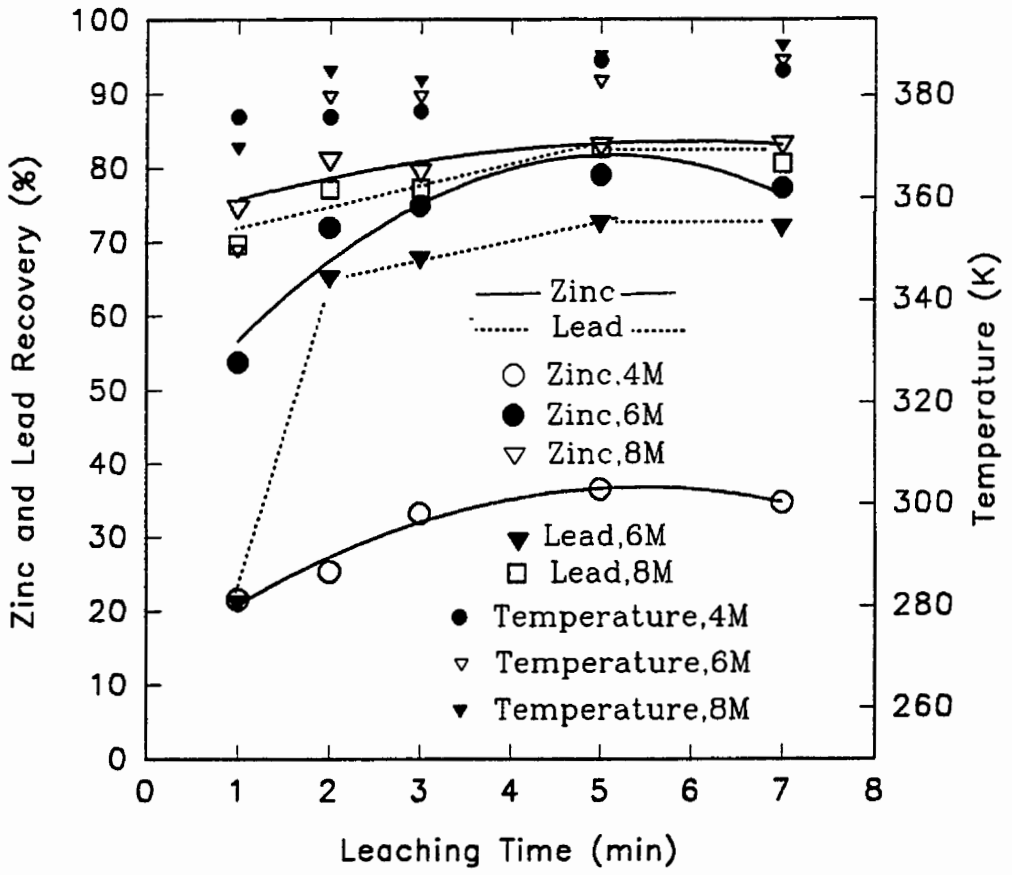

Figure 39. Effect of Caustic Concentration on Zinc and Lead Recoveries (%)

4-6-6. CHEMISTRY OF MICROWAVE LEACHING OF EAF DUST

Some experiments were performed using synthetic zinc ferrite under the following conditions: 60 g/l solids concentration, 6M caustic soda, 18 minutes and 100% power level. Figure 40 shows an XRD pattern for the leach residue of zinc ferrite. It shows that, even under such strong leaching conditions, most of the zinc ferrite remains unchanged. Also, as has been discussed in Chapter 2 for the non-microwave leaching of zinc ferrite, hematite is produced as zinc ferrite is dissolved.

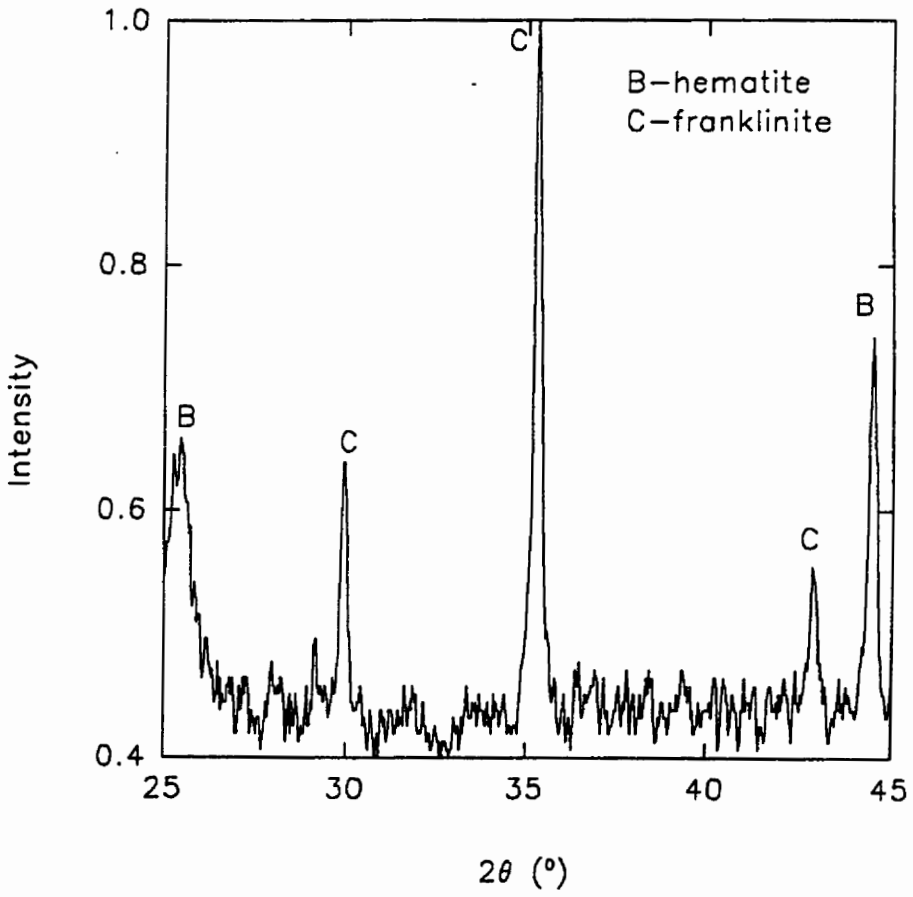

Figure 40. An XRD Pattern for Zinc Ferrite Leaching Residue

Figure 41 shows another XRD pattern of the leach residue of EAF dust. The leaching conditions employed for this experiment are as follows: microwave for five minutes, 6M caustic concentration and 60 g/l solids/liquid ratio. It shows that the predominent phases which are detected by XRD are the zinc ferrite and hematite, suggesting that all the zinc oxide has been dissolved, while most of the zinc ferrite is not dissolved.

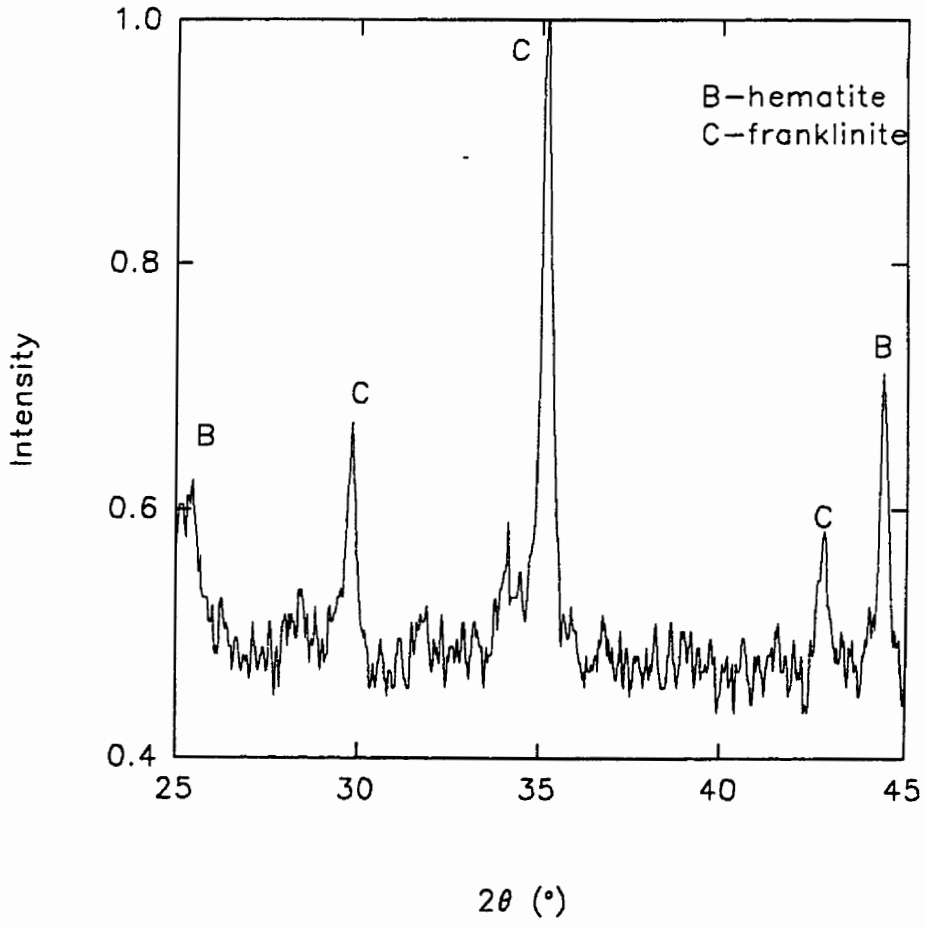

Figure 41. An XRD Pattern for EAF Dust Leaching Residue

Because the leaching reactions were non-thermal under microwave irradiation. Thus, the leaching reactions could be expressed by the following inequalities:

$$ZnFe_2O_4 + 2[OH^-] \rightarrow ZnO_2^{2-} + Fe_2O_3 + H_2O \quad (4\text{-}6)$$

$$ZnO + 2[OH^-] \rightarrow ZnO_2^{2-} + H_2O \quad (4\text{-}7)$$

$$PbO + 2[OH^-] \rightarrow PbO_2^{2-} + H_2O \quad (4\text{-}8)$$

4-6-7. BEHAVIOR OF OTHER ELEMENTS IN EAF DUST DURING MICROWAVE LEACHING

The behavior of some other elements, such as cadmium, chromium and iron, were investigated. The results are shown in Table XXXVIII, in which EAFD signifies EAF dust; R signifies leach residue; the first number after R signifies caustic concentration (M), and the last number signifies leaching time (min). For example, R6-1 represents the residue which was from the experiment in which the following conditions were employed: 6M and 1 minute leaching.

From the table, it can be seen that the dissolution of cadmium increases with the the increase of caustic concentration and leaching time. Cadmium is dissolved faster and more completely than zinc and lead, which implys that the cadmium may be present as phases which are more readily soluble in caustic solution than those phases which contain zinc and lead. In other words, cadmium may not be present as a substitute for zinc in zinc ferrite.

The table also shows that chromium is generally hard to dissolve; thus it may be mostly present as a ferrite.

Table XXXVIII. Behavior of Elements in the Leaching of EAF Dust

Material	Composition (%)				
	Zn	Pb	Fe	Cd	Cr
EAFD	24.93	2.28	12.81	0.32	0.13
R6-1	11.51	1.126	25.96	0.048	0.11
R6-2	6.975	0.625	26.57	0.049	0.12
R6-3	6.245	0.595	26.40	0.064	0.13
R6-5	5.231	0.540	26.69	0.051	0.12
R6-7	5.653	0.546	28.76	0.064	0.13
R8-1	6.301	0.573	29.71	0.065	0.15
R8-2	4.700	0.488	28.72	0.051	0.15
R8-3	5.087	0.487	29.30	0.065	0.13
R8-5	4.226	0.450	29.45	0.054	0.16
R8-7	4.193	0.426	28.28	0.051	0.15

4-6-8. COMPARISON OF CONVENTIONAL AND MICROWAVE LEACHING

Some experiment data were plotted in Figure 42, where the solid lines are the results from microwave leaching and the dashed line represents the results from the conventional leaching. The

conventional leaching conditions were as follows: 10M, 70 g/l solids, 366K(93^0 C) and 180 minutes. Under conventional conditions, the zinc recovery reaches a plateau at about 180 minutes with a maximum zinc recovery of about 72%. In microwave leaching, the zinc recovery reaches a plateau

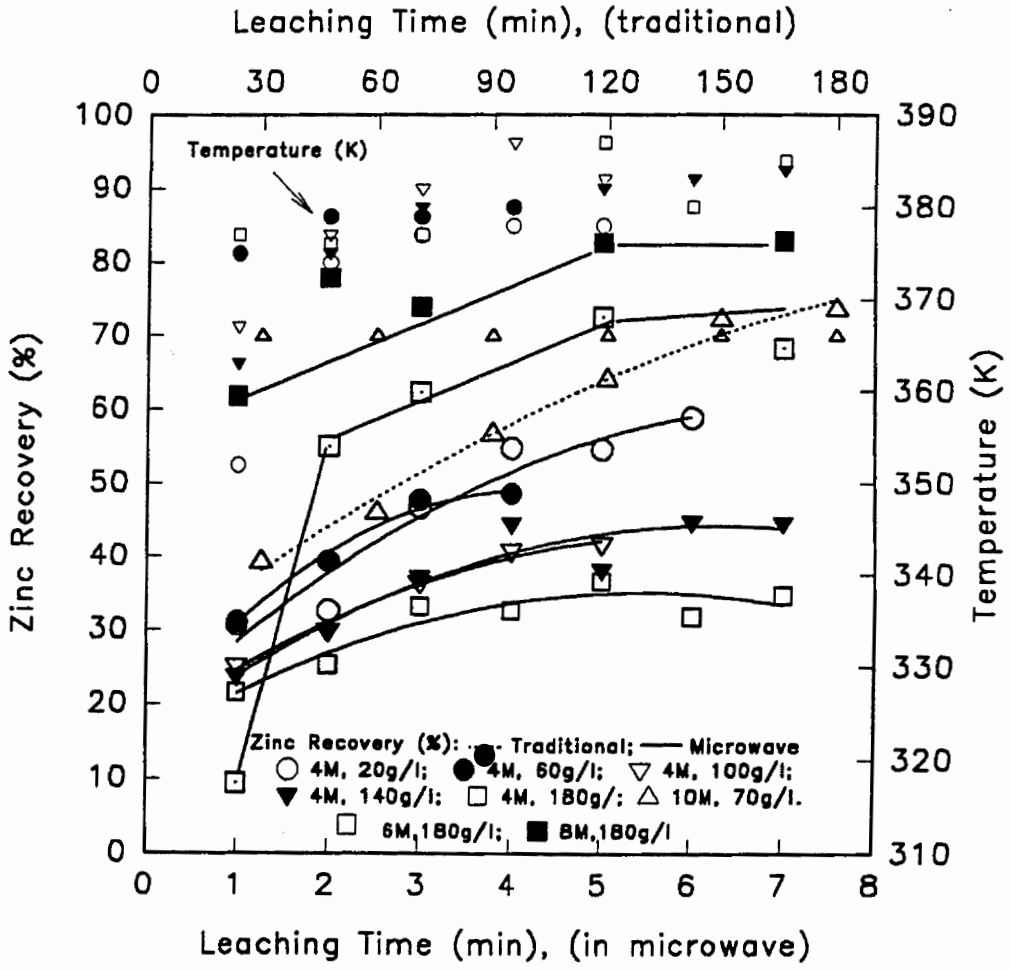

Figure 42. Comparison of Trational and Microwave Leaching

within a few minutes for all the experiments, indicating a very fast dissolution rate. For example, under the following leaching conditions: 8M, 180 g/l solids and boiling temperature, the zinc recovery reaches a maximum at about 5 minutes with a zinc recovery of about 80%. The fast dissolution rate in microwave leaching could be attributed to the following factors:

(1) Superheating;

(2) Favorable interactions of microwaves with EAF dust solids;

(3) Violent boiling of the leach solution.

Under microwave irradiation, most polar solvents have an inherent ability to be heated over their conventional boiling points. This phenomenon has been observed by a number of researchers [162, 180-182]. Baghurst and Mingos[162] explained this effect using a model of nucleation-limited boiling point. During a boiling process, bubbles nucleate preferentially at sites (cavities, pits, and scratches) on the vessel wall, allowing growth of the vapor phase. With conventional heating, the vessel wall and liquid surface are generally hotter than the bulk. In microwave processes, however, the vessel wall is cooler than the bulk solution due to convective heat losses from the surface, allowing the bulk to attain temperatures above the conventional boiling point before the boiling process commences.

The interactions of microwaves with the solids would intensify the supperheating effect. The temperature inside the solid particles may be much higher than that measured for the bulk solution.

The violent boiling and burning of the sodium ions, on the other hand, faciliated the transformation of the reactant species in the solution. Thus, the dissolution rates are further increased.

4-7. CONCLUSIONS

(1) Microwave leaching was very fast. Leaching was completed within minutes, while it took several hours for the conventional leaching process.

(2) The dissolution rate increased with the decrease of solids concentration. This effect was not significant at concentrations below 60 g/l.

(3) The effect of power level was significant. At higher power levels, the dissolution rates were faster and more zinc was dissolved.

(4) The effect of caustic concentration on the metal recovery was also significant. 8m was found to be the optimum concentration for lead, and 6m for zinc.

(5) Unlike conventional leaching in which more lead was dissolved than zinc, in the microwave leaching process, more zinc was dissolved than lead. This phenomenon was attributed to the different behaviour of zinc and lead compounds under microwave irradiation. Zinc oxide and zinc ferrite are better microwave absorbers than lead oxide and lead sulfate.

Chapter Five

A NOVEL HYBRID PROCESS FOR THE TREATMENT OF EAF DUST

SUMMARY

The problems associated with the hydrometallurgical treatment of EAF dust are reviewed. In this research, caustic soda was employed to decompose zinc ferrite in a low temperature roasting process. It was found that both synthetic zinc ferrite and the zinc ferrite which is present in EAF dust were decomposed. The zincite (ZnO) and sodium zincate (Na_2ZnO_2) were soluble and the hematite (Fe_2O_3) was insoluble. The zinc recovery was found to be about 95% after the low temperature roasting and a dilute caustic leaching process, while the majority of iron remained in the leach residue. Also, the distribution of other metal elements, such as lead, cadmium and chromium in this process, was investigated.

Finally, based on the experimental findings, a hybrid low temperature roasting and a dilute caustic leaching process followed by zinc cementation and electrowinning process is proposed and discussed. It is believed that this proposed hybrid EAF dust treatment process is superior to any other process which has been proposed.

5-1. INTRODUCTION

As discussed in Chapters One to Four, one common problem with hydrometallurgical treatment of EAF dust is the low zinc recovery in the leaching process due to the insoluble zinc ferrite which is present in the dust. Usually, the zinc ferrite accounts for 20-50% of the total zinc in the dust[10]. As a result, the zinc recovery in the leaching stage is only about 50-80% for most EAF dust treatment processes. In order to increase the zinc recovery, the zinc ferrite must be decomposed.

As demonstrated in Chapter 3, in concentrated caustic leaching, the fraction of zinc ferrite which was decomposed increased with the leaching temperature. In atmosphere, the maximum amount of decomposed zinc ferrite fraction was only about 9%, when it was dissolved in concentrated caustic solutions at about the boiling temperature. Initially, because of the high leaching temperatures which could be achieved, a caustic pressure leach process was considered in order to break up the zinc ferrite. This approach was abandoned for a number of reasons. Firstly, a study by Farrow and Burkin[183] demonstrated that magnetite was essentially insoluble in concentrated caustic solutions at temperatures up to 553K(280^0 C). According to Lu and Muir[111], when leached in acidic solutions, magnetite was over ten times more reactive than zinc ferrite. In other research on caustic pressure leaching of chromium minerals, the electron microprobe was employed and the results showed that a spinel-type structure which was rich in iron was left, as the chromite mineral was dissolved[183]. Since chromite has an inverse spinel structure, then it should be easier to dissolve than zinc ferrite which has a normal spinel structure. During this alkali pressure leaching process, the chromite initially dissolved very slow and eventurally the reaction ceased. Furthermore, the research on microwave leaching (in Chapter 4) indicated that the majority of the zinc ferrite could not be dissolved. In the microwave leaching process, it believed that the actual reaction temperature

at the interface between the EAF dust solids and caustic solution could be much higher than that which was measured for the bulk leaching solution (usually about 388K(115^0 C)).

In the Cardiff process [89](Chapter One), a reduction roasting process was combined with a conventional leaching process. The residue from the first caustic leaching stage was dried and then roasted at about 1273K(1000^0 C) in order to decompose the zinc ferrite. The total metal recovery of this process was about 80% for zinc and 90% for lead, as compared with 65-85% for zinc and 70-85% for lead for the Cebedeau process[85-88](in Chapter 1), in which no roasting processes were employed. This shows that the metal recovery, even after roasting, was still low.

Degliomini[184] has also carried out some research aimed at breaking up the zinc ferrite in the dust. In his work, two research routes were employed and the results are shown in Tables XXXIX and XXXX, respectively. The roast conditions of the two routes were the same and they are as follows: 10% coke, 1223K(950^0 C), 2 hours and a CO atmosphere.

The results shows that the second route gives both higher zinc and Cl, Na and K extractions than the first route, but zero lead extraction. Zero lead recovery suggests that the roasting process was over reducing and the insoluble metallic lead was produced. Again, after roasting and leaching, the zinc recovery was still very low at only about 83%.

It is clear that above roasting research, although preliminary, was relatively ineffective. In order to achieve an optimum roasting process, more experiments need to be performed. In the optimum roasting process, all of the zinc ferrite would be decomposed, the lead would be in the form of soluble compounds, and the iron would remain in the form of insoluble oxides. Thus, both high zinc and lead recoveries would be attainable in the following leaching stage, while iron would be mostly

Table XXXIX. ROUTE ONE [184]

Water Leach→First NaOH Leach→Roast→Second NaOH Leach Process

Water leach	Cl	Na	K	Ca	Pb	
EAF feed (350.0g), %	2.93	0.96	0.99	3.57	4.43	
H_2O residue (330.2 g) , %	0.44	0.34	0.12	3.69	4.57	
H_2O liquor, g/l	8.98	4.24	3.12	1.45	< 0.005	
Extraction, %	87	80	89	11	0	
First NaOH leaching	Zn	Pb	Fe	Cr	Cu	Cd
H_2O residue feed (292 g) , %	21.7	4.57	30.9	0.14	0.27	0.06
NaOH leach residue (230 g) , %	12.5	0.82	41.0	0.2	0.34	0.07
NaOH leach filtrate (1.17 l), g/l	31.6	10.1	0.04	<0.005	0.24	0.04
Metal extraction, %	53	86	<1	0	26	22
Second NaOH leaching	Zn					
Roasted residue (150 g), %	11.8					
NaOH residue (146 g), %	10.8					
NaOH liquor, g/l	0.89					
Zinc extraction, %	6.5					

Table XXXX. ROUTE TWO [184]

Roast→Water Leach→NaOH Leach Process

Water leaching	Cl	Na	K	Ca	Pb	
Roasted oxides (290 g), %	3.26	1.58	1.06	3.79	4.83	
H_2O liquor (0.41 l), g/l	10.1	4.8	3.2	0.38	<0.001	
H_2O residue (275 g), %	0.1	0.08	0.06	3.87	5.07	
Extraction, %	92	95	95	3	0	
NaOH leaching	Zn	Pb	Fe	Cr	Cu	Cd
H_2O residue feed (239 g), %	23.3	5.7	37.5	0.047	0.44	0.032
NaOH leach residue (189.3 g), %	5.02	7.2	47.3	0.06	0.56	0.001
NaOH leach liquor, g/l	50.1	<0.001	0.03	<0.001	<0.001	<0.001
Metal extraction, %	83	0	<1	0	0	1

retained in the leach residue. However, due to the very sensitive nature of the metal oxides to a reducing atmosphere, a successful roasting process would be elaborate in both process control and reactor design. The high roasting temperature and the carbon oxides emission to the atmosphere would be major disadvantages in the development of such a process.

5-2. PRINCIPLES OF PROPOSED ROASTING PROCESS

Any method which is employed to break up zinc ferrite and/or other insoluble compounds in EAF dust is usually performed at high temperatures, such as the high temperature reduction roasting process. Since the reactions occur at the interface between EAF dust solids and reducing agent, such as gaseuous CO and solid carbon, then the effectiveness of the reactions are not only dependent on the roasting temperatures, but also on the actual contact area between the reactants. As a result, a specially designed reactor, such as a fluidized-bed reactor, in which the reactions can take place effectively is usually required.

It is noteworthy that a roasting process could take place at low temperatures without reducing the reaction rate. Under reduced pressures, any reactions which produce gaseous products are favored and thus, the reactions occur at lower temperatures. But, again, a specially designed reactor is required. Another method to improve the reaction efficiency is to add some materials (such as borate) in the roasting process. When combined with such a material, the roasting temperature is reduced. Also, the reaction rate would be increased because of the improved reaction interfacial area. However, these advantages could be outweighed by other disadvantages.

Based on the very unique physical and chemical properties of caustic soda, a novel roasting process was proposed. As shown in Table XXXXI[185], unlike the hydroxide of alkaline-earth metals which decompose into their respective oxide and water when heated, the hydroxides of the alkali metals are quite stable. Instead of decomposing, they will be melting when heated. Among the various alkali metal hydroxides, caustic soda is the least expensive and it is compatible with the subsequent caustic leaching process. When EAF dust and caustic soda are mixed, the roasting

reactions occur at the interface between the EAF dust solids and the melted caustic soda at temperatures as low as 601K (328^0 C). The roasting reactions could be expressed as follows:

$$ZnO + 2NaOH = Na_2ZnO_2 + H_2O \quad (5\text{-}1)$$

$$ZnFe_2O_4 + 2NaOH = Na_2ZnO_2 + Fe_2O_3 + H_2O \quad (5\text{-}2)$$

Table XXXXI. Some Properties of Metal Hydroxides [185]

Hydroxide	LiOH	NaOH	KOH	RbOH	CsOH
Melting Point, ^{0}C/K	450/723	328/601	360/633	300/573	275/548
Enthalpy of Dissolution, kcal/m	4.8	10.4	13.2	14.7	16.8
Solubility, m/l, in water at 15^{0}C	5.3	26.4	19.1	17.9	25.8
Alkalinity	caustic	caustic	caustic	caustic	caustic

In principle, these roasting reactions are actually the same as those which occur in the leaching process. The major difference is that the lixiviant here is pure and the leaching temperature is much higher than that which could be achieved by the conventional leaching process. As a result, the metal values could be recovered in a very simple leaching process in which a dilute caustic solution

could be employed and the leaching time could be reduced. Due to the unique reaction nature, no emissions except some water vapour would be exhausted from this roasting process.

5-3. EXPERIMENTAL

5-3-1. RAW MATERIALS

The raw materials used were synthetic zinc ferrite and as-received COSTEEL-LASCO EAF dust. For the production of zinc ferrite, two temperatures were employed. At a temperature of 1473K(1200^0 C) and a sintering time of three hours, the zinc ferrite which was produced had a grey colour, while the zinc ferrite produced at 1073K(800^0 C) for six hours had a brown colour. Both zinc ferrites were characterized with XRD and quantified with AAS. The zinc ferrites were ground and sieved into a size range of −150+200 mesh. The chemical composition of the zinc ferrites is shown in Table XXXXII, while the XRD patterns are shown in Figures 43 and 44, respectively.

Table XXXXII. Composition of Synthetic Zinc Ferrite

Zinc Ferrite	Synthesis Temperature	Composition, %	
	K/^{0}C	Zn	Fe
A	1473/1200	28.80	48.18
B	1073/800	31.02	50.70

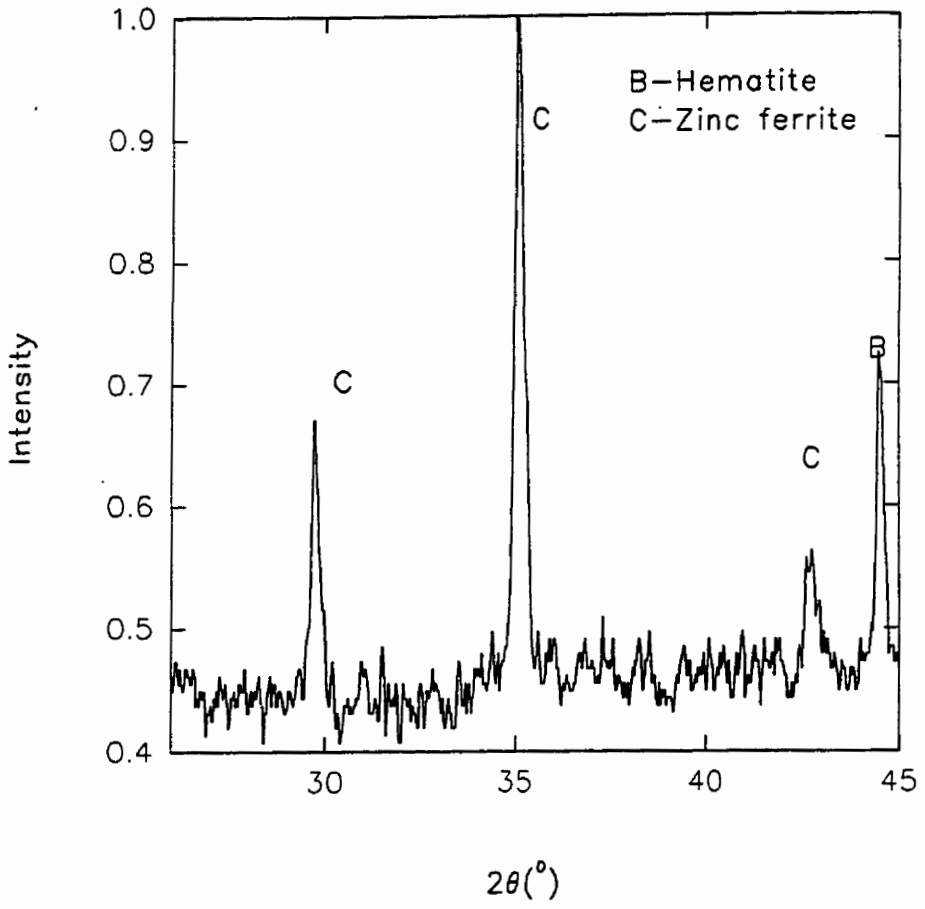

Figure 43. XRD Pattern of High Temperature Zinc Ferrite

The EAF dust used had a chemical composition which was shown in Table XXXXIII. The EAF dust was dried at about 473K(200 ^{0}C) for about 24 hours. It had a water content of about 0.5%.

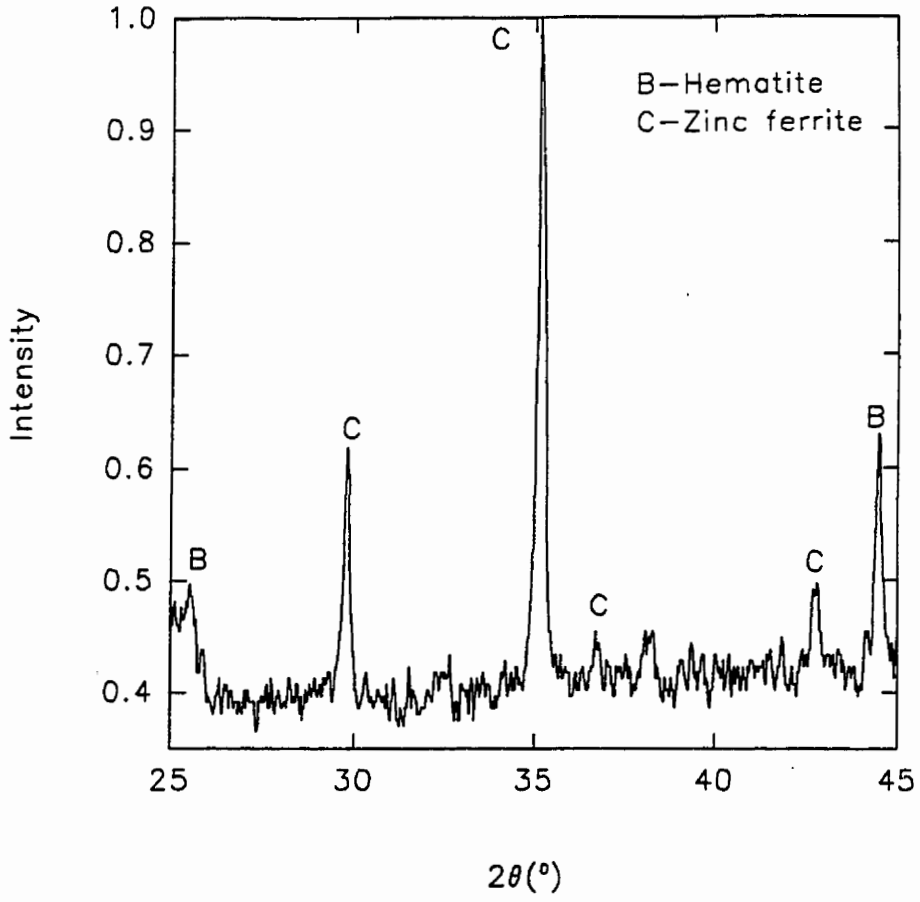

Figure 44. XRD Pattern of Low Temperature Zinc Ferrite

Table XXXXIII. Chemical Composition of COSTEEL-LASCO EAF Dust

Element	Zn	Fe	Pb	Cd	Cr
Composition (%)	22.87	12.80	2.2822	0.3249	0.1264

5-3-2. EXPERIMENTAL PROCEDURE

In each experiment, a sample of about 5 or 10 grams was employed and placed into a steel or nickel crucible. Both a Thermolyne 46100 high temperature furnace with molybdenum disilicide heating elements and a Lindberg high temperature furnace were used to heat the samples. The charged crucible was placed in the isothermal zone of the furnace, which was open to the atmosphere. Once the furnace attained the set temperature, then the temperature would drop a few degrees before it returned back to the constant value. This time was considered to be the start of the experiment.The roasted sample was allowed to cool in air and was finally stored in a desiccator for analysis.

5-3-3. ANALYSIS

In the XRD analysis, a small amount of water was added for some samples in order to provide a smooth sample surface. In the chemical analysis, all the solid samples were weighed using a METTLER AT 201 electronic digital scale and were fully digested using aqua regia. Then, a small amount of sample was taken and diluted using a 5% HCl solution.

The metal recovery was calculated according to the following equation.

Apparent recovery $R' = (C - C_1)100 / C$

where C is the mass percentage of zinc in the EAF dust and C_1 is the mass percentage of zinc in the leach residue.

The actual recovery was calculated according to the following equation:

$R = (WC - W_1C_1)100 / WC$

where W is the mass (g) of EAF dust and W_1 is the mass (g) of leach residue (g).

5-4. RESULTS AND DISCUSSION

5-4-1. ROASTING-LEACHING OF ZINC FERRITE

Zinc ferrite was roasted under various conditions in an air atmosphere. The roasting conditions are shown in Table XXXXIV.

Table XXXXIV. Zinc Ferrite Caustic Roasting Conditions and the Composition of the Leach Residues

Experiment No	Zinc Ferrite gram	Caustic gram	Mix Method hw *	Temp. C^0 / K	Time min	Roast-Leach Residue Comp. Zn%	Fe%
96-11-1	5.01585**	5.01839	hw	450/723	45	2.23	
96-11-2	5.01485	2.50015	hw	450/723	45	2.80	
96-11-3	5.01567	1.65645	hw	450/723	45	3.34	
96-11-4	5.03415	7.49699	hw	450/723	45	1.46	
96-11-5	5.03262	4.99783	hw	400/673	40	2.24	56.23
96-11-6	5.00785	2.48471	hw	400/673	40	6.52	60.79
96-11-7	5.02089	1.61429	hw	400/673	40	11.1	60.19
96-11-8	5.01812	7.49707	hw	400/673	40	2.01	49.28
96-11-9	4.96638	4.87731	hw	350/623	40	2.09	53.25
96-11-10	4.99286	2.57763	hw	350/623	40	14.10	61.43
96-11-11	4.98102	1.65327	hw	350/623	40	13.18	65.37
96-11-12	4.98231	7.49863	hw	350/623	40	7.18	62.88

*: Hand mixing with a few millilitres of water. **: Zinc ferrite B

After roasting, the residues were removed from the crucibles. Some of the residues were easy to remove from the crucibles, while others were difficult to remove, especially those which had larger amount of caustic soda and more water in the initial mixture. The residues which stuck to the crucible wall could easily be removed by adding some moisture.

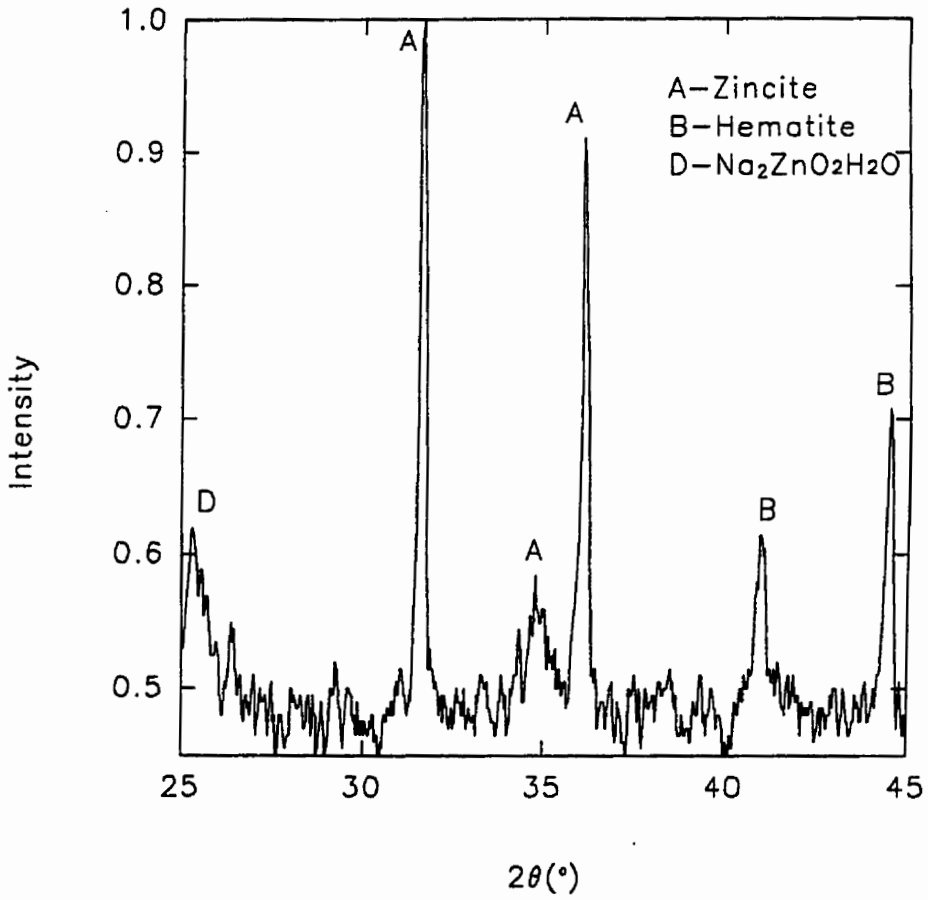

Figure 45. An XRD Pattern of the Roast Residue from Test 96-11-1

Figure 45 shows a typical XRD pattern of those samples which were obtained by water dissolution of the roast residue. It shows that the zinc ferrite decomposed during the caustic roasting process and zincite and hematite were the two predominant phases. The presence of zincite and hematite could be attributed to the following reactions.

$$\text{Roast reaction: } ZnFe_2O_4 + 2NaOH = Na_2ZnO_2 + Fe_2O_3 + H_2O \qquad (5\text{-}3)$$

$$\text{Water dissolution: } Na_2ZnO_2 + H_2O = ZnO + 2NaOH \qquad (5\text{-}4)$$

It was likely that the zincite would precipitate out onto the hematite particles, which served as nuclei for the precipitated zinc oxide. As a result, the hematite would be shielded during the water dissolution. Thus, the exposure of hematite to XRD would be improved by grinding.

Some XRD patterns for other tests are shown in Figures 46, 47, 48, 49 and 50, respectively. They all show similarities in terms of the phases which have been detected by XRD. In a few cases, zinc ferrite was detected. However, its amount was negligible, as suggested by the very weak XRD peaks. Instead of zincite, sodium zincate was detected as a major phase for those samples which were not dissolved in water. In conclusion, the zinc ferrite was decomposed during the roasting process under the conditions which were given in Table XXXXIV.

All roast samples were then leached with 4M NaOH at about 363K (90^0C) for one hour. Stirring was occasionally performed by hand. The leach slurries were filtered in a vacuum. The residues were dried and stored in a separate desiccator for AAS analysis.

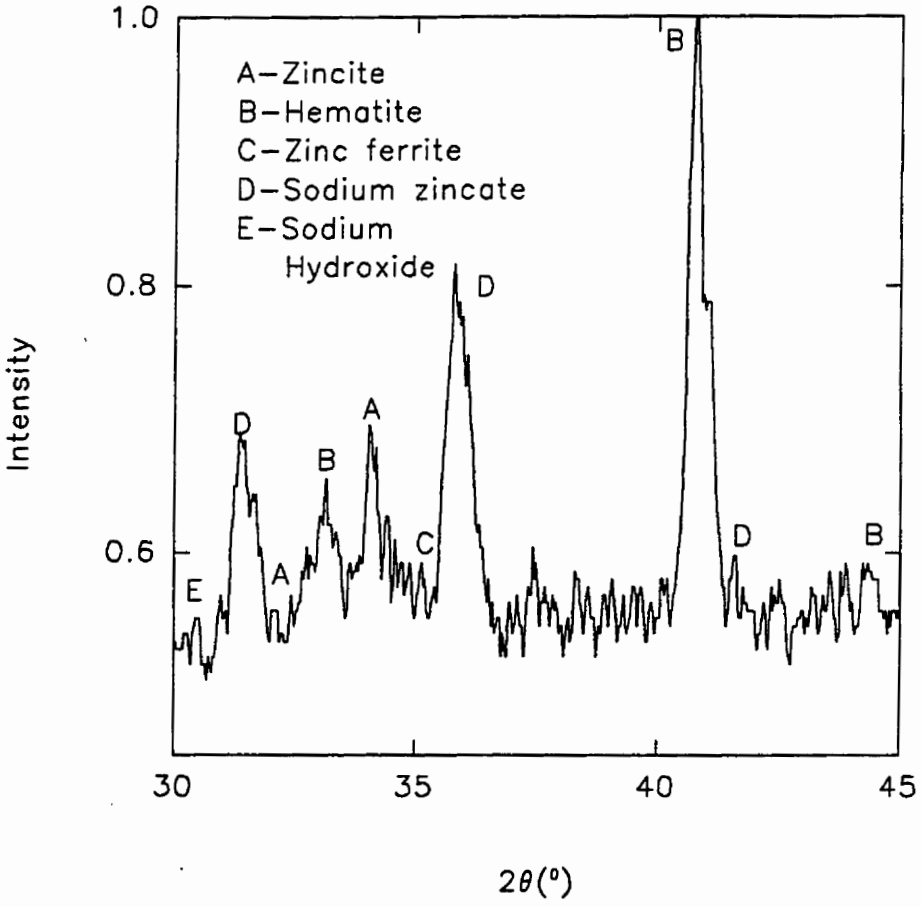

Figure 46. An XRD Pattern of the Roasting Residue from Test 96-11-2

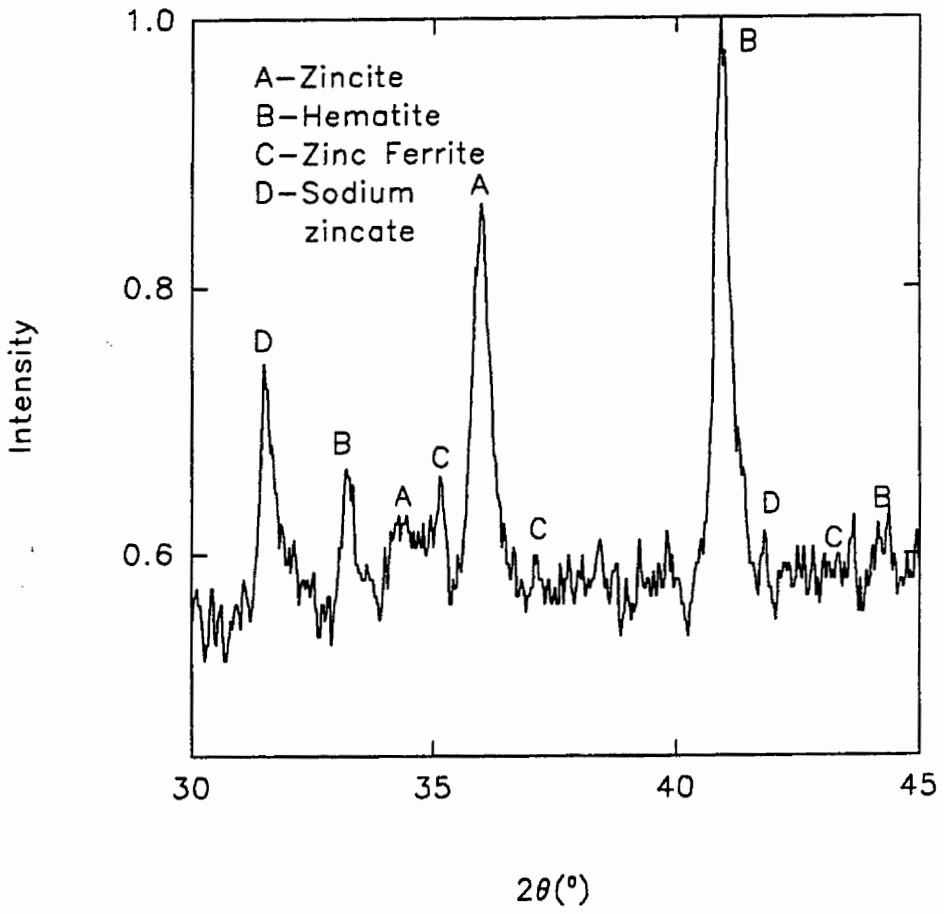

Figure 47. An XRD Pattern of the Roasting Residue from Test 96-11-3

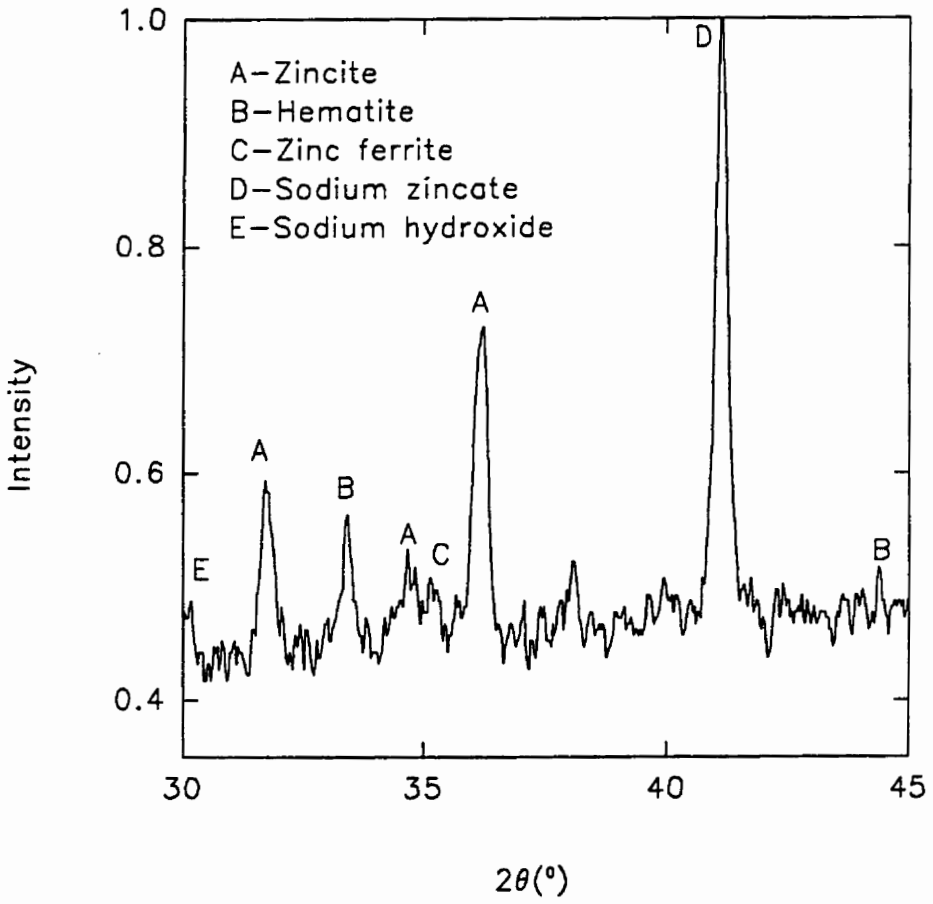

Figure 48. An XRD Pattern of the Roasting Residue from Test 96-11-4

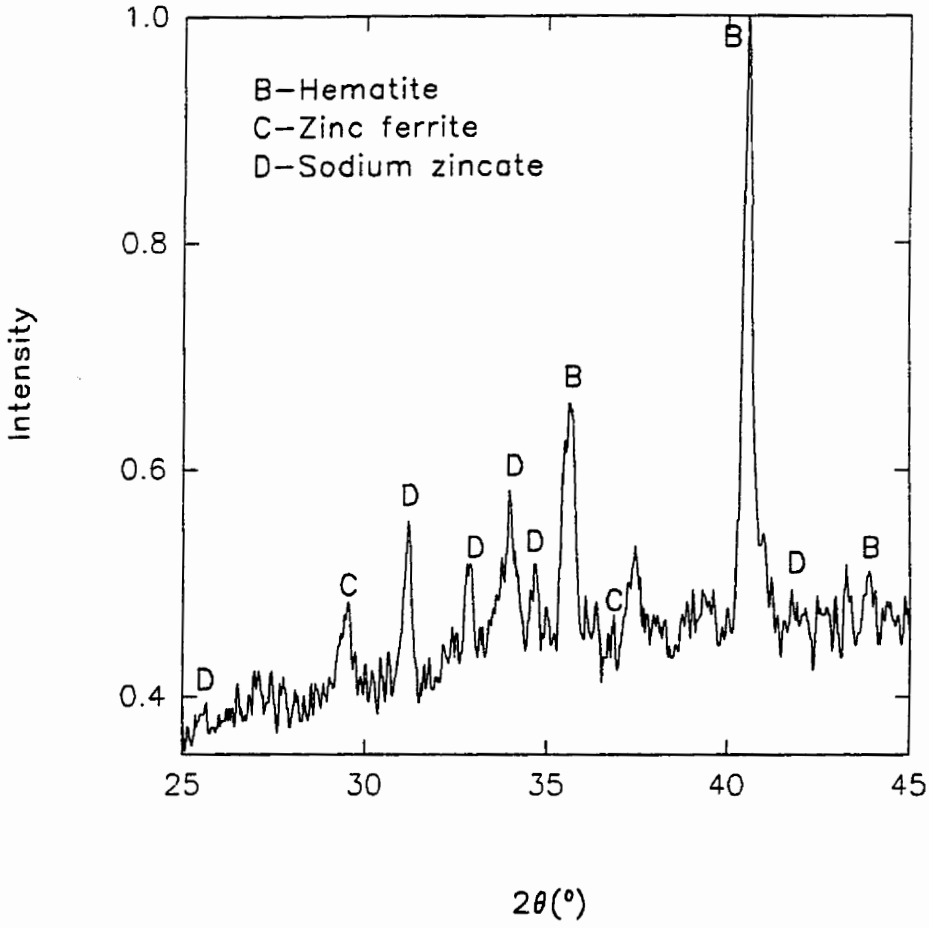

Figure 49. An XRD Pattern of the Roasting Residue from Test 96-11-5

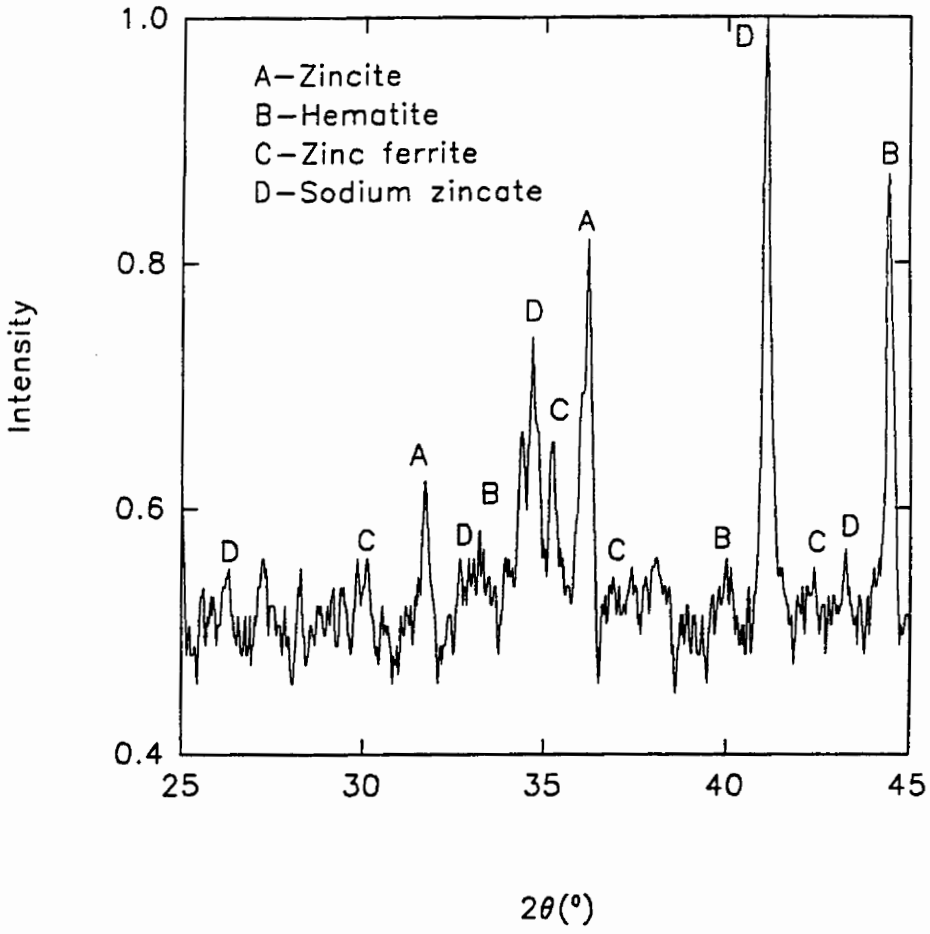

Figure 50. An XRD Pattern of the Roasting Residue from Test 96-11-8

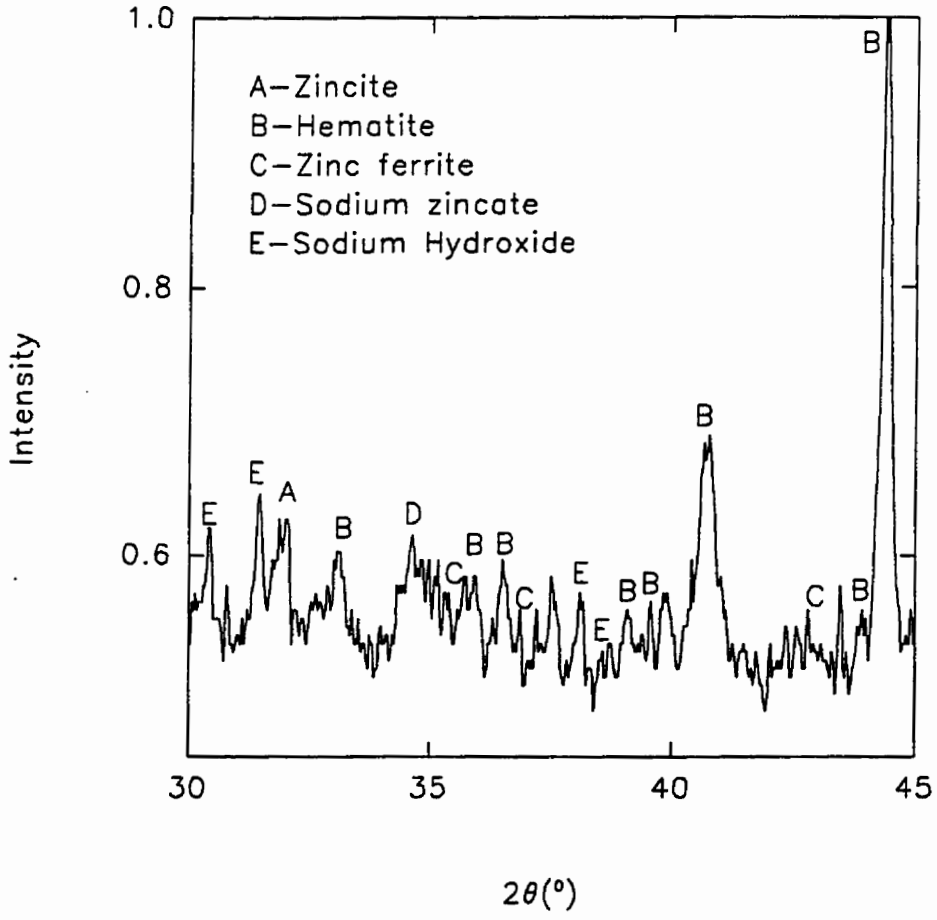

Figure 51. An XRD Pattern for the Leach Residue from Test 96-11-1

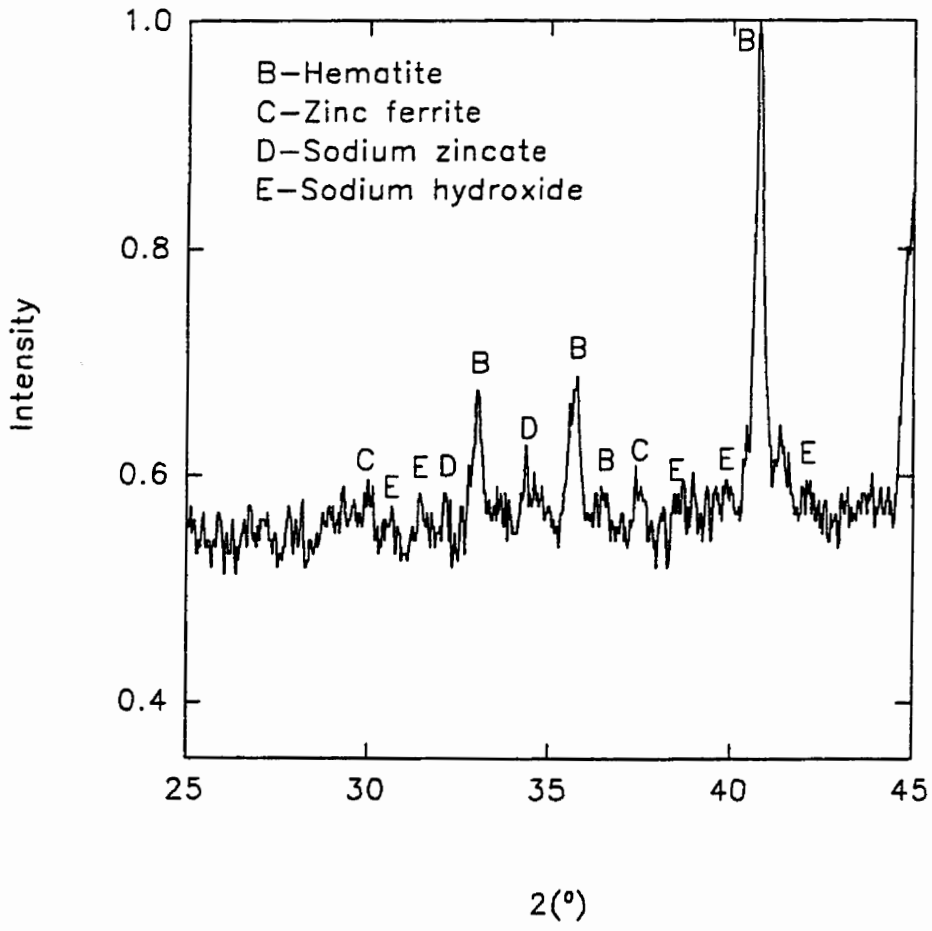

Figure 52. An XRD Pattern for the Leach Residue from Test 96-11-9

As shown in Figures 51 and 52, only hematite was detected by XRD as the predominant phase for these leach residues. Other phases, such as zincite, sodium zincate, zinc ferrite and sodium hydroxide were also detected. However, they were all present as a minor phase.

The chemical composition of some leach residues is given in Table XXXXV. Generally, it shows that zinc ferrite has been decomposed during roasting and the majority of zinc in the roast residues was dissolved. It also shows that the greater the amount of the zinc ferrite which was decomposed, the lower was the iron content of the leach residue, indicating that more iron was also dissolved.

5-4-2. ROASTING-LEACHING OF EAF DUST

A set of experiments were performed in order to investigate the effect of caustic roasting on the decomposition of zinc ferrite in EAF dust. The various roasting conditions which were employed are shown in Table XXXXV. To improve the mixing of the EAF dust particles and the caustic soda, a few millilitres of water were added to the mixture. After simple mechanical mixing, the materials were roasted in an air atmosphere.

After roasting, most of the samples were red in colour, indicating that the zinc ferrite in the dust had already broken down and hematite had been produced. This observation agreed with the XRD analysis of the roasted sample, which is shown in Figure 53.

To quantify the effectiveness of the roasting process, all the roasted samples were leached with dilute caustic solutions for about one hour. Initially, the leach slurries were filtered under a vacuum. It was later found that the filtering process was easier with these roast-leach slurries than with those

non-roasted leach slurries. As a result, the filtering was performed using a conventional filter in atmosphere.

Table XXXXV. Roasting Conditions for EAF Dust

Experiment No	EAFD g	Caustic g	Mixing hw/hwo	Temperature ^{0}C/K	Time min
EAFD-1	10.02523	4.29945	hw	400/673	40
EAFD-2	9.90161	6.33592	hw	400/673	40
EAFD-3	10.07628	8.81701	hw	400/673	40
EAFD-4	10.03609	10.53595	hw	400/673	40
EAFD-5	10.01011	13.38788	hw	400/673	40
EAFD-6	9.99250	4.25553	hw	400/673	30
EAFD-7	10.01886	6.31372	hw	400/673	30
EAFD-8	9.98453	8.86871	hw	400/673	30
EAFD-9	10.08646	10.31796	hw	400/673	30
EAFD-10	10.01742	13.33893	hw	400/673	30
EAFD-11	10.01295	2.35501	hwo	350/623	30
EAFD-12	10.06056	4.38986	hwo	350/623	30
EAFD-13	10.02206	6.10803	hwo	350/623	30
EAFD-14	10.01912	8.64830	hwo	350/623	30
EAFD-15	9.99367	10.06406	hwo	350/623	30

hwo: sample mixed with a few millilitres of water.

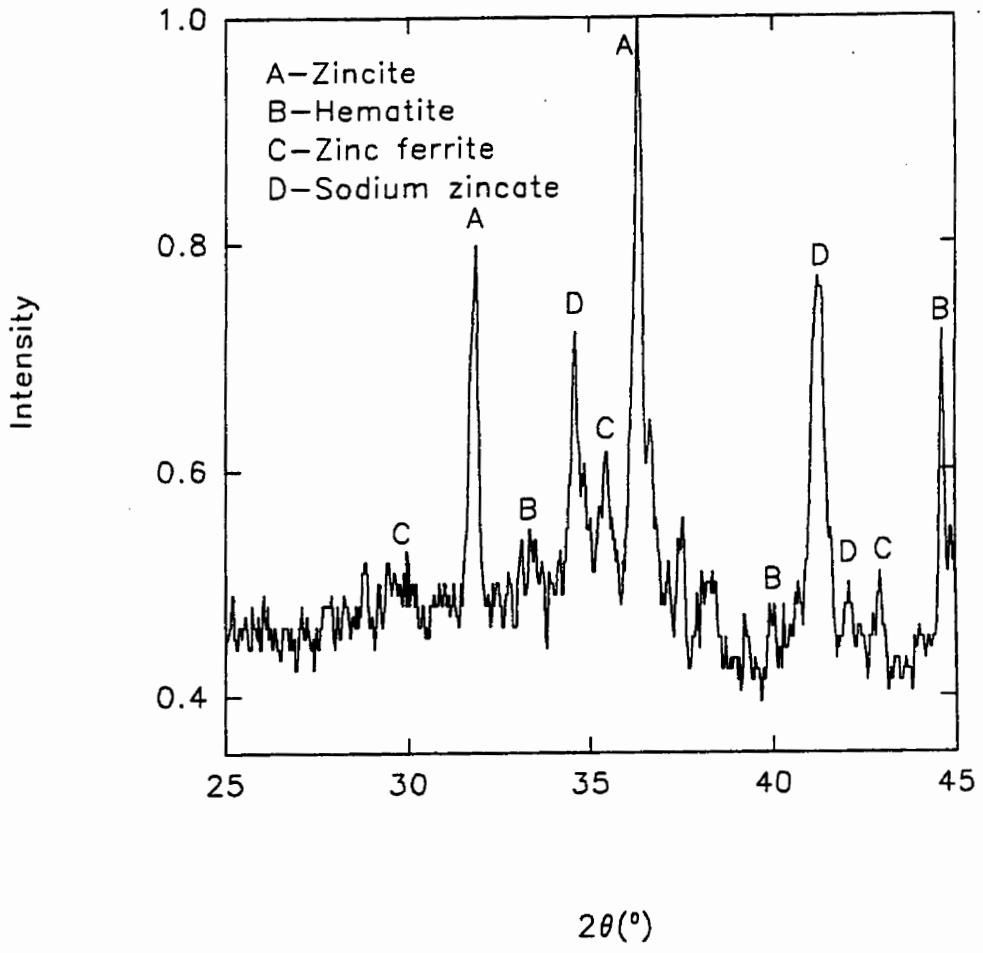

Figure 53. An XRD Pattern of the Roasted Sample from Test EAFD-1

In the caustic leaching process, problems are usually encountered in the solid-liquid separation process, because of the very fine zinc ferrite particles which are difficult to precipitate in the leach

slurries. However, during the caustic roasting process, most of these fine particles have been decomposed, and the hematite particles which were produced, although fine in size, were easy to precipitate. Accordingly, the filtering difficulties were overcome. With this improvement, it is likely that in a large scale test, a conventional filtering process could replace the costly and complex solid-liquid separation process which was employed in the Cardiff process[89].

Table XXXXVI. Leaching Conditions and Zinc Recovery

Experiment	Caustic	Temp.	Time	Stirring	Residue Composition, %		Zinc Recovery R' %
No	M	^{0}C/K	min	osw*	Zn	Fe	Zn
EAFD-1	4	90/363	60	oswh	1.04	18.49	95.45
EAFD-2	4	90/363	60	oswh	0.86	20.38	96.24
EAFD-3	4	90/363	60	oswh	0.48	17.96	97.90
EAFD-4	4	90/363	60	oswh	0.55	18.76	97.60
EAFD-5	4	90/363	60	oswh	0.41	19.06	98.21
EAFD-6	4	90/363	60	oswh	7.3528	32.7342	67.85
EAFD-7	4	90/363	60	oswh	1.7805	18.3661	92.21
EAFD-8	4	90/363	60	oswh	1.3741	24.0013	93.99
EAFD-9	4	90/363	60	oswh	1.2338	22.5706	94.61
EAFD-10	4	90/363	60	oswh	0.7419	17.7589	96.76
EAFD-11	4	90/363	60	oswh	9.6154	25.8774	57.96
EAFD-12	4	90/363	60	oswh	6.8659	26.5606	69.98
EAFD-13	4	90/363	60	oswh	5.6996	25.8427	75.08
EAFD-14	4	90/363	60	oswh	3.8185	27.4361	83.30
EAFD-15	4	90/363	60	oswh	3.0049	26.3133	86.86

*: oswh: Occasionally stirring by hand.

The chemical composition of the leach residues are shown in Table XXXXVI and indicates that, after caustic roasting, the zinc recovery was dramatically improved as compared to conventional roasting and leaching processes. The zinc recovery was usually about 95% for the caustic roasting and a dilute caustic leaching process, as compared with 65-85% for the Cebedeau process[85-88] and 80% for the Cardiff process[89]. Tables XXXXV and XXXXVI also show that the effect of roasting time and the amount of caustic which was added to the dust in the mixing process did not have a significant effect on zinc recovery, if the dust was roasted above 673K.

Based on the above preliminary results, another set of experiments was performed in order to determine the actual zinc recoveries, and to investigate the behaviour of the other elements in this hybrid EAF dust treatment process. Also, it was of interest to determine the effect of the water which was added to the mixture before roasting. The roasting and leaching conditions for this set of experiments and their corresponding results are shown in Table XXXXVII.

Table XXXXVII shows that the actual zinc recovery in the leachates was about 95% for most of the experiments, while the majority of iron in the dust remained in the leach residues as was indicated by very small iron recovery in the leachate. These experimental results also demonstrate that the mixing of the materials with water before roasting obviously improved the zinc recovery, if the materials were roasted at 623K(350^0C). However, mixing of the materials with or without water did not have a significant effect on zinc recovery, if the materials were roasted at 673K(400^0C).

The experimental results also show that the mixing of the materials with water before roasting improved the lead recovery. After roasting and leaching, the lead content was reduced from about

Table XXXXVII. Roasting and Leaching Conditions and Corresponding Results

Experiment No	EAFD-16	EAFD-17	EAFD-18	EAFD-19	EAFD-20	EAFD-21	EAFD-22	EAFD-23
				Roasting Conditions				
EAFD (g)	10.00217	10.01940	10.03524	10.00877	10.00131	10.03365	9.92165	9.97070
Caustic (g)	8.80556	7.20656	8.85190	10.01371	8.65338	10.05591	9.00061	10.05488
Mixing*	hwo	hwo	hw (3ml)	hw (3ml)	hwo	hwo	hw (3mi)	hw (3ml)
Temp.(^{0}C/K)	350/623	350/623	350/623	350/623	400/673	400/673	400/673	400/673
Time (min)	60	60	30	30	30	30	45	45
Residue (g)	18.78916	17.11157	18.77828	19.91531	18.53516	19.93107	18.71038	19.83345
				Leaching Conditions				
Caustic (M)	4	4	4	4	4	4	4	4
Temp.(^{0}C/K)	90/363	90/363	90/363	90/363	90/363	90/363	90/363	90/363
Time (min)	90	90	90	90	90	90	90	90
Residue (g)	6.53386	6.52934	6.49273	6.51196	6.61383	6.62493	6.25215	6.26864
				Chemical Composition (%)				
Zn	2.5566	2.9723	1.2856	1.7448	2.5634	1.8928	1.5332	1.3148
Fe	19.4746	19.1252	20.1689	21.3299	19.2683	19.2344	20.1918	20.1169
Pb	1.5659	1.3059	0.4987	0.6988	1.1465	1.1510	0.5715	0.4323
Cd	0.0515	0.0519	0.0560	0.0559	0.0537	0.0558	0.0537	0.0559
Cr	0.0361	0.0330	0.1170	0.1118	0.0390	0.0406	0.1270	0.1424
				Metal Recovery in Leachate R (%)				
Zn	92.70	91.53	96.36	95.04	92.59	94.54	95.78	96.39
Fe	0.6121	2.6286	nil	nil	0.4529	0.7821	0.5944	1.1905
Pb	55.18	62.71	85.86	80.08	66.78	66.70	84.22	88.09
Cd	89.66	89.59	88.83	88.81	89.07	88.65	89.58	89.19
Cr	81.33	83.02	40.06	42.45	79.59	78.79	36.68	29.13

*: hwo-hand mixing without water; hw-hand mixing with water.

2.28% to 0.43% for those materials which were roasted at 673K for 45 minutes and were leached with 4m caustic solutions at 363K(90^0C) for 90 minutes.

Under the experimental conditions, the recovery of cadmium did not change significantly. Usually, the cadmium content could be reduced from about 0.32% in the dust to about 0.034% in the leach residue.

However, the mixing of the materials with or without water did have a significant effect on the chromium recovery. Mixing of the materials without water favored the recovery of chromium in the leachate. It is likely that the roasting of the materials with water favored the formation of a chromium compound which was difficult to dissolve in comparison to that which was formed when roasting the materials without a water addition.

5-5. PROPOSED HYBRID PROCESS FOR THE TREATMENT OF EAF DUST

Based on the above findings, a hybrid low temperature pyrometallurgical and hydrometallurgical process is proposed for the treatment of EAF dust. Figure 54 shows a schematic flowsheet of this process.

5-5-1. PROCESS DESCRIPTION

In the process, the as-received EAF dust is first mixed with concentrated caustic solution or solid caustic soda. If the as-received EAF dust has a high halide content which could interfere with the quality of the electrolytic zinc, then, a water wash process can be employed in order to remove the

majority of the halides in the dust. According to the literature[10], after an EAF dust was leached at room temperature with water at a 1:3 solid-liquid ratio for one hour, about 91.5% of the chloride was removed. Another option to remove chlorides would be to bleed off a certain amount of spent

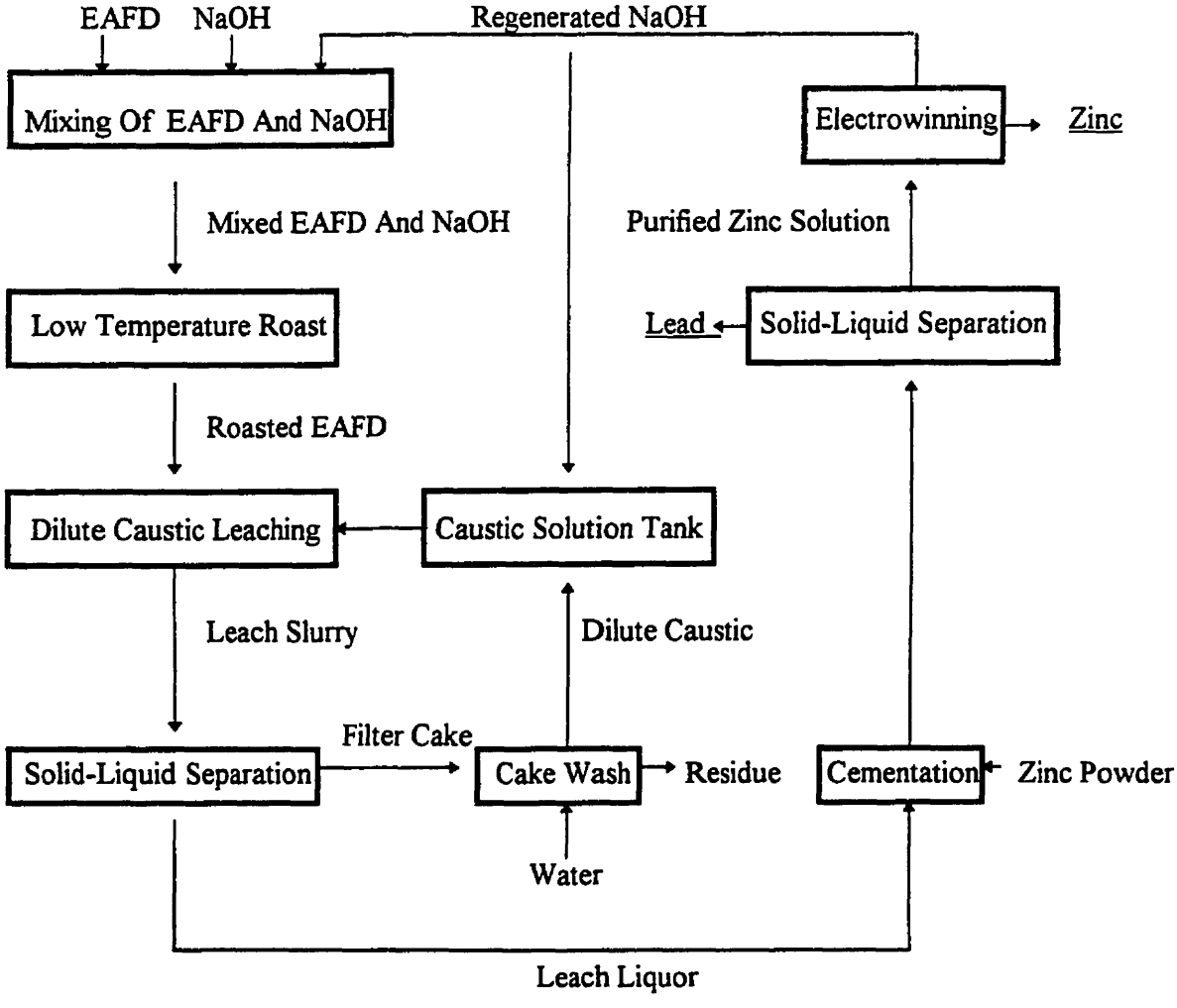

Figure 54. Schematic Flowsheet of Proposed EAF Dust Treatment Process

electrolyte from the electrowinning process, followed by a simple evaporation step in which the salts such as NaCl and KCl could be precipitated[85-88].

Then the mixed EAF dust and caustic soda are introduced to the roasting process. During roasting, the materials are dried and react to become soluble compounds. For example, zinc ferrite ($ZnFe_2O_4$), which is insoluble, would be decomposed and form soluble sodium zincate ($Na_2ZnO_2H_2O$) and insoluble hematite (Fe_2O_3). The roasting process does not need a complex reactor, since it involves a solid (EAF dust)-liquid (molten NaOH) reaction at temperatures as low as 603K (330^0 C) to 673K (400^0 C).

The only emission from this process is water vapour and thus there are significant environmental benefits.

In the conventional roasting processes, reducing agents, such as carbon, are usually added to reduce metal-containing compounds, such as zinc ferrite, at temperatures as high as about 1273K (1000^0 C). In addition to the high energy consumption, the emission of CO_2, CO and halides is unavoidable. Another problem is that the operating conditions need to be carefully controlled; otherwise, lead is not easily recovered.

In the caustic roasting process the EAF dust can be easily leached with a dilute caustic solution. During the leaching process, metals, such as zinc, lead and cadmium are readily dissolved at temperatures between 333K (60^0 C) and 363K (90^0 C) for only about 60 to 90 minutes, while the iron remains in the solid residue.

The slurry from the leaching process is then introduced to a solid-liquid separation process. In this process, the difficulties which are usually encountered in the solid-liquid separation process due to the very fine zinc ferrite particles are avoided, since these fine particles have been decomposed during the caustic roasting process. As a result, conventional solid-liquid separation methods can be used.

After washing with water, the filter cake can be removed from the process as an inert solid residue. It can be recycled to the steelmaking process or land-filled at conventional sites.

The leach liquor can be purified by the addition of zinc powder. During this stage, any metal ions which are chemically more noble than zinc ions, such as lead, cadmium, silver and copper ions, would be precipitated from the leach liquor. The cemented lead which also contains other metals can be sold to lead smelters as a raw material, or it can be further treated in order to separate the metal values.

Finally, zinc is recovered from the purified liquor as pure zinc powder in an electrowinning process. During this stage, the caustic is regenerated and can be recycled to be used in the roasting and leaching processes.

5-5-2. FEATURES OF THE PROCESS

This proposed process has the following features.

(1) The process is very simple and basically a closed system.

(2) Roasting is conducted without any reducing agent at very low temperatures (around 623K/350^0 C). During roasting, only water vapour is released to the atmosphere.

(3) The process has great flexibility in both the kind and quantity of the materials to be treated. For example, electric arc furnace dust of any chemical composition and mineralogy, and of both small and large tonnage, can be treated effectively and economically.

(4) A complex reactor is not required for this process. Actually, due to the very low roasting temperatures, one reactor could be employed for both the roasting and leaching processes.

(5) Zinc and lead can be recovered separately in metallic form. The leach residue can be recycled to the steelmaking process, or land-filled at a conventional site.

5-6. CONCLUSIONS

The treatment of EAF dust has been a troublesome problem for EAF steelmakers for many years. Treatment processes which are both economic and environmentally safe have not been found.

Pyrometallurgical processes are usually energy intensive due to the high processing temperatures, and have less economic benefits due to the lower value and impure metal products. Hydrometallurgical processes, on the other hand, are complex and also uneconomic, due to the extended process flowsheet and inefficient metal recoveries which are due to the insoluble zinc ferrite in the dust.

Based on the present research results in which both synthetic zinc ferrite and the zinc ferrite in the dust have been decomposed and become soluble compounds during the roasting process, a hybrid low temperature roasting and dilute caustic leaching process followed by zinc cementation and electrowinning has been proposed for the treatment of EAF dust.

In this hybrid process, it is possible that the EAF dust can be treated economically due to the high metal recoveries and the low energy consumption. The metals can be recovered in metallic form and the leach residue can be recycled to the steelmaking process or land-filled in a conventional site. The process is environmentally safe and has a great potential for both the treatment of EAF dust and other similar zinc-bearing materials.

ORIGINAL CONTRIBUTION OF THIS THESIS RESEARCH

Due to the high concentration of zinc ferrite in EAF dust and since the zinc ferrite is insoluble when it is leached, the recovery of zinc is usually low in the hydrometallurgical treatment of EAF dust.

The present research on the kinetics of zinc ferrite formation (in Appendix) contributes to an improved understanding of the reaction mechanism involved in zinc ferrite formation during roasting and dust formation processes in pyrometallurgical processes.

The research on the kinetics of zinc ferrite leaching in caustic media (in Chapter Two) is the first research which has been performed on pure synthetic zinc ferrite. It contributes to an improved understanding of the zinc ferrite dissolution mechanism. The following leaching reaction was experimentally verified: $ZnFe_2O_4 + 2[OH^-] = ZnO_2^{2-} + Fe_2O_3 + H_2O$.

The research on the leaching of EAF dust in caustic media (in Chapter Three) provided an improved understanding of the problems which could be encountered in the leaching process. It demonstrated that the leaching temperature was the major variable in the leaching process which could be employed to increase the metal recovery. However, even at the boiling point of the solution, the recovery of the zinc was low.

The research on the microwave leaching of EAF dust (in Chapter Four) was the first process to use microwaves for the leaching of EAF dust. It was found that the dissolution reactions in microwaves were violent and very fast, indicating that the actual reaction temperature was much higher than that

which was measured for the solution. This research showed that there are many advantages in the application of microwaves as a novel energy source in the leaching process.

The research on the low temperature roasting of both the synthetic zinc ferrite and EAF dust (in Chapter Five) resulted in a novel process in which the insoluble zinc ferrite was decomposed at low temperatures and the zinc oxide was soluble and thus the zinc could be recovered in the subsequent caustic leaching process. The main features of this roasting process are the low operating temperature, thermal efficiency, high zinc recovery and environmental benefits. At the present time, these features can not be achieved by any other conventional roasting processes.

Overall, this thesis research resulted in the development of a hybrid EAF dust treatment process, in which the EAF dust can be roasted at low temperatures and high metal recoveries can be achieved in the subsequent caustic leaching process. Impurities can be removed by zinc cementation and zinc can be recovered in metallic form in an electrowinning process. The process is essentially a closed system and no emissions are exhausted to the atmsphere except for water vapour. This proposed process is superior in many aspects to other hybrid processes which have been proposed.

Appendix

KINETICS OF ZINC FERRITE FORMATION IN THE RATE DECELERATION PERIOD

SUMMARY

The initial surface chemical reaction involved in zinc ferrite formation is very rapid at any given temperature, and the reactants quickly become covered with zinc ferrite. Then the reaction rate becomes decelerated. In this work, the kinetics of zinc ferrite formation during this rate deceleration period was studied in the temperature range of 873 K to 1073 K. The experimental data were found to be best described by Jander's model and the activation energy was found to be about 168 kJ mol^{-1}. This activation energy indicates that diffusion is rate controlling. The effect of briquetting pressure was more significant at low compaction pressures and sample size had no effect in the range studied. These results contribute to an improved understanding of the formation mechanism of some soft ferrites, such as MnZn-ferrite and NiZn-ferrite, which are employed in the electronics industry, and also the formation of zinc ferrite during roasting and dust formation in pyrometallurgical processes.

A-1. INTRODUCTION

Zinc ferrite formation is of interest to both the electronics and the metallurgical industries. In the electronics industry, it has been found that both the magnetic and the electrical properties of ferrites can be substantially improved if some zinc oxide is present[186-188]. For example, the addition of zinc ferrite ($ZnFe_2O_4$) to magnetite (Fe_3O_4), manganese ferrite ($MnFe_2O_4$) and nickel ferrite ($NiFe_2O_4$) results in the formation of ferrites which have substantially higher magnetic moments than the pure ferrites[186-189]. It is noteworthy that in its pure form, zinc ferrite has a magnetic moment of zero[186-188]. In the metallurgical industry, zinc ferrite is found in the calcine from the roasting of zinc ores and also in the dust which is generated when galvanized scrap is melted in the electric arc furnace (EAF). The zinc, in the zinc ferrite, is difficult to recover, since it is insoluble in both dilute sulphuric acid and caustic solutions.

Ferrite formation is a relatively simple solid state reaction and is often selected as a model system for homogeneous rate processes[190]. Some previous research has been performed on the formation of zinc ferrite. As early as 1931, Guillissen and Van Rysselberghe investigated the effects of temperature and time on zinc ferrite formation[191]. A fine mixture of zinc oxide and iron oxide was heated at successively higher temperatures for various time increments. Then, the unreacted zinc oxide in the mixture was extracted with an ammoniacal solution. They found that above 873 K, the reaction proceeded rapidly. It began at 853 K and was completed at 1343 K. Their results also showed that for the first 3 hours the reaction followed a linear relationship in accordance with Tammann's law[192]:

$$C = A\log t + B \qquad \text{(A-1)}$$

where C is the fraction of ferrite formed at time t for a given temperature and A and B are constants. A similar study by Kedesdy and Katz employed X-ray diffraction to measure the extent of reaction between the constituent oxides[193]. The mixed oxides were pressed at about 1,758 kg cm^{-2} and heated for 5 hours at various temperatures in air. Then, the compacts were quenched, ground and examined by X-ray diffraction. Their results showed that only a small amount of reaction took place below 873 K and the reaction was complete at about 1373 K. Heating to higher temperatures merely increased the crystallinity of the reaction product. In their study of the reaction, Furuichi et al[194] modified Jander's equation:

$$[1-(1-X)^{1/3}]^2 = kt \qquad \text{(A-2)}$$

by incorporating the condition that the initial surface reaction was much faster than the later diffusion-controlled process. Their modified Jander's equation is as follows:

$$\{1-[1-(X-X_s/1-X_s)]^{1/3}\}^2 = kt / (1-X_s)^{2/3} \qquad \text{(A-3)}$$

where X is the total fraction reacted, X_s is the fraction reacted in the surface reaction and k is the rate constant. This equation can be employed to investigate the initial surface reaction, since the thickness of the product layer, X_s, can be calculated. However, since the X_s value could only be determined by fitting the experimental data to a straight line, which passes through the origin, then errors were introduced[195]. In fact, there is no difference between this modified equation and Jander's equation, if only the kinetic data from the later stages are employed. Recently, Shimada et al[195] used this equation in their research and demonstrated that the zinc oxide was the more mobile constituent and migrated to the surface of the α-Fe_2O_3 particles in the initial rapid reaction

stages. The zinc ferrite layer which formed on the surface had a characteristic texture. This observation was in agreement with the results of other authors[196-201]. Their results also showed that the initial particle size of the hematite (Fe_2O_3) had an effect on the initial surface reaction with zinc oxide, but it had no influence on the diffusion process[195]. Some investigators, such as Hedvall[202] and others[203-205], believed that structure-sensitive factors, such as impurities and imperfections would exert a major influence on the reactivity of solids, such as zinc oxide and hematite. On the other hand, other investigators[206-212] believed that geometrical factors, such as the contact area and the shape of the reactant particles, would have a more significant effect on the kinetics of zinc ferrite formation.

In summary, zinc ferrite formation is a complex process which depends on both the structural and the geometrical factors. In many cases, the results of the various researchers can not be directly compared, because of the difference in the composition, the structure, and/or the geometry of the original materials. In the past, research was more focussed on the earlier stages of zinc ferrite formation rather than on the later stages or the deceleration period. Since it is comparatively easy for the initial surface reaction to take place, then the final stages appear to be more significant than the earlier stages. Thus, in the present research, emphasis was placed on the later stages of the zinc ferrite formation process. The effects of temperature, time, briquette compacting pressure and sample size were investigated.

A-2. EXPERIMENTAL

A-2-1. RAW MATERIALS AND SAMPLE PREPARATION

Commercial purity zinc oxide (>99.9%) and alpha-hematite (>99.5) were employed as the raw materials. Both materials were heated to 753 K for sixty minutes to remove moisture. Then the powders were ball milled and sieved into various size fractions. The zinc oxide particles were in the size range of 73.7 to 104.1 microns while the alpha-hematite was in the size range of 53.3 to 73.7 microns. Equi-molar amounts of zinc oxide and alpha-hematite were dry mixed in an alumina mortar and pestle for thirty minutes. Then the powders were fully mixed in an automatic alumina mortar and pestle for one-hundred-and twenty minutes.

The mixed powders were compacted into briquettes in an alloy steel mold with one movable plunger. The briquettes, which had a diameter of 25.5 mm, were again heated to 753 K for thirty minutes in order to remove any water and/or organic mold lubricant, which could interfere with the reaction. The standard three-gram sample had a height of 2.1 mm. A Thermolyne 46100 high temperature furnace with molybdenum disilicide heating elements was used to heat the sample to the reaction temperatures. Each briquette was placed on a porous alumina plate, which was within the constant temperature zone of the furnace for each reaction temperature. Cylindrical alumina crucibles were used for the powder samples (i.e. zero compaction pressure). Initially, when the sample was placed into the furnace, the temperature, would drop by a few degrees during the first three to four minutes. At the completion of the test, the reacted samples were removed and cooled in air.

A-2-2. PRODUCT ANALYSIS

The reacted samples were crushed with a mortar and pestle and the unreacted zinc oxide was extracted using 4M NaOH for 4 hours. The resulting solutions were analyzed using Atomic

Absorption Spectroscopy (AAS). Standards were prepared by dissolving known amounts of analytical grade zinc oxide in the same 4 M NaOH solution. In order to obtain reproducible results, the following procedures were followed in the AAS analysis: (1) a nitrous-acetylene flame was employed to minimize the interference from zinc; (2) the burner was cleaned before each analysis in order to minimize the accumulation of caustic elements.

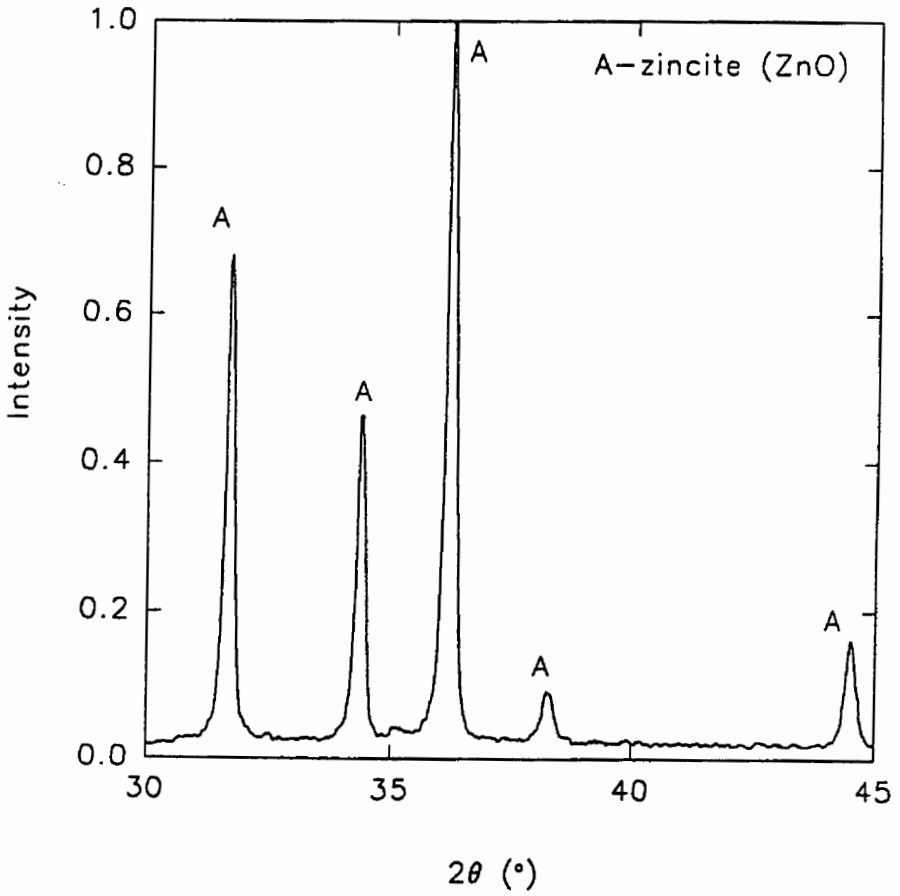

Figure 55: (a) XRD Pattern for Zinc Oxide

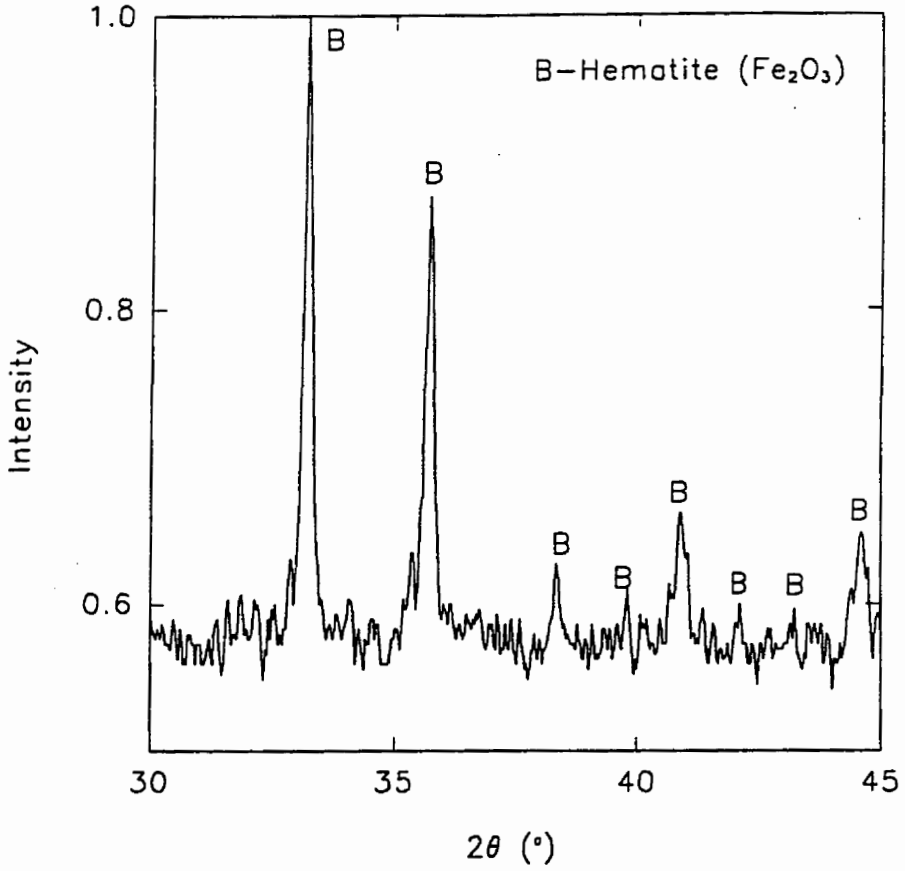

Figure 55: (b) XRD Pattern for Iron Oxide

X-ray diffraction (XRD) analysis was employed to identify the various phases in the reacted samples. The XRD patterns for zinc oxide, alpha-iron oxide and the mixed powder are shown in Figure 55.

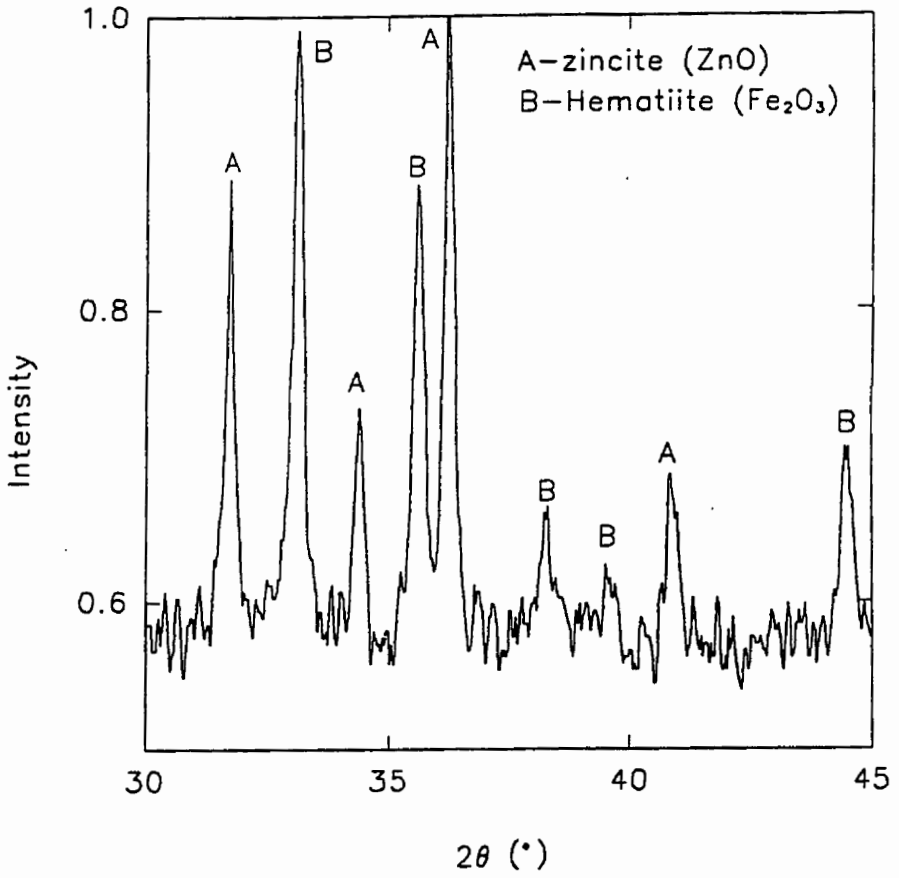

Figure 55: (c) XRD Pattern for Mixed Powders

A-3. RESULTS AND DISCUSSION

Table XXXXVIII shows the experimental conditions and the AAS results. The behaviour of the reaction with time under various experimental conditions is shown in Figure 56. It can be

Table XXXXVIII. Experimental Conditions and the AAS Results

Experiment No (#)	Temp (K)	Sample Mass (g)	Briq. Pressure (Kg cm-2)	Time (min)	Residual ZnO (%)	Fraction Reacted (%)
F-1	873	3	282	60	26.96	18.94
F-2	873	3	282	120	24.17	27.33
F-3	873	3	282	180	21.54	35.24
F-4	873	3	282	240	19. 46	41.49
F-5	873	3	141	60	28.41	14.58
F-6	873	3	141	120	25.52	23.27
F-7	873	3	141	180	23.57	29.13
F-8	873	3	141	240	21.70	34.76
F-9	873	3	0	60	30.63	7.91
F-10	873	3	0	120	29.09	12.54
F-11	873	3	0	180	26.85	19.27
F-12	873	3	0	240	25.99	21.86
F-13	973	5	282	60	12.23	63.23
F-14	973	5	282	120	30.72	7.64
F-15	973	5	282	180	5.21	84.34
F-16	973	5	282	240	4.03	87.88
F-17	973	3	282	60	12.08	63.68
F-18	973	3	282	120	7.61	77.12
F-19	973	3	282	180	5.10	84.67
F-20	973	3	282	240	2.55	92.33
F-21	973	1	282	60	11.05	66.78
F-22	973	1	282	120	6.55	87.61
F-24	973	1	282	240	3.27	90.17
F-25	973	3	141	60	15.51	53.37
F-26	973	3	141	120	10.86	67.35
F-27	973	3	141	180	8.32	74.98
F-28	973	3	141	240	7.05	78.80
F-29	973	3	0	60	25.91	22.10
F-30	973	3	0	120	23.54	29.22
F-31	973	3	0	180	21.66	34.88
F-32	973	3	0	240	20.63	37.97
F-33	1073	3	282	60	1.74	94.77
F-34	1073	3	282	120	0.96	97.11
F-35	1073	3	282	180	0.77	97.68

seen that a considerable amount of zinc oxide is reacted within the first sixty minutes of reaction. For example, for loose powder (not briquetted), the fraction reacted at 873 K was about 8 percent,

while for a compacted sample (282 kg cm^{-2}) at 1073 K, the fraction reacted was over 90 percent. The XRD patterns for these experiments, F-9 and F-33, are shown in Figure 57, from which it is clear that zinc ferrite was detected at 873 K and became the predominant phase at 1073 K. This indicates that the initial nucleation process and the surface reaction are rapid. As shown by Kingery[213], this can be attributed to the relatively easy repositioning of the various ions, which is

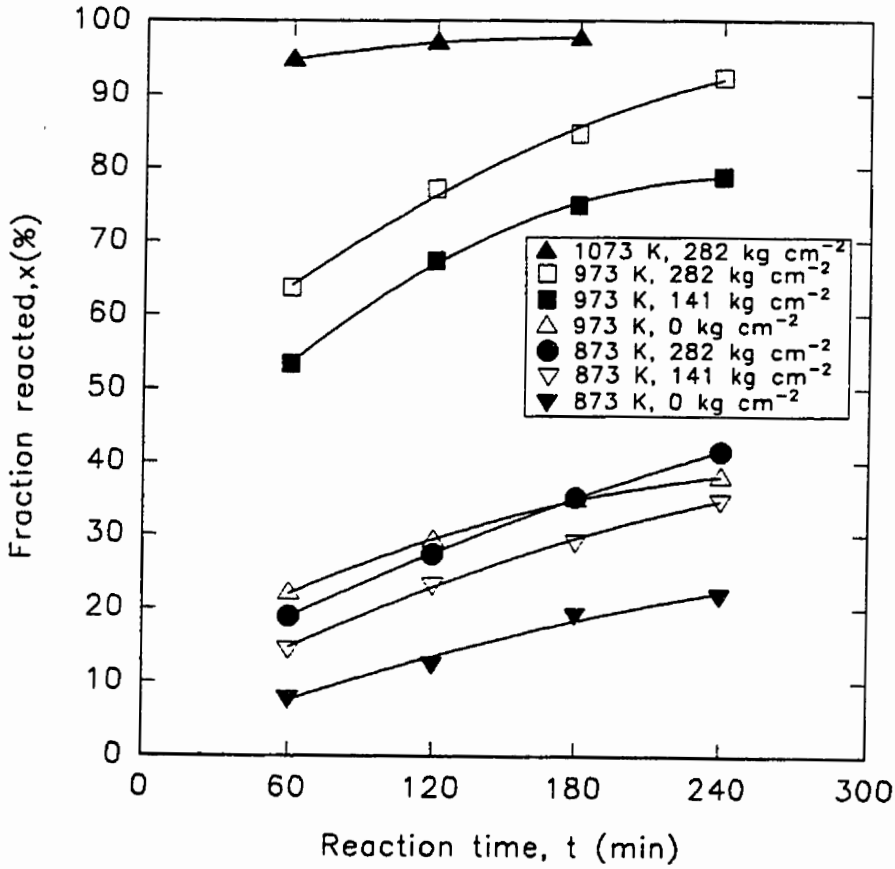

Figure 56. Fraction Reacted (X) versus Reaction Time (t).

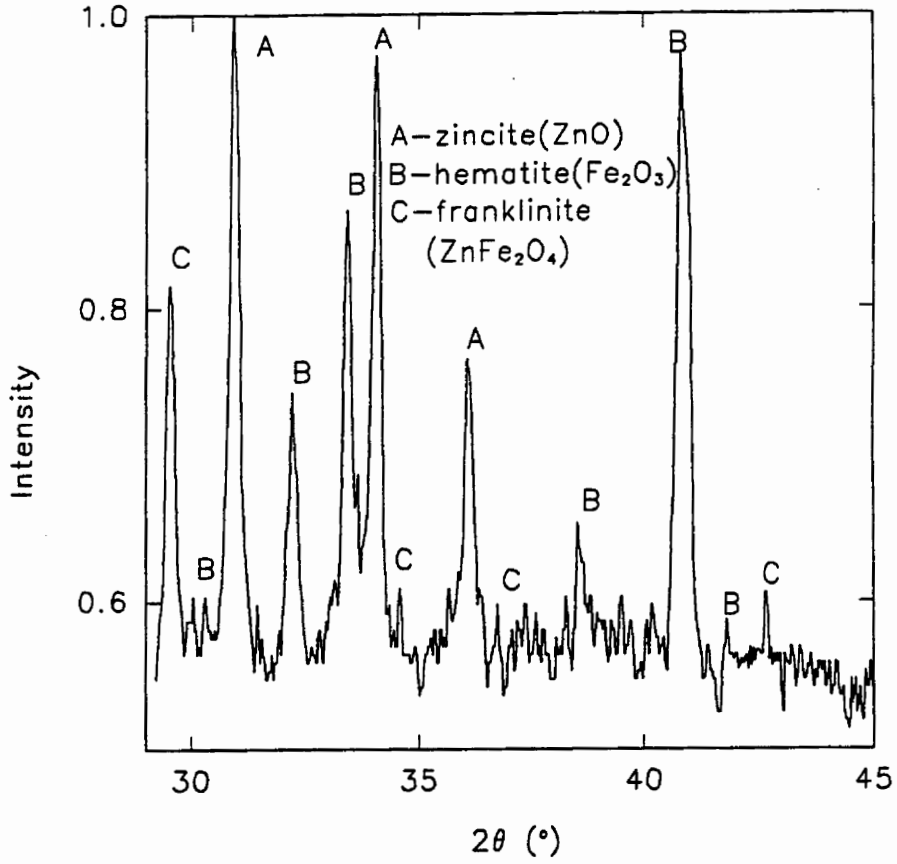

Figure 57. (a) XRD Pattern for Experiment F9

required to convert the zinc oxide and the ferric oxide into zinc ferrite. Ferric oxide is rhombohedral, with all the ferric ions being located in the octahedral interstitial sites, while the zinc oxide is hexagonal, with the zinc ions in the octahedral sites. In order to form zinc ferrite, which has a normal spinel structure, i.e. the zinc ions occupy the A sites (tetrahedral) and the iron ions the B

sites (octahedral), the only ion that must be repositioned is zinc. Also, the oxygen lattice has to be slightly displaced in order to accommodate both of the constituent oxides. With both increasing temperatures and compaction pressures, the repositioning of the ions and the diffusion processes are promoted. However, once a barrier layer of zinc ferrite has formed around the ferric oxide particles[194], then the reaction rate is diminished, since the growth of the product layer requires one or more of the reacting species to diffuse across the barrier layer. Thus, the kinetics of the process changes from chemical control to diffusion control.

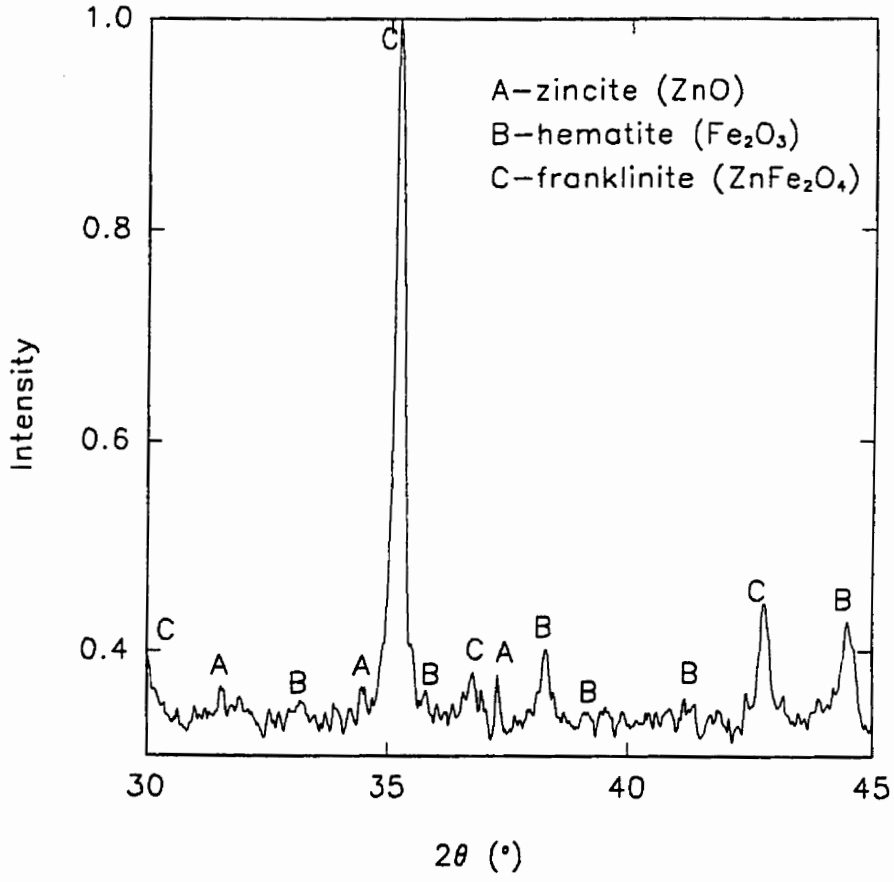

Figure 57. (b) XRD Pattern for Experiment F33

The effect of briquetting pressure on the kinetics of zinc ferrite formation is shown in Figure 56. The following relationships were determined at the indicated temperatures for the effect of briquetting pressure on the rate constant:

$$k=3.26\times10^{-7}p+3.367\times10^{-5} \qquad \text{at 873 K} \qquad \text{(A-4)}$$

$$k=3.76\times10^{-6}p+9.004\times10^{-5} \qquad \text{at 973 K} \qquad \text{(A-5)}$$

where k is the rate constant, min^{-1}, and p is the briquetting pressure, kg cm^{-2}. For the above equations, the correlation coefficients were 0.9970 and 1.0 respectively. It is clear from Figure 56 that above a critical briquetting pressure of about 141 kg cm^{-2} there is no significant increase in the reaction kinetics. At a given temperature and above the critical briquetting pressure, further increases in the conversion rate could only be obtained by using smaller size particles of the raw materials, or by introducing additional imperfections or strains into the particles.

The effect of sample mass (weight) on the conversion rate is shown in Table XXXXVIII. It is clear that the size of the sample, in the range of 1 to 5 grams has no influence on the conversion rate. Sample size would not be expected to have an effect on the kinetics of the reaction for the range of sample sizes employed in the present investigation. However, if the sample size was large enough, then heat transfer could become the rate-limiting factor.

The experimental data were examined by more than eight different diffusion-based models[214-219]. The best fit to the data for reaction times up to four hours at 873, 973, and 1073 K was obtained with Jander's model [220]. The results are fitted to Jander's equation in Figure 58 and the

correlation coefficients for the various experimental conditions are shown in Table XXXXIX. It can be seen that the correlation coefficients are, in general, over 0.98.

Table XXXXIX. Linear Regression Analysis of the Data Using Equations (A-2), (A-6), (A-7) and (A-8)

Experimental Conditions									
Temperature (K)	873	873	873	973	973	973	973	973	1073
Sample Mass (g)	3	3	3	5	3	1	3	3	3
Briq. Pressure (kg cm^{-2})	282	141	0	282	282	282	141	0	282
Analysis of Results									
Equation (A-2) (Jander's Model: $[1-(1-X)^{1/3}]^2 = kt$)									
k ($\times 10^4$) (min^{-1})	1.2431	8.2636	0. 3221	9.8430	13.5090	11.0490	6.2908	0.8628	65.3690*
Correl. Coeff. (R^2)	0.9916	0.9960	0.9753	0.9910	0.9801	0.9780	0.9852	0.9934	1.0
Equation (A-7) (Ginstling-Brunhstein's Model: $(1+X)^{2/3} + (1-X)^{2/3} = kt$)									
k ($\times 10^4$) (min^{-1})	1.0916	0.7455	0.3037	5.8389	7.4935	6.2245	4.2489	9.5506	38.0767*
Correl. Coeff. (R^2)	0.9940	0.9974	0.9757	0.9807	0.9946	0.9624	0.9757	0.6435	1
Equation (A-8) (Valensi-Carter's Model: $\{z-[1+(z-1)X]^{2/3} - (z-1)(1-X)^{2/3}\} / (z-1) = kt$, assuming $z = 1.48$)									
k ($\times 10^4$) (min^{-1})	1.4622	1.0161	0.4272	6.7332	8.5391	7.0986	5.0707	1.0227	44.7780*
Correl. Coeff. (R^2)	0.9952	0.9981	0.9761	0.9775	0.9959	0.9585	0.9722	0.9911	1
Equation (A-6): $\ln[-\ln(1-X)] = n\ln t + \ln B$									
n	0.68	0.71	0.82	0.55	0.64	0.55	0.52	0.47	0.22
Correl. Coeff. (R^2)	0.9960	0.9990	0.9855	0.9974	0.9757	0.9943	0.9959	0.9964	0.9964

* Due to the very high reaction rate at 1073 K, k was calculated based on the data at one hour.

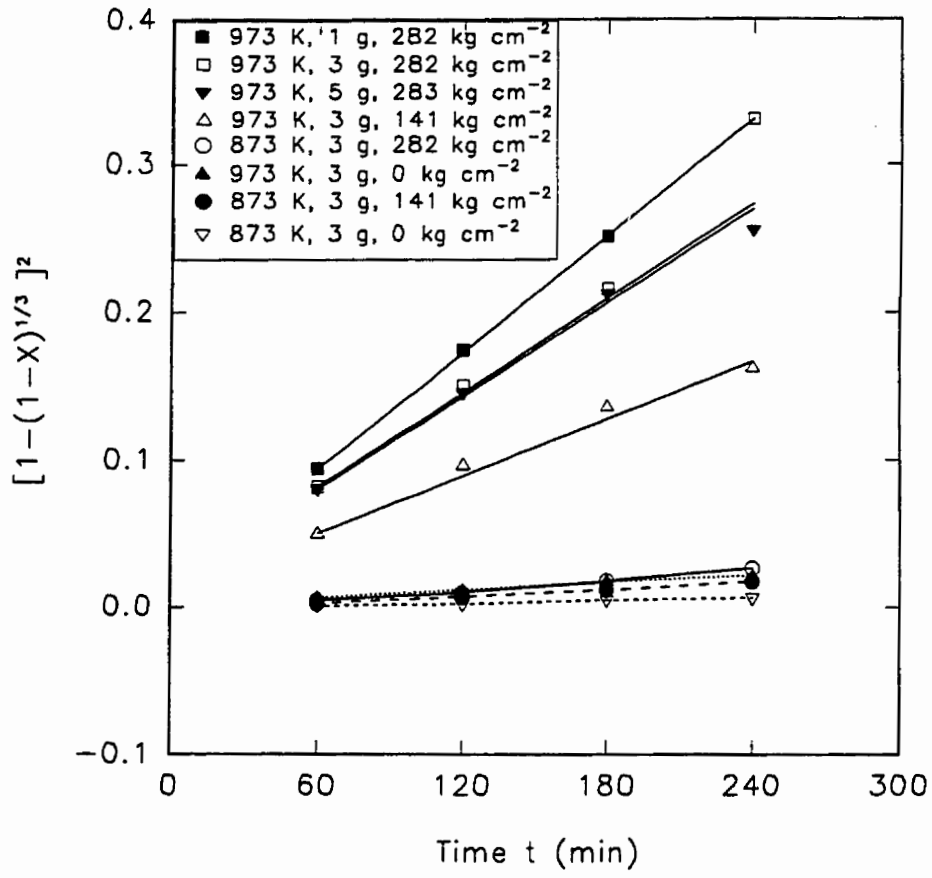

Figure 58. Plot of the Data According to Jander's Equation

The data were further analyzed using the following equation[214-216]:

$$\ln[-\ln(1-X)] = n\ln t + \ln B \qquad \text{(A-6)}$$

where n is a diagnostic and can be used to differentiate among various theoretical mechanisms, and B is a constant. For diffusion controlled models, the value of n should be between 0.53 and 0.58, while for phase boundary reaction controlled models the value should be between 1.07 and 1.11, and between 2.00 and 3.00 for the nucleation models. It is shown in Table XXXXIX that the value of n was generally in the range of 0.47 to 0.82 for the present experimental conditions.

The experimental data were also fitted to the Ginstling-Brounshtein's equation as follows[221]:

$$1-2/3X-(1-X)^{2/3} = kt \qquad \text{(A-7)}$$

and the Valensi-Carter's expression as follows[220]:

$$\{Z-[1+(Z-1)X]^{2/3}-(Z-1)(1-X)^{2/3}\}/(X-1)=kt \qquad \text{(A-8)}$$

The Ginstling-Brounshtein's equation was derived from Fick's second law with a constant diffusion coefficient, while the Valensi-Carter's expression employed the parameter Z, which is the ratio of the volume of zinc ferrite formed to the volume of alpha hematite consumed. The volume of Z should not exceed 2[216-219]. Based on the reported specific gravities[222-224], Z was assumed to be 1.48 in the present work. The analyses of the results using equations (A-7) and (A-8) are also shown in Table XXXXIX.

The data in Table XXXXIX were fitted to the Arrhenius equation using the three different models and the results are plotted in Figure 59. The Arrhenius equations for the three different models: the Jander's model, the Ginstling-Brounshtein's model and the Valensi-Carter's model are as follows, respectively:

$$\ln k = -20265.24/T+14.10 \quad \text{(A-9)}$$

$$\ln k = -18081.01/T + 11.42 \quad \text{(A-10)}$$

$$\ln k = 18689.86/T + 12.16 \quad \text{(A-11)}$$

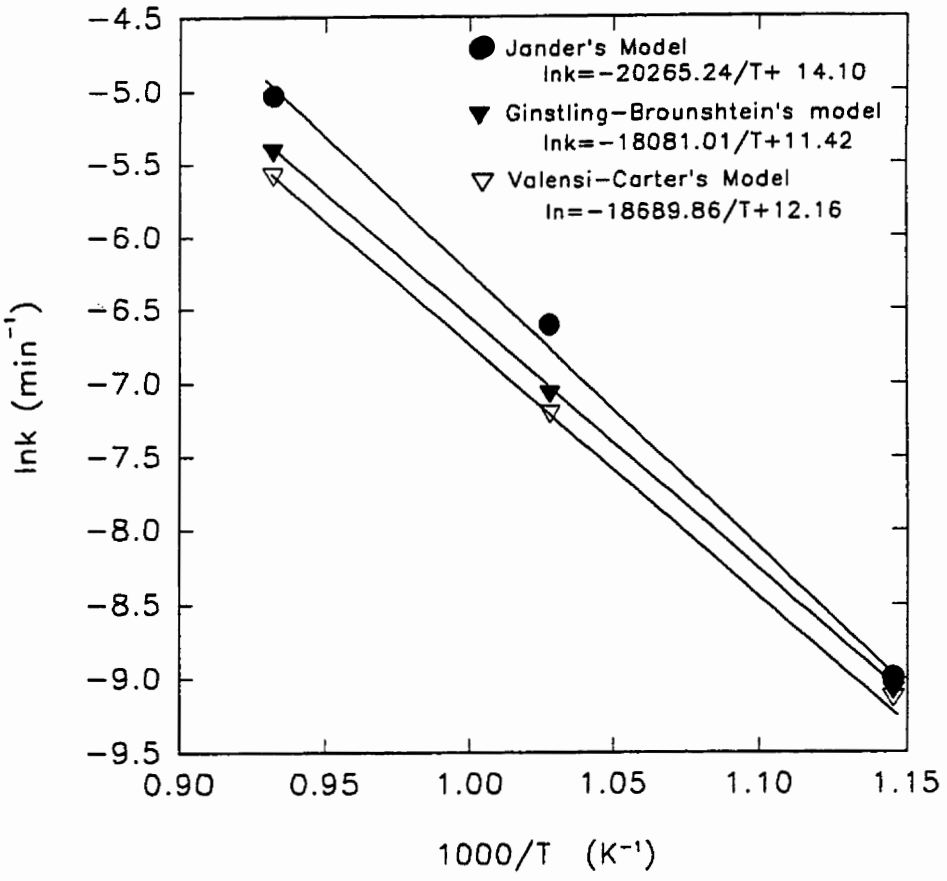

Figure 59. Arrhenius Plots for the Three Diffusion-Controlled Models

Using Jander's equation, the activation energy in the temperature range of 873 K to 1073 K was 168.49 kJ mol^{-1}. Duncan and Steward also showed that the rate process obeyed Jander's model and

they found an activation energy of 300 kJ mol^{-1} in the temperature range of 963 K to 1033 K[198]. Shimada et al[195] used Furuichi's equation[211] to study the kinetics of zinc ferrite formation in the temperature range of 973 K to 1273 K. They found an activation energy of 180 kJ mol^{-1}. Halikia and Milona, who used the Ginstling-Brounshtein's equation, found an activation energy of 117 kJ mol^{-1} [221]. Thus, it is clear that there is considerable variation in the activation energy values reported which ranged from 117 kJ mol^{-1} to 300 kJ mol^{-1}. One possible reason for the variation in the activation energies is that all of the diffusion models include experimental data from the initial stages of the reaction. In this period, it would be expected that the reaction would be controlled by the chemical reactions at the surface and eventually by mixed chemical and diffusion processes. This would be particularly important in the lower temperature range. If the process were to be examined within the period where diffusion control was the only rate limiting step, for example, after one hour of reaction, then it would be expected that there would be better agreement among the activation energies. It is also possible that the variation in the reported activation energies can be attributed to the different raw materials and the experimental methods employed. For example, the purity and the presence of imperfections in the starting powders can affect the conversion rate. Furthermore, grinding and/or pulverizing of the particles introduces more imperfections and strains in the particles which again affects the kinetics of the process.

Using the experimental data in the present work two other values of the activation energy were calculated in addition to the value of 168.49 kJ mol^{-1}, which was obtained previously from an analysis of the data based on Jander's model. The two other values of 150.33 kJ mol^{-1} and 155.39 kJ mol^{-1} were calculated using the Ginstling-Brounshtein's equation and the Valensi-Carter's

expression, respectively. It can be seen that they are both similar to the value obtained using Jander's equation. The various activation energies are compared in Table XXXXX.

Table XXXXX. Comparison of Activation Energies from Various Sources

Equation Used	Temperature Range	Activation Energy	Reference
Jander's: $[1-(1-X)^{1/3}]^2=kt$	963K-1033K	300 kJ mol^{-1}	198
Furuichi's: $\{1-[1-(X-X_s/1-X_s)]^{1/3}\}^2 = kt / (1-X_s)^{2/3}$	973K-1273K	180 kJ mol^{-1}	195
Ginstling-Brounshtein's: $(1+X)^{2/3} + (1-X)^{2/3} = kt$	873K-1073K	117 kJ mol^{-1}	221
Jander's: $[1-(1-X)^{1/3}]^2=kt$	873K-1073K	168 kJ mol^{-1}	this work

Therefore, although zinc ferrite formation from mixed powders of ZnO and Fe_2O_3 is strongly dependent on both the structure-sensitive and the geometric factors, which makes each kinetic model very specific and limited, the diffusion of reactant species through the product layer, after one hour, is rate controlling and the activation energy is 168 kJ mol^{-1}.

A-4. CONCLUSIONS

The kinetics of zinc ferrite formation were studied in the temperature range of 873 K to 1073 K. The data were collected from one to four hours of reaction time. The experimental results were

found to be best described by Jander's diffusion model. The data were fitted to the Arrhenius equation as follows:

$$\ln k = -20265.24/T + 14.10$$

The activation energy was found to be 168.49 kJ mol^{-1}.

Under a given set of experimental conditions, the conversion to zinc ferrite increased with briquetting pressure. The effect was more significant at low briquetting pressures and could be described by the following equations:

$k=3.26\times10^{-7}p+3.37\times10^{-5}$ at 873 K

$k=3.76\times10^{-6}p+9.00\times10^{-5}$ at 973 K

The sample mass, which was varied in the range of 1 to 5 grams, did not have a significant effect on the conversion kinetics. These experimental results contribute to an improved understanding of the reaction mechanism involved in zinc ferrite formation.

REFERENCES

[1] Smithyman, C. M.: Alternate Iron Sources for the EAF, I & SM, (8)(1996):47-50.

[2] Nyirenda, R. L.: The Processing of Steelmaking Flue-Dust: A Review, Minerals Engineering, 4(7-11)(1991):1003-1025.

[3] James, S. E.: Recycling Lead and Cadmium, as well as Zinc, from EAF Dust, in Mackey, T. S. and Prengaman, R. D. eds.: Lead-Zinc '90, The Minerals, Metals & Materials Society, 1990:477-495.

[4] Kola, R.: The Treatment of EAF-Dust in Europe, Proceedings: Recycling Lead and Zinc, The Challenge of the 1990's, Rome, Italy, June 11-13, 1991:279-295.

[5] Yasuda, K.: Current and Proposed Regulations Affecting Recycling in Japan, Proceedings: Recycling Lead and Zinc, The Challenge of the 1990's, Rome, Italy, June 11-13, 1991:445-451.

[6] Bosley, J. J. : Technoeconomic Assessment of Electric Steelmaking Through the Year 2000, Research Project 2787-2, Final Report, Pittsburgh, PA:Center for Metals Production, 1987.

[7] Steiner, B. A.: Electric Arc Furnace Emission Control, in C. R. Taylor ed.: Electric Furnace Steelmaking, The Iron and Steel Society, U.S.A., 1985:49-50.

[8] Morris, J. P.: The Cause of Fuming in Oxygen Steelmaking, U.S. Bureau of Mines Report 7047, 1967.

[9] Rossi, G. and Perin, A.: J. Iron Steel Inst., 207(1969):1365.

[10] QUESTOR ENGINEERING LIMITED: Caustic Leaching-Electrowin Process for Treating Electric arc Furnace Baghouse Dust, Final Report, Queen's University Micromedia, Req. No. 1-9092, July 5, 1983:7,12.

[11] Dreisinger, D. B., Peter, E., and Morgan, G.: The Hydrometallurgical Treatment of Carbon Steel Electric Furnace Dust by the UBC-Chaparral Proces, Hydrometallurgy, 25(1990):137-152.

[12] Ellis, A. F. and Glover, J.: J. Iron Steel Inst., 209(1971):593.

[13] Kosmider, H.: Stahl u. Eisen, 74(1954):1045.

[14] Harding, T. W.: In: Goldstein, J. L., Porter, J. R. and Keyer, N. H. eds.: Characterization, Recovery and Recycling of Electric Arc Furnace Flue Dust, Section V, Final Report, Prepared for the U.S. Department of Commerce Under Project Number 99-26-09886-10, Lehigh University, Bethlehem, 1982.

[15] Jha, M. C.: A Two-Stage Leaching Process for Selective Recovery of Zinc from Steel Plant Dusts, In Taylor, P. R., Sohn, H. Y., and Jarrett, N. eds.: Recycle and Secondary Recovery of Metals, The Metallurgical Society of AIME, Fort Lauderdale, Florida, Decenber 1-4, 1985:143-157.

[16] Hogan, J. C., in Lu, W. K. ed: Waste Oxide Recycling in Steel Plants, MacMaster University, Hamilton, 1974, p.2-1.

[17] Barnard, P. G., Starliper, A. G., Dressel, W. M. and Fine, M. M.: in Proceedings of the 3rd Mineral Waste Utilization Symposium, U.S. Bureau of Mines/IIT Research Institute, Chicago, 1972:63.

[18] Barnes, T. M.: Can. Met. Quart., 15(1976):53.

[19] Akerlow, E. V.: Iron and Steel Engineer, 52(1975):39.

[20] Goodwill, J. E. and Schmitt, R. J.: An Update on Electric Arc Furnace Dust Treatment in the United States, in Mahant, P., Pickles, C. and Lu, W-K eds.: Resource Conservation and Environmental Technologies in Metallurgical Industries, CIM, Toronto, Ontario, August 20-25, 1994:25-34.

[21] Goodfellow, H. D. and Katrusiak, J. M.: EAF and Integrated Steel Mill Dust, A Canadian Perspective. Private Communication.

[22] Tsuneyama, N., Takewaki, M. and Yasukawa,M.: Production of Zinc for Zinc Smelting Process from EAF Dust at Shisaka Works, in Mackey, T. S. and Prengaman, R. D. eds.: Lead-Zinc '90, The Minerals, Metals &Materials Society, 1990:465-476.

[23] Law, S. L.: Characterization of Steelmaking Dusts from Electric Arc Furnace, U. S. Bureau of Mines Report 8750, 1983.

[24] Wu, L. and Themelis, J.: The Flash Reduction of Electric Arc Furnace Dusts, JOM, January, 1992:35-39.

[25] Lopez, F. A., Gonzalez, P., Sainz, E. and Balcazar, N.: Electric Arc Furnace Flue Dust: Characterization and Toxicity with Photobacterium Phosphoreum, International Journal of Environment and Pollution, 3(4)(1993):269-283.

[26] Stephen, L. L., Wayne, F. L., Janet, G. S. and Gary, W. K.: Bureau of Mines, Report of Investigation 8750, 1983.

[27] Hagni, A. M. and Hagni, R. D.: Significance of Mineralogy of Electric Arc Furnace (EAF) Dust in Pyrometallurgical Treatment to Render the Dust Non-Hazardous, in Hager, J., Hansen, B., Imrie, W. and Ramachandran, V. eds.: Extraction and Processing for the Treatment and Minimization of Wastes, The Minerals, Metals and Materials Society, 1993:1137-1148.

[28] Cruells, M., Roca, A. and Nunez, C: Electric Arc Furnace Flue Dust: Characterization and Leaching with Sulphuric Acid, Hydrometallurgy, 31(1992):213-231.

[29] Hagni, A. M. and Hagni, R. D.: Reflected Light and Scanning Electron Microscopic Study of Electric Arc Furnace (EAF) Dust, in Reddy, R. G. ed: Residues and Effluents: Processing and Environmental Considerations, The Minerals, Metals and Materials Society, Warrendale, PA, 1991:117-125.

[30] Arthur D. Little, Inc: Electric Arc Furnace Dust--1993 Overview, Report No.93-1 for Center for Materials Production, Pittsburgh ,PA, 1993.

[31] Mac Rae, D. R.: Electric Arc Furnace Dust-Disposal, Recycle, and Recovery, Report No. 85-2, Bethlehem Steel Corporation for Center for Materials Production, Pittsburgh, PA, 1985.

[32] Frenay, J, Hissel, J., and Ferlay, S.: Recovery of Lead and Zinc From Electric Steelmaking Dusts By The Cebedeau Process, in Taylor, P., Sohn, H. Y. and Jarret, N. eds.: Recycle and Secondary Recovery of Metals, TMS, Fort Landerdale, Florida, December 1-4, 1985:195-201.

[33] Keyser, N. H.: Characterization, Recovery and Recycling of Electric Arc-Furnace Dust, A paper presented at the Symposium on Iron and Steel Pollution Abatement Technology, Chicago, 1981.

[34] Li, C-L and Tsai, M-S: A Crystal Phase Study of Zinc Hydroxide Chloride in Electric-Arc-Furnace Dust, Journal of Materials Science, 28(1993):4562-4570.

[35] Law, S. L.: Characterization of Steelmaking Dusts from Electric Arc Furnaces, U. S. Bureau of Mines Report 8750, 1983.

[36] Simmons, G. W. and Music, S.: Characterization of Electric Arc Furnace Dust by Mossbauer Spectroscopy, in Goldstein, J. L., Porter, J. R. and Keyser, N. H. eds.: Characterization, Recovery and Recycling of Electric Arc Furnace Dust, Final Report for the U.S. Department of Commerce , P. III, D-87, 1982.

[37] Dressel, W. M., Barnard, P. G. and Fine, M. M.: US Bureau of Mines, Report of Investigation 7927, 1974.

[38] Eacott, J. G., Robinson, M. C., Busse, E., Burgener, J. E. and Burgener, P. E.: CIM Bull. 1984:75.

[39] Thomas, B. K. and Fray, D. J.: Metall. Trans. B, 12(1981):281.

[40] Fray, D. J.: Trans. Inst. Min. Metall. 95(1986)55.

[41] Li, C-L and Tsai, M-S: Mechanism of Spinel Ferrite Dust Formation in Electric Arc Furnace Steelmaking, ISIJ International, 33(2)(1993): 284-290.

[42] Aota, J, Mikhail, S. A., Liang, D. T. and Howell, W. N.: Low Temperature EAF Dust Vitrification Process, CANMET Mineral Science Laboratories, For Distribution at 33rd Conference of Metallurgists, Aug. 20-25, 1994, Toronto, Canada.

[43] Aune, J. A., Bergwitx-Larsen, K, Eikeland, I. J. and Pedersen, T. H.: Elkem Multi-Purpose Furnace Technology for Reclamation of Metal Values in the Treatment of Hazardous Materials, Proceeding: Recycling of Metalliferous Materials, Metalliferous Materials Conference, Institute of Mining and Metallurgy, Birmingham, England, April 23-25, 1996:11-19.

[44] Kotraba, N. L. and Lanyi, M. D.: Metal Recovery from EAF Dust Using Rotary Reduction Process, SEM Conference, Denver, February, 1991.

[45] Zunkel, D.: What to do with your EAF Dust, Steel Times International, July, 1996:46-50.

[46] Nicolle, R. and Lu, W. K.: in Lu, W. K. ed.: Waste Oxide Recycling in Steel Plants, MacMaster University, Hamilton, 1974, p.12-1.

[47] Taylor, J. C. and Zunkel, A. D.: J. of Metals, 40(1988):27.

[48] Moser, W. S., Mahler, G. T., Kneooer, T. R., Kuba, R. M. and Pusateri, J. E.: Metals Recycling from Steelmaking and Foundry Waste by Horsehead Resource Development, 50th

Electric Furnace Conference Proceedings, Iron and Steel Society of the AIME, Warrendale, PA, USA, 1992:145-157.

[49] Candy, I. M. and Wrona, L. M.: Selection of a Process for the Treatment of Carbon Steel Electric Arc Furnace Dust, private communication.

[50] Kola, R.: The Processing of Steelworks Waste, in Mackey, T. S. and Prengaman, R. D. eds.: Lead-Zinc '90, The Minerals, Metals and Materials Society, Warrendale, PA, USA, 1990: 453-464.

[51] Yatsunami, N., Miyashita, T., Tajima, O., Watanabe, H. and Suzawa, Y.: New Process for Treating Electric Arc Furnace Dust (The HRT Process), 39th Electric Arc Furnace Proceedings, Iron and Steel Society of AIME, Warrendale, PA, USA, 1981:188-196.

[52] Kotraba, N. L. and Lanyi, M. D.: Metal Recovery fron EAF Dust Using Rotary Reduction Process, SME Annual Meeting, Denver, CO, USA, Feb.25-28, 1991, total page: 14.

[53] Santen, S. O.: Recovery of Metals from Steelmaking Dusts, Pretreatment and Reclamation of Dusts, Sludges and Scales in Steel Industry, 21st McMaster Symposium on Iron and Steelmaking, Hamilton, Ont, Canada, 1993.

[54] Herlitz, H., Johansson, B. and Santen, S.: EAF Dust Decomposition and Metals Recovery at Scandust, Proceedings of the 45th Electric Furnace Conference, Iron and Steel Society, Warrendale, PA, 1987:81-87.

[55] Eriksson, S., Herlitz, H. and Santen, S.: Operating Experience with the Plasmadust Process, Proceedings of the 44th Electric Furnace Conference, Iron and Steel Society, Warrendale, PA, 1986:425-430.

[56] Lightfoot, R. and Stockham, J. B.: The Treatment of EAF Dust Using the Davy Hi-Plas Process, Pretreatment and Reclamation of Dust, Sludges and Scales in Steel Industry, 21st McMaster Symposium on Iron and Steelmaking, Hamilton, Ont, Canada, 1993.

[57] McAloon, T. P.: Decision Time for EAF Dust Generators, I & SM, 2(1990): 15-20.

[58] Bosley, J. J.: Proceedings of the 1992 CMP Electric Arc Furnace Dust Treatment Symposium, The EPRI Center for Materials Production, Pittsburg, PA, June, 1992: Appendix I.

[59] Cowx, P., Chapman, C. Heanley, C. P. and Pargeter, J.: The Processing of Electric Arc Furnace Dust in the Tetronics Plasma Furnace, Lead-Zinc '90, The Minerals, Metals & Materials Society, Warrendale, PA, 1990:497-510.

[60] Cowx, P. M. and Roddis, B.: The Recovery of Alloy Elements from EAF/AOD Fume in the Tetronics Plasma System, Proceedings of the 44th Electric Arc Furnace Conference, Iron and Steel Society, Warrendale, PA, 1986:443-450.

[61] Chapman, C. D., Cowx, P., Pargeter, J. and Pocklington, D. N.: Tetronics Plasma Process for Recovery of Zinc, Lead, and other Metals from Secondary Sources, Recycling of Metalliferous Materials, IMM, England, 1990:47-55.

[62] Heanley, C. P. and Cowx, P. M.: The Smelting of Ferrous Ores Using a Plasma Furnace, Disposal, Recycling and Recovery of Electric Arc Furnace Exhaust Dust, Iron and Steel Society, Warrendale, PA, 1987:127-135.

[63] Bounds, C. O. and Pusateri, J. F.: EAF Dust Processing in the Gas-Fired Flame Reactor Process, in Mackey, T. S. and Prengaman, R. D. eds.: Lead-Zinc '90, The Minerals, Metals & Materials Society, Warrendale, PA, 1990:511-528.

[64] Lehmkuhler, H. J., Staeubner, H. and Hanewald, R. H.: Reclamation of Iron and Steelmaking Dusts, Sludges and Scales Using the INMETCO Technology, Pretreatment and Reclamation of Dusts, Sludges and Scales in Steel Industry, 21st McMaster Symposium on Iron and Steelmaking, Hamilton, On, Canada, 1993.

[65] Kawata, Y.: Recovery of Zinc Oxide from Steelmaking Dust at Onahama Plant of Ryoho Recycle Company, in Tozawa, K. ed.: Zinc '85-Proceedings of International Symposium on Extractive Metallurgy of Zinc, The Mining and Metallurgical Institute of Japan, Tokyo, Japan, 1985:797-805.

[66] Monden, S. and Okami, M.: The Use of Secondary Materials at Miike Smelter, in Tozawa, K. ed.: Zinc '85-Proceedings of International Symposium on Extractive Metallurgy of Zinc, The Mining and Metallurgical Institute of Japan, Tokyo, Japan, 1985: 807-823.

[67] Matsuoka, T., Kurozu, S. and Koyabu, Y.: New Technology for Treating Electric Arc Furnace Dust, Iron and Steel Engineer, February, 1991:37-40.

[68] Bosley, J. J.: Proceedings of the 1992 CMP Electric Arc Furnace Dust Treatment Symposium, The EPRI Center for Materials Production, Pittsburgh, PA, June, 1992: 2-6

[69] Dogan, Z. M. and Karayazic, F.: Cinkur's Waelz Plant in Turkey: Operational Results and Problems, Mining Magzine, (8)(1984):98-103.

[70] Kashiwada, M. and Kumagai, T.: Waelz Process for Leach Residues at Nisso Smelting Company Ltd., Aizu, Japan, AIME Symposium on Mining and Metallurgy of Lead and Zinc, New York, II(1970):402-422.

[71] Best, T. E. and Pickles, C. A.: Treatment of EAF Baghouse Dusts in Carbon Monoxide, in Sohn, H. Y. ed: Metallurgical Processes for the Early Twenty-first Century, Vol. 1, San Diego, CA, 1994:543-562.

[72] Schoukens, A. F. S., Nelson, L. R. and Barcza, N. A.: Plasma-Arc Treatment of Steel-Plant Dust and Zinc-Containing Slag-Theoretical and Practical Considerations, Proceedings: Recycling Lead and Zinc, The Challenge of the 1990's, Rome, Italy, June 11-13, 1991:361-369.

[73] Bamrim, A., Flamant, G . and Lecadet, J.: Separation of Metals from Dusts in a Plasma Spouted Bed Reactor, Private communication with author, P.8, 1997.

[74] Kishimoto, Y., Tobo, H., Hara, Y. and Sakuraya, T.: Development of Dust Treatment System Based on Hollow Cathode DC Technology, In: Plasma for Industry and Environment, Sep. 25-27, 1990, England, Paper no. 2.4.

[75] Pocklington, D. N. and Cowx, P. M.: The Commercial Application of Plasma Technology to Steel Dust Treatment, In: Plasma for Industry and Environment, Sep. 25-27, 1990, England, Paper no. 2.3.

[76] Flamant, G., Bamrim, A. Badie, J. M. and Lecadet, J.: Plasma Beneficiation of Lead-rich Dusts, Journal of High Temperature Chemical Processes, Colloque, Supplement au 1(3) (1992):239-246.

[77] Bamrim, A., Flamant, G. and Badie, J. M.: Transport Phenomena During the Vaporization of Metallic Waste Particle in a Plasma Jet, Private communication with author, P.5, 1997.

[78] Herlitz, H. G.: Plasma Technology for Metal Recovery from Oxidic Waste, Private communication with author, 1995

[79] Lherbier, L. W.: Flash Smelting Efficiency in the Flame Reactor Processes, 1988 Center for Pyrometallurgy Conferences, June 16-17, Salt Lake City, Utah, 1988.

[80] Pusateri, J. F., Chew, R. and Stanze, A. E.: Treatment of EAF Dust Via the Flame Reactor, the 44th Electric Furnace Conference, ISS-AIME, Dallas, TX, December 10-12, 1986.

[81] Bounds, C. O. and Pusateri, J. F.: The Flame Reactor Process: A Solution for Lead/Zinc Industry Problems, TMS Annual Meeting, Phoenix, AZ, 1988.

[82] Olper, M.: The EZINEX Process- A New and Advanced Way for Electrowinning Zinc from a Chloride Solution, in Mathew, I. J. ed: World Zinc '93, Proceedings of the International

Symposium on Zinc, The Australasian Institute of Mining and Metallurgy, Parkville, Victoria, 1993: 491-494.

[83] Nogueira, E. D., Regife, J. M., Martin San Lorenzo, D. and Nogueira, G. D.: Using Zinc Secondaries to Feed an Electrowinning Plant, in Tozawa, K. ed: Zinc'85-Proceedings of the International Symposium on Extractive Metallurgy of Zinc, The Mining and Metallurgical Institute of Japan, Tokyo, Japan, 1985: 763-781.

[84] Diaz, G. and Martin, D.: Modified Zincex Process: the Clean, Safe and Profitable Solution to the Zinc Secondaries Treatment, in Resources, Conservation and Recycling, Elsevier Science B. V, 10(1994)43-57.

[85] Frenay, J. N. and Hissel, J.: ATB Metallurgie, XXIV(1984):233.

[86] Frenay, J., Ferlay, S. and Hissel, J.: Zinc and Lead Recovery from EAF Dusts by Caustic Soda Process, 44th Electric Furnace Conference Proceedings, Iron and Steel Society of the AIME, Warrendale, PA, USA, 1986:417-421.

[87] Geutskens, R. in Mackey, T. S. and Prengaman, R. D. eds: Lead-Zinc'90, TMS, Warrendale, 1990:529.

[88] Frenay, J., Hissel, J. and Ferlay, S.: Recovery of Lead and Zinc From Electric Steelmaking Dusts, in Taylor, P, Sohn, H. Y. and Jerrett, N. eds: Recycle and Secondary Recovery of Metals, TMS, Fort Landerdale, Florida, December 1-4, 1985:195-201.

[89] Wheatley, B. I.: Production of Zinc Powder from Arc and Smelter Flue Dusts, In Recycling of Metalliferous Materials, IMM, London, 1990:291-299.

[90] Burrows, W. H.: US Patent, No. 3,849,121, 19 November, 1974.

[91] Pearson, D.: Recovery of Zinc from Metallurgical Dusts and Fumes, in Kuhn, M. C. ed: Process and Fundamental Considerations of Selected Hydrometallurgical Systems, Chapter 14, Society of Mining Engineers of AIME, New York, 1981:153-168.

[92] Duyvesteyn, W. P. C., Wicker, G. R. and Doane, R. E.: An Omnivorous Process for Laterite Deposits, in Evans, D. J. I., Shoemaker, R. S. and Veltman, H. eds: International Laterite Symposium, Chapter 28, Society of Mining Engineers of AIME, New York, 1979: 553-570.

[93] Ohtsuka, T., Yamada, T., Abe, H. and Aoki, K.: Progress of Zinc Residue Treatment in the Iijima Refinery, at 107th Annual AIME Meeting, Denver, 1978: A78-7.

[94] Duyvesteyn, W.: US Patent, No. 4,610,721, September 9, 1986.

[95] Barrett, E. C., Nenniger, E. H. and Dziewinski, J.: A Hydrometallurgical Process to Treat Carbon Steel Electric Arc Furnace Dust, Hydrometallurgy, 30(1992):59-68.

[96] Thorsen, G., Grislingas, A. and Steintveit, G.: JOM, 33(1)(1981):24-29.

[97] Duyvesteyn, W. and Jha, M. C.: US Patent, No. 4,572,771, February 25, 1986.

[98] Duyvesteyn, W. and Jha, M. C.: US Patent, No. 4,614,543, September 30, 1986.

[99] Peters, M.: US Patent, No. 4,071,357, January 31, 1978.

[100] Cuadra, A. D. and Limpo, J. L.: Ouimica e Industria, 38(1)(1992):27-34.

[101] Caravaca, C., Cobo, A. and Alguacil, F. J.: Proceedings, Materials and Ecology, SNMT-TANGER, Frydek-Mistek, Chzechoslovakia, April 1992:103-114.

[102] Caravaca, C, Cobo, A, and Alguacil, F. J.: Considerations about the Recycling of EAF Flue Dusts as Source for the Recovery of Valuable Metals by Hydrometallurgical Processes, Resources, Conservation and Recycling, Elsevier Science B. V., 10(1994)35-41.

[103] North-East Institute of Technology: Zinc Metallurgy(in Chinese), Metallurgical Industrial Publishing House, Beijing, 1974:29-31.

[104] Xu, C. D., Lin, R. and Wang, D. C.: Physical Chemistry for Zinc Metallurgy (in Chinese), Shanghai Scientific and Technological Publishing House, Shanghai, 1979: 69-141.

[105] Rodier, D. D.: An Overview of Silver and Trace Metal Recovery Strategies in the Zinc Industry, in Mackey, T. S. and Prengaman, R. D. eds.: Lead, Zinc'90 Proceedings, 1990 World Symp. on Metallurgical and Environmental Control. TMS, Warrendale, Pa.1990:57-85.

[106] Monhemius, A. G.: The Electrolytic Production of Zinc, in Burkin, A. R. ed.: Topics in Non-Ferrous Extractive Metallurgy, Society of Chemical Industry, Oxford, U.K., 1980:104-130.

[107] Krauss, C. J.: Effects on Minor Elements on the Production of Electrolytic Zinc from Zinc Sulfide Concentrates, in Tozawa, K. ed.: Zinc'85 Proceedings, International Symp. on Extractive Metallurgy of Zinc, Tokyo, 1985:467-481.

[108] Elgersma, F., Witkamp, G. J. and Van Rosmalen, G. M.: Simultaneous Dissolution of Zinc Ferrite and Precipitation of Ammonium Jarosite, Hydrometallurgy, 34(1993):23-47.

[109] Merril, C. C. and Lang, R. S.: Experimental Caustic Leaching of Oxidized Zinc Ores and Minerals and the Recovery of Zinc from Leach Solution. Report of Investigations 6576, Bureau of Mines, United States Department of the Interior, 1964:1-23.

[110] Bhat, K. L., Natarajan, K. A. and Ramachandran, T.: Electroleaching of Zinc Leach Residues, Hydrometallurgy, 18(1987):287-303.

[111] Lu, Z. Y. and Muir, D. M.: Dissolution of Metal Ferrites and Iron Oxides by HCl under Oxidising and Reducing Conditions, Hydrometallurgy, 21(1988):9-21.

[112] Sarma, V. N. R., Deo, K. and Biswas, A. K.: Dissolution of Zinc Ferrite Samples in Acids, Hydrometallurgy, 2(2)(1976):171-184.

[113] Ryczaj, K. and Riesenkampf, W.: Kinetics of the Dissolution of Zinc-Magnesium Ferrites in Sulfuric Acid Solutions Related to Zinc Leach Processes, Hydrometallurgy, 11(2)(1983):171-184.

[114] Nunez, C. and Vinals, J.: Kinetics of Leaching of Zinc Ferrite in Aqueous Hydrochloric Acid Solutions, Metall. Trans. B., 24B(1984):211-228.

[115] Filippou, D. and Demopoulos, G. P.: A Reaction Kinetic Model for the Leaching of Industrial Zinc Ferrite Particulates in Sulfuric Acid Media, Can. Metall. Q., 31(1992):41-54.

[116] Nii, K. and Hisamatsu, Y.: Study on Zinc Ferrite (V): The Promotion of Acid Dissolution of Zinc Ferrite, Trans. Nat. Res. Inst. Metals, 8(1966):27-33.

[117] Elgersma, F., Kamst, G. F., Witkamp, G. J. and Van Rosmelen, G. M.: Acid Dissolution of Zinc Ferrite, Hydrometallurgy, 29(1992):173-189.

[118] Elgersma, F., Witkamp, G. J. and Van Rosmelen, G. M.: Kinetics and Mechanism of Reductive Dissolution of Zinc Ferrite in H_2O and D_2O, Hydrometallurgy, 33(1993): 165-176.

[119] Elgersma, F., Witkamp, G. J. and Van Rosmelen, G. M.: Simultaneous Dissolution of Zinc Ferrite and Precipitation of Ammonium Jarosite, Hydrometallurgy, 34(1993): 23-47.

[120] Filippou, D. and Demopoulos, G. P.: On the Various Dissolution Kinetics of Zinc Ferrite in Acid Media, The Canadian Journal of Chemical Engineering, 71(1993): 790-801.

[121] Frenay, J.: Leaching of Oxidized Zinc Ores in Various Media, Hydrometallurgy, 15(1985):243-253.

[122] Nirdosh, I., Kalia, R. K. and Muthuswami, S. V.: Bench Scale Investigations on the Electrolytic Recovery of Zinc Powder from Galvanizer's Ash, Hydrometallurgy, 20(1988): 203-217.

[123] Nii, K. and Hisamatsu, Y.: Trans. Nat. Res. Inst. Metals, 1966:183.

[124] Nii, K. and Hisamatsu, Y.: Trans. Nat. Res. Inst. Metals, 1964:78.

[125] Nii, K. and Hisamatsu, Y.: Trans. Nat. Res. Inst. Metals, 1965:9.

[126] Nii, K. and Hisamatsu, Y.: Trans. Nat. Res. Inst. Metals, 1966:193.

[127] QUESTOR ENGINEERING LIMITED: Caustic Leaching-Electrowin Process for Treating Electric arc Furnace Baghouse Dust, Final Report, Queen's University Micromedia, Req. No. 1-9092, July 5, 1983, vol 1:1-78; vol 2.

[128] Pourbaix, M.: Atlas of Electrochemical Equilibria in Aqueous Solutions, Pergamon Press, Brussels, 1966:313,409.

[129] National Research Council: Microwave Processing of Materials, National Academy Press, Washington, D. C., 1994:1-149.

[130] Atomic Energy of Canada Limited Research Company and Voss Associates Engineering Ltd.: Microwaves and Minerals, Ontario, Canada, 1990:1-77.

[131] McGill, S. L. and Walkiewicz, J. W.: Applications of Microwave Energy in Extractive Metallurgy, Journal of Microwave Power and Electromagnetic Energy, 22(3)(1987):175-177.

[132] Bradhurst, D. H. and Worner, H. K.: The Applications of Microwave Energy in Mineral Processing and Pyrometallurgy in Australia, Sprechsaal International Glass Magazine, 123(2)(1990): 194-197.

[133] Peng, J., Yang, H. and Tang, X.: Applications of Microwave Energy in Pyrometallurgy, Rare-Earth Metals and Hard Alloys (in Chinese), 113(6)(1993):1-4.

[134] Xia, D. K. and Pickles, C. A.: Microwave Applications in Extractive Metallurgy, a Review, In Pickles, Hancock and Wynnyckyi eds.:Proceedings,Challenges in Process Intensification, 35th Annual Conference of Metallurgists, CIM, Montreal, Aug.24-29,1996:183-207.

[135] Walkiewicz, J. W., Clark, A. E. and McGill, S.: Microwave-Assisted Grinding, IEEE Transactions on Industry Applications, 27(2)(1991):239-243.

[136] Pickles, C. A. and Xia, D. K.: Microwave Drying of Ferric Oxide Pellets, Proceedings,56th Ironmaking and 80th Steelmaking Conference, Chicago, USA, April 13-16, 1997.

[137] Standish, N. and Pramusanto: Reduction of Microwave Irradiated Iron Ore Particles in CO, ISIJ International, 31(1)(1991):11-16.

[138] Wu, W. and Huang, W.: Microwave Drying and Roasting of Pellets, In: Sohn, H. Y. ed: Metallurgical Processes for Early Twenty-First Century, TMS, 1994:889-894.

[139] Standish, N. and Huang, W.: Microwave Application in Carbothermic Reduction of Iron Ores, ISIJ International, 31(3)(1991):241-245.

[140] Standish, N. and Worner, H.: Microwave Application in the Reduction of Metal Oxides with Carbon, Iron and Steelmaker, 18(5)(1991):59-61.

[141] Ghoreshy, M. and Pickles, C. A.: Microwave Processing of Electric Arc Furnace Dust, Electric Furnace Conference Proceedings, ISS-AIME, Nashville, USA, 52(1994):187-195.

[142] Hatton, B. D. and Pickles, C. A.: Microwave Treatment of Ferrous Slags, Steelmaking Conference Proceedings, ISS-AIME, Chicago, USA, 72(1994):435-442.

[143] Durance, C., McCrea, J. and Pickles, C. A.: Microwave Preheating of High Alumina Steelmaking Ladle Refactories,14th Process Technology Conference, ISS-AIME, Orlando, Florida, November, 1995.

[144] Kruesi, P. R.: Microwave Processes for Gold Recovery, Randol Gold Forum, Randol International Ltd., Golden, Colorado, 4(1986):11701-11708.

[145] Haque, K. E.: Microwave Irradiation Pretreatment of a Refractory Gold Concentrate, In Salter, R. S et al. eds: Proc. Int. Symposium on Gold Metallurgy, Winnipeg, Canada, Pergamon Press, New York, 1987:327-339.

[146] Woodcock, J. T.: Possibilities for Using Microwave Energy in the Extraction of Gold, Proc. First Australian Symp. on Microwave Power Applications, Wollongong, Australia, 15-17 February, 1989.

[147] Kruesi, P. R. and Frahm, V. H. Jr.: U.S. Pat. 4311520, Jan.19, 1982.

[148] Kruesi, P. R. and Frahm, V. H. Jr.: U.S. Pat. 4321089, March 23,1982.

[149] Kruesi, P. R and Frahm, V. H. Jr.: U.S. Pat. 4324582, April 13,1982.

[150] Cato Res. Corp.: French Pat. C22B03, 2477181, September, 1981.

[151] Kruesi, W. H. and Kruesi, P. R.: Microwaves in Laterite Processing, In Ozberk, E. and Marcuson, S. W. eds: Nickel Metallurgy, Proceedings, CIM, 1(3)(1986):1-11.

[152] Liu, C. and Peng, J.: The Physicochemical Properties of Nickel Bearing Pyrrhotite and Kinetics of Elemental Sulphur Produced under Controlled Oxygen Potential in the Microwave Field, In: Hager J. P. ed: EPD Congress 1993, TMS:499-510.

[153] Lui, C., Zhu, Z. Xu, Y. and Peng, J.: A Novel Combined Process for Obtaining High Grade Ni-Cu Matte from Ni-Cu Sulphide Concentrates Directly, In Reddy, R. G. and Weizenbach, R. N. eds: Extractive Metallurgy of Copper, Nickel and Cobalt, Vol. I Fundamental Aspects, TMS and CIM, 1993:1063-1080.

[154] Peng, J and Liu, C.: Rate of Temperature Increase of PbS and PbO and their Reaction Kinetics, J. of China Non-Ferrous Metals (in Chinese), 3(1)(1993):25-31.

[155] Peng, J and Liu, C.: Kinetics of $FeCl_3$ Leaching of Sphalerite in Microwave Irradiation, J. of China Non-Ferrous Metals (in Chinese), 2(1)46-49.

[156] Neas, E.: Microwave Chemistry: A Young Science with Great Potential, Presentation to the National Materials Advisory Board Committee on Microwave Processing of Materials, USA, December 1992.

[157] National Research Council: Microwave Processing of Materials, National Academy Press, Washington, D. C. 1994:1-150.

[158] Westbrook, W. T. and Jefferson, R. H.: Dissolution of Samples by Heating with a Microwave Oven in a Teflon Vessel for Instrumental Analysis, J. Microwave Power, 21(1)(1986):25-32.

[159] Mattes, S. A., Farrell, R. F. and Mackie, A. J.: A Microwave System for the Acid Dissolution of Metal amd Mineral Samples, U. S. Bureau of Mines Technical Progress Report 120, April 1983:1-9.

[160] Kingston, H. M. and Jassie, L. B.: Fundamental Relationships in Acid Decomposition of Samples for Elemental Analysis Using Microwave Energy, in Sutton, W. H., Brooks, M. H. and Chabinsky, I. J. eds.: Microwave Processing of Materials, Vol 124, Materials Research Society, Pittsburgh, PA, 1988:121-128.

[161] Kingston, H. M. and Jassie, L. B.: Introduction to Microwave Sample Preparation: Theory and Practice, American Chemical Society Professional Reference Book, American Chemical Society, Washington, 1988.

[162] Baghurst, D. R. and Mingos, D. M. P.: Superheating Effects Associated with Microwave Dielectric Heating, Journal of the Chemical Society, Chemical Communications, 9(1992):674-677.

[163] Kingston, H. M.: Microwave Applications in Analytical Chemistry, In Congress Proceedings: First World Congress on Microwave Chemistry, International Microwave Power Institute, Clifton, Virginia, 1992.

[164] Roussy, G. and Pearce, J. A.: Foundations and Industrial Applications of Microwaves and Radio Frequency Fields, John Wiley & Sons, New York, NY, USA, 1995:1-475.

[165] Sutton, W. H.: Microwave Processing of Ceramic Materials, Ceramic Bulletin, 68(2)(1989): 376-386.

[166] Roussy, G. A., Mercier, A., Thiebaut, J. M. and Vaubourg, J. P.: Temperature Runaway of Microwave Heated Materials: Study and Control, Journal Microwave Power, 20(1)(1985):47-51.

[167] Roussy, G. A., Bennani, A. and Thiebaut, J. M.: Temperature Runaway of Microwave Irradiated Materials, Journal of Applied Physics, 62(4)(1987):1167-1170.

[168] Tian, Y. L., Feng, J. H., Sun, L. C. and Tu, C. J.: Computer Modeling of Two Dimensional Temperature Distributions in Microwave Heated Ceramics, In Beatty, R. L., Sutton, W. H., and Iskander, M. F. eds: Materials Research Society Symposium Proceedings, Materials Research Society, Pittsburgh, Pennsylvania, 269(1992):41-46.

[169] Kriegsmann, G. A.: Thermal Runaway and its Control in Microwave Heated Ceramics, In Beatty, R. L., Sutton, W. H., and Iskander, M. F. eds: Materials Research Society Symposium Proceedings, Materials Research Society, Pittsburgh, Pennsylvania, 269(1992):257-264.

[170] Barmatz, M. and Jackson, H. W.: Steady State Temperature Profile in a Sphere Heated by Microwaves, In Beatty, R. L., Sutton, W. H., and Iskander, M. F. eds: Materials Research Society Symposium Proceedings, Materials Research Society, Pittsburgh, Pennsylvania, 269(1992):97-103.

[171] Johnson, D. L., Skamser, D. J., and Spotz, M. S.: Temperature Gradients in Microwave Processing: Boon and Bane, In Clark, D. E., Tinga, W. R. and Saia, J. R. eds: Ceramic Transactions, American Ceramic Society,Westerville,Ohio 36(1993):133-146.

[172] Ford, J. D. and Pei, D. C. T.: High Temperature Chemical Processing via Microwave Absorption, J. Microwave Power, 2(2)(1967):61-64.

[173] Wong, D.: Microwave Dielectric Constants of Metal Oxides at High Temperature, M.Sc. Thesis, 1975, University of Alberta.

[174] Tinga, W. R.: Microwave Dielectric Constants of Metal Oxides, Part 1 and Part 2, Electromagnetic Energy Reviews, 1(5)(1988):2-6; 2(1)(1989):1-6.

[175] Chen, T. T., Dutrizac, J. E., Haque, K. E., Wyslouzil, W. and Kashyap, S.:The Relative Transparency of Minerals to Microwave Radiation, Canadian Metallurgical Quarterly, 23(3)(1984):349-351.

[176] Walkiewicz, J. W., Kazonich, G. and McGill, S. L.: Microwave Heating Characteristics of Selected Minerals and Compounds, Minerals and Metallurgical Processing, 5(1)(1988):39-42.

[177] McGill, S. L. and Walkiewicz, J. W.: Applications of Microwave Energy in Extractive Metallurgy, J. Microwave Power, 22(3)(1987):175-177.

[178] McGill, S. L., Walkiewicz, J. and Smyres, G. A.: The Effects of Power Level on the Microwave Heating of Selected Chemicals and Minerals, In Sutton, W. H., Brooks, M. H. and Chabinsky, I. J. eds: Microwave Processing of Materials, Reno, Nevada, 124(1988):247-252.

[179] Church, R. H. and Webb, W. E.: A Measurement Technique for Determining the Dielectric Properties of Low Loss Materials, J. Microwave Power, 21(2)(1986):113-114.

[180] Mingos, D. M. P.: The Applications of Microwaves in Chemical Synthesis, in Burka, M., Weaver, R. D. and Higgins, J. eds: Proceedings:Microwave-Induced Reactions Workshop, Pleasant Hills, California: Electric Power Research Institute, EPRI TR-102252(1993)A-8-1– A-8-11.

[181] Neas, E.: Basic Theoretical Considerations in Microwave Chemistry, In Congress Proceedings: First World Congress on Microwave Chemistry, International Microwave Power Institute, Clifton, Virginia, 1992.

[182] Majetich, G.: The Use of Commercial Microwave Oven in Organic Chemistry, In Congress Proceedings: First World Congress on Microwave Chemistry, International Microwave Power Institute, Clifton, Virginia, 1992.

[183] Farrow, C. J. and Burkin, A. R.: Alkali Pressure Leaching of Chromium (III) Oxide and of Chromite Mineral, in Burkin, A. R. ed: Leaching and Reduction in Hydrometallurgy, The Institute of Mining and Metallurgy, London, 1975:20-27.

[184] Degliomini, P.A.: Monthly Progress Report-February 1983 Chemical Metallurgy, Corporate Research and Technical Service-AMAX Caustic Leach Process Testwork, Project No. 912 (CJ-778), 1983:1-5.

[185] Yin, J. Z and Shen, B. W.: Inorganic Chemistry, Vol 2 (in Chinese), People's Education Publishing House, Beijing, 1980:366.

[186] Fuller, A. J. B.: Ferrites at Microwave Frequencies, Peter Pererinus Ltd., London, UK., 1987,8-17.

[187] Roberts, J.: High Frequency Applications of Ferrites, The English Universities Press LTD, London, UK, 1960, 10, 11,33-35.

[188] Lax and K.J. Button: Microwave Ferrites and Ferromagnetics, McGraw-Hill Book Company, Inc., New York, USA,

[189] Aulock: Handbook of Microwave Ferrite Materials, Academic Press, New York, USA, 1965,341-347,379-394.

[190] Bamford and C.F.H.Tipper ed.: Comprehensive Chemical Kinetics, Elsevier, New York, 1980(22),41.

[191] Guillisen, G. and Van Rysselberghe, R. J.: Trans. Am. Electrochem. Soc., 59(1931):95.

[192] Tammann, G.: Z. angew. Chem., 39(1926): 869.

[193] Kedesdy, H. and Katz, G.: Ceram. Age, 62(1953): 29.

[194] Furuichi, R, Ishii, T. and Bamba, S.: Z. Anorg. Allg. Chem., 437(1977):293.

[195] Shimada, S., Soejima, K. and Ishii, T..: Reactivity of Solids, 8(1990):51-61.

[196] Hopkins, D. W.: J. Electrochem. Soc., 96(1949):195.

[197] Hauffe, K. and Pschera, K.: Z. Anorg. Chem., 262(1950):147.

[198] Dunkan, J. F. and Stewart, D. J.: Trans.Faraday Soc., 63(1967):1031.

[199] Parder, R., Riden, C. J. and Tinsley, C. J..: Trans. Faraday Soc., 65(1969):219.

[200] Schnitt, G. and Kleinert, P.: Z. Anorg. Allg. Chem., 398(1973):41.

[201] Mackenzie, K. J. D.: Rev. High Temp. Mater., 5(1984):251.

[202] Hedvall., J. A.: Solid State Chemistry-Whence,Where and Whither, Elsevier, Amsterdam, 1966:6.

[203] Boldyrev, V. V., Bulens, M. and Delmon, B.: The Control of the Reactivity of Solids (Studies in Surface Science and Catalysis, vol.2), Elsevier, Amsterdam, 1979:3.

[204] Kubo, T.: in T.Okabe ed.: Reactivity of Solids, Japanese Chemical Society, Tokyo, 1975:1.

[205] Gohn, J. G.: in T.J.Gray et al ed.: Kinetics of Reaction in Ionic Systems, Plenum, New York, 1969:7.

[206] Komatsu, W.: React. Solid. Int. Symp. 5th, 1965,1964:82.

[207] Bak, T, Haber, J. and Ziolkowski, J.: Bull. Acad. Pol. Sci., Ser. Sci. Chim., 19(1972):489.

[208] Bamford , C. H. and Tipper ed., C. F. H.: Comprehensive Chemical Kinetics, Elsevier, New York, 22(1980):253.

[209] Feltz, A. and Martin, A.: Mater. Sci. Monogr., 28A(1985):137.

[210] Toolenaar, F. J. C. M.: J. Mater. Sci., 24(1989):1089.

[211] Furuichi, R., Tani, K., Kamada, K. and Ishii, T.: React. Solids, 1(1986): 309-318.

[212] Halika, I. and Milona, E.: Can. Met. Quart.,1994, 33(2):99-109.

[213] Kingery, W. D. ed.: Kinetics of High-Temperature Processes, The Technology Press of MIT and John Wiley & Sons, Inc., New York, 1959:245.

[214] Bamford, C. H. and Tipper ed, C. F. H.: Comprehensive Chemical Kinetics, Elsevier, New York, 22(1980): 41.

[215] Sharp, G. H., Brindley, G. W. and Achar, B. N. N.: J.Am.Ceram.Soc., 49(1966):379.

[216] Hurbert, S. F.: J. Br. Ceram. Soc., 6(1967):11.

[217] Hancock, J. D. and Sharp, J. H.: J. Am. Ceram. Soc., 55(1972):74.

[218] Carter, R. E.: Chem. Phys., 34(1961):2010.

[219] Carter, R. E.: Chem. Phys., 35(1961):1137.

[220] Jander, W.: Z. Anorg. Allg. Chem., 163(1927):1 ; Angew. Chem., 41(1928):79.

[221] Ginstling, A. M. and Brounshtein, B. I.: Zh. Prikl. Khim., 23(1950):1327.

[222] North-East Institute of Technology: Zinc Metallurgy (in Chinese), Metallurgical Industrial Publishing House, Beijing, 1974:10.

[223] Tottle, C. R.: An Encyclopaedia of Metallurgy and Materials, Macdonald & Evans Ltd., Great Britain, 1984:132.

[224] Berry, L. G.: Powder Diffraction File, Set 6-10, Joint Committee on Powder Diffraction Standards, Philadelphia, 295,813.